Alma Mater Studiorum – Università di Bologna

DOTTORATO DI RICERCA IN

SCIENZE E TECNOLOGIE AGRARIE, AMBIENTALI E ALIMENTARI

Ciclo XXXII

Settore Concorsuale: 07/B1

Settore Scientifico Disciplinare: AGR/02

TITOLO TESI

REMOTE SENSING AND SITE SPECIFIC CROP MANAGEMENT IN PRECISION AGRICULTURE

Presentata da: Abid Ali

Coordinatore Dottorato

Prof. Massimiliano Petracci

Supervisore

Dr. Lorenzo Barbanti

Co-supervisore

Dr. Roberta Martelli

Esame finale anno 2020

Table of Contents

List of Abbreviations

AA	Above Average
AVHRR	Advanced Very High Resolution Radiometer
BA	Below Average
BW	Bread wheat
CEC	Cation Exchange Capacity
CO	Coriander
CV	Coefficient of Variation
DEM	Digital Elevation Mapping
DNS	Digital Numbers
DOS1	Dark Object Subtraction 1
DSpD	Degree of Spatial Dependence
DSS	Decision Support System
DW	Durum wheat
EC	Electrical Conductivity
ECa	Apparent Electrical Conductivity
EM	Electromagnetic
ER	Electrical Resistivity
ETc	Crop Evapotranspiration
ETM+	Enhanced Thematic Mapper Plus
EVI	Enhanced Vegetation Index
FOV	Field of View
GCI	Green Chlorophyll Index
GIS	Geographic Information System
GNDVI	Green Normalized Difference Vegetation Index
GNSS	Global Navigation Satellite Systems
GOES	Geostationary Operational Environmental Satellites
GPS	Global Positioning System
GY	Grain Yield
HY	High Yielding
HYS	High Yielding and Stable
IFOV	Instantaneous Field of View
IPM	Integrated Pest Management
K-S	Kolmogorov-Smirnov
L1TP	Level-1 Precision Terrain
LIDAR	Light Detection and Ranging
LS	Landsat
LY	Low Yielding
LYS	Low Yielding and Stable
MAE	Mean Absolute Error
MODIS	Moderate-Resolution Imaging Spectroradiometer
MRE	Mean Relative Error
MZs	Management Zones

NDVI	Normalized Difference Vegetative Index
NOAA	National Oceanic and Atmospheric Administration
OLI	Operational Land Image
P	Precipitation
PA	Precision Agriculture
QGIS	Quantum Geographic Information System
R^2	Coefficient of Determination
RGB	Red, Green and Blue
RMSE	Root Mean Square Error
R_{NIR}	Near-Infrared Reflectance
R_{RED}	Red reflectance
RRMSE	Relative Root Mean Square Error
RS	Remote Sensing
RTK	Real Time Kinetics
SAR	Synthetic Aperture Radar
SAVI	Soil Adjusted Vegetation Index
SpD	Spatial Dependence
SD	Standard Deviation
SF	Sunflower
SK	Simple Kriging
SR	Simple Ratio
SpR	Spatial Resolution
SSCI	Site-Specific Crop Input
SSCM	Site-Specific Crop Management
SSMZs	Site-Specific Management Zones
TM	Thematic Map
USGS	United State Geological Survey
UTM	Universe Transverse Mercator
VIs	Vegetation Indices
VRI	Variable Rate Inputs
VRT	Variable-Rate Technology
YSCs	Yield Stability Classes
YZs	Yield Zones

Abstract

Application of variable crop inputs in the right quantity and place is very important for optimizing plant growth and final yield through efficient use of finite resources and minimum environmental impacts. Precision agriculture (PA) practices have a great potential to enhance the global food demand, as well as sustain the environmental resources. Among sustainable farming, remote sensing (RS) and site-specific crop management (SSCM) have been considered the core of modern PA practices, involving crop inputs to be applied according to the inherent spatio-temporal characteristics within field. Under variable rate technology, the profit highly depends on the input rates based on the specific factors which influence crop productivity.

In this framework, actions were carried out to support the adoption of PA: In Chapter 1 several remotely sensed vegetation indices (VIs) from Landsat 5, 7 and 8 missions were used to estimate the spatial crop yields of winter cereals (durum and bread wheat) and spring dicots (sunflower and coriander) over five consecutive years. Crop growth stages showing highest correlations between studied VIs and final yield were considered as the critical growing periods for each crop. Pixel level correlations through spatial maps were also investigated between original VIs data and kriged crop yield data. Results showed that spatial variability of crops can be effectively assessed through Landsat imagery with 30 m resolution even on a relatively small area (11.07 ha). Simple ratio (SR) and normalized difference vegetation index (NDVI) were shown slightly better indices during vegetative to reproductive stages as compared to enhanced vegetation index (EVI), soil adjusted vegetation index (SAVI), green normalized difference vegetation index (GNDVI) and green chlorophyll index (GCI). Pixel level study also demonstrated a good agreement between five classes of VIs and grain yield (GY). Past literature demonstrated that correlation between VIs and GY highly depends on the stage of crop growth, hot and cold weather conditions, lodging, pest and disease attacks. Furthermore, the high value of VIs before grain filling stage, alone, cannot always be a predictor for estimating the final yield: sometimes higher values only contribute to the development of plant biomass structure because of proper water availability to crop plants during early stages.

In Chapter 2, three yield stability classes (YSCs) were developed using spatio-temporal yield maps over five years: high yielding and stable (HYS, relative yield > 100 %; CV < 30 %), low yielding and stable (LYS, relative yield < 100 %; CV < 30 %) and unstable class (Unstable, CV > 30 %). Thereafter, we evaluated the YSCs by

following the simple correlations between stable soil properties and spatiotemporal yield variability within YSCs, and as a function of the differences in soil properties among the three classified classes. In addition, we examined the time trends of ambient moisture, i.e. the balance between precipitation and evapo-transpiration during the five growing seasons. Results showed that spatial maps were more consistent with the YSCs map than the temporal stability map. Unstable class was found to be slightly more productive than LYS class. Yield classes were found considerably consistent with soil properties. Lower values of soil apparent electrical conductivity (ECa), in the average, were consistent with HYS class featuring maximum crop yield (122 %), compared to LYS and unstable class. However, higher soil ECa and sand content in unstable class were associated with slightly higher yield (83 %) than LYS (80 %), implying that higher ECa and sand content had not exerted a negative influence on crop yield, despite higher variability in the unstable area, in the given field conditions. It is perceived, therefore, that ECa has complex interactions with soil properties and environmental factors, which may influence ECa values and the final yield performance. The balance between precipitation and evapo-transpiration, and temperature erratic patterns support the fluctuations of yield across years in the unstable area. Owing to this uncertainty, the establishment of yield stability classes based on spatio-temporal maps over multiple years appears the best practice for delineating SSCM, as these maps apparently comprise all factors influencing crop yield.

Scientific production and patents during 3 years' PhD period

PhD activities:

I. Ali, A., Martelli, R., Lupia, F., & Barbanti, L. (2019). Assessing Multiple Years' Spatial Variability of Crop Yields Using Satellite Vegetation Indices. *Remote Sensing*, 11(20), 2384. **IF 4.118,** ISI & Scopus Journal.

II. Ali, A., Barbanti, L., Scudiero E., Martelli, R., Falsone, G. Soil and Weather Factors Drive Spatiotemporal Variability of Yields in a Crop-Rotation Field under Uniform Management. Under draft.

General activities:

I. Hassan, M. U., Chattha, M. U., Khan, I., Chattha, M. B., Barbanti, L., Aamer, M., Iqbal, M. M., Nawaz, M., Mahmood, A., Ali, A. & Aslam, M. T. (2020). Heat stress in cultivated plants: nature, impact, mechanisms, and mitigation strategies-A review. *Plant Biosystems-An International Journal Dealing with all Aspects of Plant Biology*, (just-accepted), pp.1-56. **IF 1.525,** ISI & Scopus Journal.

II. Mustafa, G., Ali, A*., Ali, S., Barbanti, L., & Ahmad, M. (2019). Evaluation of dominant allelopathic weed through examining the allelopathic effects of four weeds on germination and seedling growth of six crops. *Pakistan Journal of Botany*, *51*(1), 269-278. **IF 0.755,** ISI & Scopus Journal.

III. Chattha, M. U., Hassan, M. U., Barbanti, L., Chattha, M. B., Khan, I., Usman, M., Ali, A., & Nawaz, M. (2019). Composted Sugarcane By-product Press Mud Cake Supports Wheat Growth and Improves Soil Properties. *International Journal of Plant Production*, 1-9. **IF 0.961,** ISI & Scopus Journal.

IV. Hassan, M. U., Chattha, M. U., Khan, I., Chattha, M. B., Aamer, M., Nawaz, M., Ali, A., Khan, M. A. U., & Khan, T. A. (2019). Nickel toxicity in plants: reasons, toxic effects, tolerance mechanisms, and remediation possibilities—a review. *Environmental Science and Pollution Research*, *26*(13), 12673-12688. **IF 2.914,** ISI & Scopus Journal.

V. Aamer, M., Muhammad, UH, Abid, A., Su, Q., Liu, Y., Adnan, R., Tahir, A. K., & Huang, G. (2018). Foliar application of glycinebetaine (GB) alleviates the cadmium (Cd) toxicity in spinach through reducing Cd uptake and improving the activity of antioxidant systems. *Applied Ecology and Environmental Research*. 16, 7575-7583. **IF 0.721,** ISI & Scopus Journal.

Conference proceedings:

I. Ali A., Martelli R., Lupia F., Barbanti L. 2019. Estimating Spatial Variability of Crop Yields Using Satellite Vegetation Indices. In: Poster Proceedings of the 12th European Conference on Precision Agriculture, July 8-11, Montpellier, France. p. 16. E-book publication. SupAgro Montpellier. ISBN 978-2-900792-49-0.

0. General Introduction

Precision agriculture (PA), also known as satellite farming or site specific crop management (SSCM), is a modern agricultural crop management paradigm in which all field operations, from sowing to harvesting, are carried out by information technology to manage the future crop farming based on spatiotemporal variability of past or current field history. (Neményi et al., 2003; Yousefi and Razdari, 2015; Shah and Wu, 2019). Amid information technology, computer based softwares such as GPS (Global Positioning System), QGIS (Quantum Geographic Information System) and ArcGIS are commonly used for the collection, spatial mapping, storing, processing, retrieving and geostatistical analysis of numerical variables, as well as to help in the decision making process related to PA practices (Gupta et al., 2010; Zhang et al., 2010). Specifically, PA uses a combination of advanced technologies such as soil and crop sensors, satellite navigation system, remote sensing technology, site-specific crop management (SSCM), various internet sources and interactions among them (Gibbons, 2000; Andreo, 2013; Schrijver et al., 2016).

0.1. Remote Sensing

Remote sensing (RS), approach widely used in PA, is the art and science of collecting information's of the earth surface without physical contact through sensors on satellites or airplanes (Elachi, 1987; Jensen, 2007; Basso et al., 2016; Toscano et al., 2019). Remote sensing is contributing an essential role in global issues related to agriculture, environment, forestry, and natural ecosystems, etc. This technology is considered as an efficient tool to solve above-mentioned issues at the earth's surface (Baghdadi and Zribi, 2016). Innovations in machine learning, artificial intelligence, and deep image analysis made it necessary to further analyze and better understand the remote data at the same time (Ma et al., 2019). All this information indicated that RS is serving as a major development opportunity in PA.

There are many platforms used in retrieving the data from the earth's surface. In the past, only visible spectrum of light was used in satellite sensing but current modern technologies made possible for retrieving spectral data from the wavelengths of infrared, thermal and microwave spectrum of a target object. Data collection using many different types of wavelengths referred to as hyperspectral data. Currently, modern satellite-missions are successfully providing enough information at lower cost over a large area at the same time. However, monitoring the land surfaces and environmental data have greatly increased during the last years, and probably remote sensing is an important approach for enhancing the agricultural yield and sustaining the natural resources.

0.1.1. Electromagnetic spectrum

The electromagnetic (EM) spectrum is the EM radiations. The EM spectrum has seven regions ranging from gamma to radio waves as shown in Figure 1. Remote sensing measures the wavelength embedded in different regions of the EM spectrum, for example, visible lights reflected or emitted infrared and microwave wavelengths, which are important in satellite sensing information (Table 1). However, the most important regions are visible light. The measurement of visible spectrum of light proceeds in spectral bands, these spectral bands known as a discrete interlude of the EM spectrum. Sensors in satellite configuration were designed in such a manner that sense the respond from spectral bands to allow the differentiation of target object. Researchers choose particular spectral bands, depending on what they want to investigate.

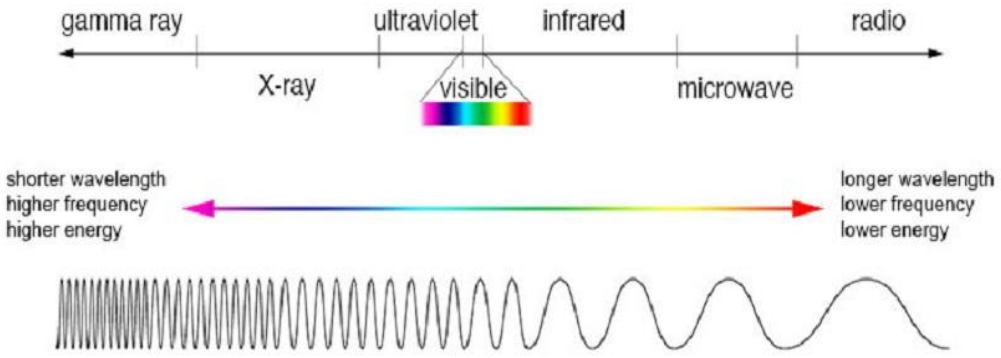

Source: NASA

Figure 1. Electromagnetic spectrum

Table 1. Wavebands of the Electromagnetic Spectrum

EM Bands	Wavelengths	Comments
Gamma Rays	< 0.03 nm	Absorbed by earth surface
X-rays	0.03 to 30 nm	
Extreme Ultraviolet	0.03 to 0.4 μm	Absorbed by the ozone layer.
Near Ultraviolet	0.3 to 0.4 μm	Available for remote sensing, the reflected from earth surface.
Visible light	0.4 to 0.7 μm	
Near-Infrared	0.7 to 100 μm	
Far Infrared	0.7 to 3.0 μm	
Thermal waves	3.0 to 14 μm	
Microwaves	0.1 to 100 cm	Images can be made with sensors that actively emit microwaves.
Radio waves	> 100 cm	Normally not used for remote sensing.

Source: NASA

0.1.2. Reflection and absorption

When radiations from the sun reach on the earth surfaces, some part of it is absorbed by earth surface and other reflected back to the atmosphere at certain wavelengths, this phenomenon occurs if earth surface become true reflector or fully black body. Anyway, these surfaces existed rarely on the earth planet. During photosynthesis, blue and red wavelengths are absorbed, whereas green light reflected back to the atmosphere. In RS, a detector measures the reflected wavelengths from the earth. These readings may support to differentiate the vegetation type on the earth's surface. The soil, water, and vegetation have different sensitivity levels to EM wavelengths. The sensitivity of one object varies to the range of EM wavelengths, this phenomenon known as the spectral signature of an object.

A sensor is a RS device that measures the wavelength of the EM spectrum. There are two types of sensors (Figure 2). The passive sensor depends on external energy, the sunlight, and acquires optical images of various spatial and spectral resolution. The active sensor has its own energy, radio waves, produces radar imagery. This type of sensor measures the amount of radiations that reflected back through the earth surfaces. Active sensors are more controlled as compare to passive ones because they do not depend and receive different light conditions. In general, these sensors collect spatial data in the form of images and provide specialized capabilities for analysis, processing, and visualizing those images by using GIS software.

Remote sensors produce the image based on the source of reflected light from the earth surface. This sensation helps us to easily visualize the differences between the earth surfaces based on green vegetation cover. In order to extract information contained in such images and use it accordingly, one needs special tools - a GIS software (QGIS and ArcGIS). Free images can be downloaded from the USGS website, or from cloud-based platforms like EOS Land Viewer with a more user-friendly interface. There you can preview, filter, and download images to a computer or save to cloud storage. These GIS tool allows analyzing the spectral characteristics of images and downloading results according to your needs and specification.

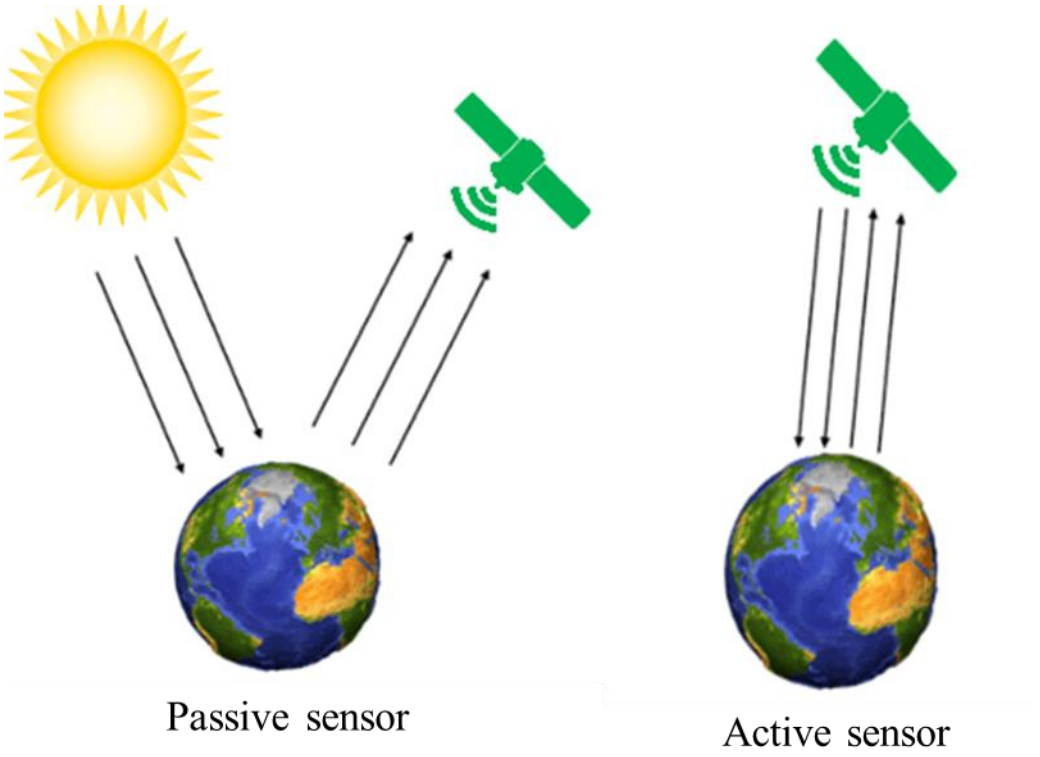

Figure 2. Passive and active sensors of remote sensing

0.1.3. Satellite sensor

The satellite sensors collect the informative data from reflected radiation in a specific path, referred to as field of view (FOV). The smallest region on the earth's surface called the sampled area, known as instantaneous field of view (IFOV) or pixel size of the sensor. This measurement takes place in one or more spectral bands. The measurement collected by each satellite sensor known as spatial, spectral or temporal resolution (Table 2).

0.1.3.1. *Spatial resolution*

The spatial resolution (SpR) is the surface area imaged by a remote sensing device for the IFOV. The IFOV of the Landsat-Thematic Map (TM) sensor i.e. 30m. Weather satellite sensors have larger SR than kilometer square. Some commercial or military satellites have less than 1m SR that are available at expensive price.

0.1.3.2. *Temporal resolution*

Temporal resolution is a measure of the frequency at which a satellite sensor revisits the same area of the earth's surface. However, revisiting frequency varies many times over a day: in typical satellites for a weather forecast, from 8- 20 times per year, for example, Landsat-TM satellite, for a moderate ground-based satellite.

0.1.3.3. *Spectral resolution*

The spectral resolution is the number and width of the spectral bands in the satellite sensor. The simplest sensor of a spectral resolution consisted on one band, senses only visible portion of the EM spectrum. A sensor having 3 bands (red, green and blue) in visible portion of light spectrum gathers the same information as human vision. By using different types of visual resolutions (RGB composites, multi-temporal NDVI index), a researcher can identify the problems associated with their crops and apply the proper solutions to affected areas. This can help the farmers to apply less or more crop inputs to the areas according to a specific need, rather than treating a whole field with evenly distributed input dosages.

Table 2. Comparison of Landsat satellite sensors

Landsat Resolution	**MSS (LS 1-5)**	**TM (Landsat 4-5)**	**ETM+ (LS 7)**	**OLI (LS 8)**
Spectral (μm)	1. 0.50-0.60, G 2. 0.60-0.70, R 3. 0.70-0.80, NIR 4. 0.80-1.10, NIR	1. 0.45-0.52, B 2. 0.52-0.60, G 3. 0.63-0.69, R 4. 0.76-0.90, NIR 5. 1.55-1.75, SWIR-1 6. 2.08-2.35, SWIR-1 7. 10.4-12.5, TIR	1. 0.45-0.52,B 2. 0.53-0.61, G 3. 0.63-0.69, R 4. 0.78-0.90, NIR 5. 1.55-1.75, SWIR-1 6. 10.31-12.36, TIR 7. 2.06-2.35, SWIR-2 8. 0.52-0.90 (Pan)	1. 0.44-0.45, Coastal/Aerosol 2. 0.45-0.51, B 3. 0.53-0.59, G 4. 0.64-0.67, R 5. 0.85-0.88, NIR 6. 1.57-1.65, SWIR-1 7. 2.11-2.29, SWIR-2 8. 0.50-0.68, Pan 9. 1.36-1.38, Cirrus 10. 10.60-11.19, TIR-1 11. 11.50-11.51, TIR-2
Spatial (m)	79X79	30x30 120x120 (TIR)	30X30 15X15 (Pan) 60x60 (TIR)	30X30 15 (Pan) 100 (TIR)
Temporal (revisit in days)	18	16	16	16

LS, landsat; MSS, multi-spectral scanner; TM, thematic map; ETM+, enhanced thematic map plus; OLI, operational land imager; G, green; R, red; B, blue; NIR, near infrared; SWIR, panchromatic and shortwave infrared; TIR, thermal infrared, Pan, panchromatic band.

0.1.4. Satellite remote sensing

Nowadays, satellite remote sensing (RS) has introduced more commonly in PA. The Landsat-TM and the National Oceanic and Atmospheric Administration (NOAA) provide multi-spectral images that can be successfully used to estimate the crop vegetation and acreage, where the normalized difference vegetative index (NDVI) is used to verify the soil factors that influence the crop yields and nutrient status.

The Advanced Very High-Resolution Radiometer (AVHRR) satellite measures the reflectance of plant canopy in the visible, near-infrared and thermal infrared

spectrum. This spectral sensitivity of the satellite sensor can be used to estimate the rapid changes in crop vegetation because the revisiting frequency of this satellite is twice a day. Unfortunately, this satellite is hardly used in PA, because the SR of this satellite goes to 1.1 km. However, thermal infrared could be used for this sensor to determine the range of temperatures; these estimations could be further used to calculate the growing degree-days of insect pests and crop plants for their model development. These models could be used in integrated pest management (IPM) programs. These predictions of spatial variability provided by satellites would allow us to use degree-day models in a better way, rather than time-spaced data from weather stations used until recently in these models. Some handheld optical sensors are also used in RS science. Handheld sensors are easy tools that can be used according to specific day and time with high spectral resolution. Remote data are also used to determine irrigation scheduling.

Through satellite RS, various other vegetation indices (VIs) have been developed to address crop growth status through specific relationships with chlorophyll, carotenoids or biomass (Sims and Gamon, 2003). These VIs provide information on biotic and abiotic stresses affecting crop growth, to be used in the prediction of final crop yield (Zarco-Tejada et al., 2005). More recent VIs have been developed to counterbalance NDVI limitations, e.g. the interference of soil reflectance with sparse canopy cover, and the low sensitivity to chlorophyll content in mature canopies. Mulla (2013) found that VIs were outperformed in specific applications to PA. Landsat satellites measure the reflected radiation from the visible EM spectrum by thermal infrared. The high SR (30 m) of Landsat sensors makes it applicable in PA. This satellite is suitable for estimating the spatial vegetation of an individual field because of its high SR and spectral response. Remotely sensed data from Landsat TM is becoming more popular in existing precision agricultural support systems.

0.1.5. Other common satellites and earth observatory missions

Table 3. Spatial, temporal and spectral resolution of commonly used satellites and earth observatory

Satellite and earth observatory	Full name and description	Spatial resolution	Temporal resolution (revisit in days)	Spectral resolution
Geos-5	Geostationary operational environmental satellite-5	1-41 km	20	multi-bands
NOAA	National oceanic and atmospheric administration	1.1 km	1	-
MODIS	Moderate-resolution imaging spectro-radiometer	250-1000 m	1	-
IKNOS	Earth observatory satellite	4m	3 to 5	-
SAR	Synthetic Aperture Radar	1 to 80 m	0.2 to 7	-
Sentinels (1-5)	Satellite platform	10m	5 & 10	-

0.1.6. Remote sensing process

Remote sensing gives the possibility to form images by detecting the reflected radiation of visible, near and short-wave infrared spectrum from target objects on the earth's surface (Figure 3). Different materials of the earth's surface absorb and reflect differently depending upon the type of wavelength. However, the targets could be identified by examining the spectral signature of remote imagery.

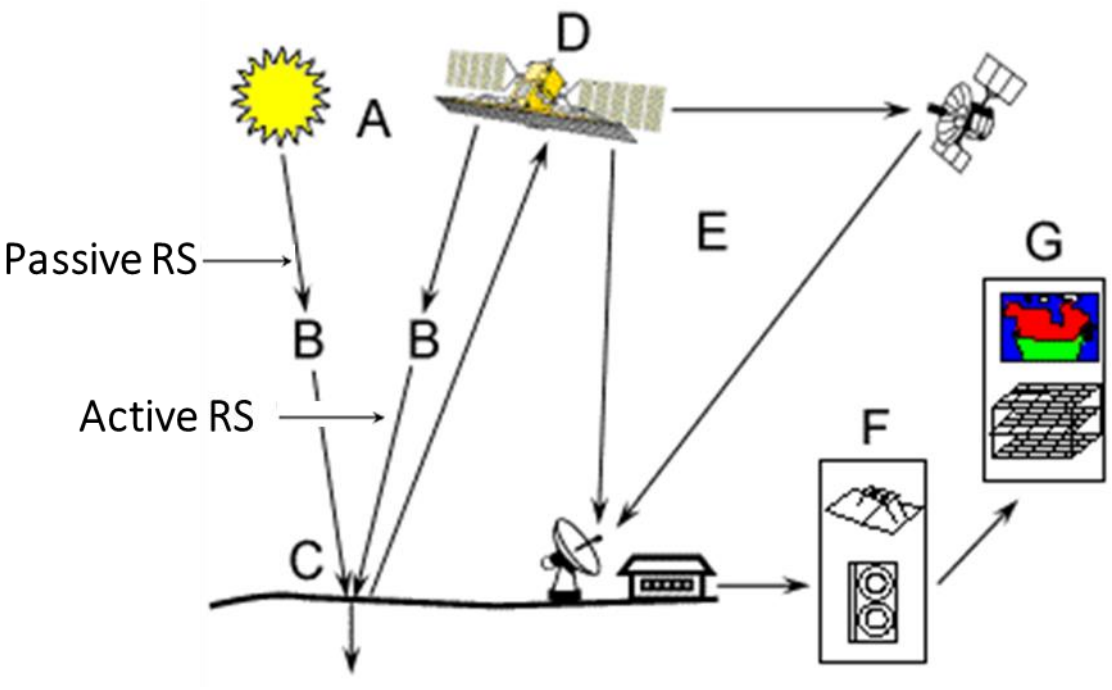

Figure 3. Sunlight (A); Atmosphere (B); Target object (C); Satellite sensor (D); Data transmission (E); Data interpretation/analysis (F); Computer application (G)

0.1.7. UAVs (Unmanned Aerial Vehicles) or Drones

An **unmanned aerial vehicle** (**UAV**) (also known as a **drone**) is a flying craft that can fly a preset course without the help of on-board pilot, but with GPS coordinates (Figure 4). UAVs are a component of an unmanned aircraft system (UAS); which include a UAV, a ground-based controller, and a system of communications between them. Sometimes the term UAV is referred to as a complete system, like ground stations and video systems. However, UAVs are commonly known as model planes and helicopters, i.e. aircrafts with both fixed and rotary wings. The flight of UAVs may be operated either under remote controller by a human operator or by onboard computer system (Pajares, 2015).

The rapid development of UAVs in agricultural field has resulted in increasing uptake of this technology in the remote sensing platform. These vehicles are providing a new possibility for the near-surface remote sensing of plant behaviour. Acquiring aerial photography with the help of UAVs offers high resolution, high accuracy, time saving, and low cost, which lead to more timely and accurate crop monitoring (Klosterman and Richardson, 2017; Maimaitijiang et al., 2017). Its spatial resolution exceeds that provided by Landsat satellite sensing, moreover it can be used for generating the orthophotographies (Yue et al., 2018). UAV remote sensing is more advantageous as compared to traditional remote sensing as it concerns flight pattern, time and cost (Geipel et al., 2014).

Drones can be regarded as the third generation of platforms providing remotely sensed data for addressing a particular problem involving detailed spatial and temporal resolution. The drone particularly addresses the spatiotemporal resolution in the acquisition of data.

Anyhow, some regulations across the world may still limit the use of UAVs in PA. This section of the general introduction will broaden the awareness, advantages of UAV in remote sensing and associated sensor technology.

Figure 4. Image of UAV aircraft

0.1.7.1. Advantages of using drones

1. Drones present less pressure on natural environment, and ensures the environmental safety.
2. This technology is used for better decision making in PA. UAVs help farmers to obtain access to a wealth of data such as crops yield data, livestock health, soil nutrient status, nutrient measurements, results of weather and rainfall, and much more. This reliable data can be used to get accurate site specific maps of existing issues. In this way, farmers can adopt better management practices in PA, and increase crop production efficiency.
3. In RS, it offers unprecedented spatial, spectral, and temporal resolution, but can also provide detailed vegetation height data and multi-angular observations.
4. Help in chemical spraying: spraying system is attached to the lower region of the UAV which has a nozzle beneath the liquid container to spray the pesticide or any other kind of liquid fertilizer downwards (Mogili and Deepak, 2018).
5. The UAVs technology can cover the whole ground and deliver the right amount of liquid in real time for even distribution to particular regions. In this way, correct amount of chemicals are sprayed in a better way increasing the production efficiency of crops. In fact, scientists estimate that sprinkler spray is five times faster with drones than traditional machinery.
6. These vehicles can stay in the air for up to 30 hours, doing repetitive tasks, day-after-day. Flight can be possible in the complete darkness or in the fog under computer control. Hence, these vehicles can fly longer hours on the areas of interest, and in this way there is no human fatigue in the plane.

7. These vehicles can perform geological survey, visual or thermal imaging of the region at the same time.
8. UAVs are capable of observing the crop with different indices (Simelli et al., 2015).
9. The drones can have more pinpoint accuracy over greater distances.
10. Through drone planting systems, plant nutrients uptake efficiency may achieve up-to 75% and decrease planting costs up-to 85% (Ahirwar et al., 2019). These systems provide all necessary nutrients in right amount to crop plants throughout the whole life cycle.
11. It is very important to monitor plant health, namely, virus, bacterial and fungal diseases during crop growing cycle. Scanning of crop plants with drones assembled with both visible and near-infrared light can determine which plants reflect the different amounts of green and NIR light. This information can produce multispectral images and identify their health status.
12. Now a days, comparatively cheap agricultural drones with advanced imagery and sensors are providing specific data to farming community. Through this data, farmers can enhance their productivity by reducing crop damages. With the application of UAVs, farmers can reduce their crop inputs such as irrigation water, pesticides, etc., and maintain their same output by using minimum economic resources. Finally, we can say that the UAVs (drones), which started as a military technology, may end as a green-tech technology.

0.2. Site-Specific Crop Management

Site-specific crop management is defined as the management of field spatial variability based on soil, environmental, topographical, anthropogenic and biological factors influencing the crop yields for optimizing the crop productivity and environmental impacts (Yakowitz et al., 1993; Oshunsanya et al., 2017). More specifically, "a sub-region within the same piece of land showing similar yield limiting factors within which different crop production practices are carried out." However, conventional agricultural practices are not following the complexity of yield-limiting factors, spatially and temporally, so it cannot fulfill the food demand of the escalating world population, as well as challenges of the future limited resource. Adopting modern farming, like PA or more precisely SSCM practices, is the only way to understand the complexity of spatial and temporal variability within

field using various approaches (Blackmore et al., 2003; Smith et al., 2009; Maestrini and Basso, 2018b; Marino and Alvino, 2019).

0.2.1. Factors responsible for yield variations within field

The soil physical-chemical properties significantly affect the crop behavior at field scale (Nielson et al., 1973). Recently, with the breakthrough of new technologies such as GPS and yield monitoring tools, various studies demonstrated that the spatial variability was influenced by the soil or other external factors under field scale (Verhagen et al., 1995; Corwin, 2013). There are many factors such as soil, biological entities, field topography, or meteorological data that could be responsible for spatiotemporal variability in crop yields. These factors might be varied, i.e. temporally, and become difficult to be measured by soil or plant sample, or an instrument.

0.2.2. Comparison between conventional vs site-specific crop management

In conventional agriculture, the whole field is treated with uniform cultivation, planting density, fertilizers, pesticides, herbicides, soil modifications, irrigation scheduling, and other inputs, without considering the inherent field variations. These farming practices may result in over dosages, but also in under dosages, of crop inputs such as seed rate, fertilizers, pesticides or irrigation water in some field parts. Consequently, lack of the knowledge of spatial and temporal variability at field scale, linked with soil internal and external factors that significantly influence the crop yields, results in reduced economic crop yield in certain parts of a field as well as increase in detrimental effects on the environment due to over dose of fertilizers, pesticides and other agro-chemicals. Furthermore, this situation leads to the wastage of public money, depletion of available resources, and degradation of soil, surface and ground water resources (Khosla et al., 2002; De Caires et al., 2015). In contrast, SSCM helps in managing the agricultural crops based on the spatial and temporal variability of soil and crop data within field to enhance crop productivity and limit the detrimental environmental impacts (Lindblom et al., 2017). SSCM is a premise of PA in which all agronomic practices and decisions take place according to field variability and crop requirements within specific sub-section within the same field (McKinion et al., 2001). However, every input must be applied to a particular zone with sound knowledge of site-specific variability.

0.2.3. Need for SSCM

World food demand poses a great challenge for agricultural scientist due to limited finite resources. Likewise, there are many negative impacts on the

environment affecting the sustainability of the crops, together with changing the climatic pattern, which resulted in limit the agricultural commodities and water scarcity. Unfortunately, conventional farming is not able to solve these issues. In addition, conventional farming continuously contributes to degradation of the natural habitat, excessive usages of fertilizers and pesticides, as well as promoting the degradation of fauna and flora. Globally, approximately 1.5 billion ha cropland has degraded under conventional agriculture (poor agriculture practices), and annual losses estimated over 5–6 million ha (World Resources Institute, 1998). SSCM addresses the drawbacks of conventional agriculture, such as spatial and temporal variation within the same piece of land. Hence, site-specific agriculture has a great potential to meet the world food demand of the escalating population through sustaining the resources and minimizing environmental impacts (Demirbaş, 2018).

0.2.4. Components of SSCM

There are five important components in SSCM: (1) spatial referencing; (2) monitoring of crop, soil and weather data; (3) mapping; (4) decision support system (DSS); and (5) differential actions. The technologies have been combined in SSCM as followed: global navigation satellite systems (GNSS), satellite sensor technology, GIS, yield monitoring and variable-rate technology (VRT) (Neupane and Guo, 2019). Geo-referenced data of soil, plant and environmental variables can be obtained through GIS, yield monitoring tools, proximal and satellite sensors (Odeha et al., 1994). Global navigation satellite systems, as the GPS, are a technology through which geo-referencing is made possible from several meters to sub-meter for accurate information that is important for downstream sensor technology, GIS and VRT. Similarly, in real-time kinetics (RTK), GPS tool is used for the measurement of field coordinates at a micro-level accuracy that can be detected during crop cultivation or harvesting, which are helpful in strip tillage, drainage or digital elevation mapping (DEM). Veris pH Manager (Veris Technologies, Salinas, KS) is a sensor technology that is used where pH is too acid or alkaline within field for variable-rate lime application or sulphur application to those areas, respectively.

Recently, apparent soil electrical conductivity (ECa) measured by EM induction (Geonics EM-38) or electrical resistivity (Veris-3100) has been successfully used to delineate the spatial map of soil physical-chemical properties (Corwin et al., 2003). Soil ECa sensors are affected by the soluble salts (as salinity) and other soil-related properties, and finally, ECa becomes measured ECa values result from a complex mixture interaction of all different soil properties (Corwin et al., 2003). In addition, ECa is influenced by various soil properties, so sensors that measure the ECa could

be considered an effective tool for delineating the management zones. This argument is supported only if ECa maps correlate with spatial yield maps. Generally, ECa map is not consistent with spatial yield in rainfed agriculture. In arid agriculture, crop sensors can provide enough information, whereas ECa sensors provide only appropriate results for irrigated crops grown under arid as well as semi-arid conditions. Generally, a DSS is an informative system that helps in the decision-making process. In SSCM context, a DSS supports us to determine the spatial and temporal variability associated with crop growth and yield parameters (Kersten et al., 2000). Through DSS system, site-specific areas are developed within field, in which variable inputs are required. Furthermore, these site-specific areas provide enough information to farmers linked to management practices during crop growing period. These areas denote a quite similar yield-limiting factor, giving the same pattern of yield over each year, in which a specific rate of crop input is fitting (Khosla et al., 2010). Variable-rate inputs such as planting density, fertilizers or irrigation time, etc., use the information from the SSMZs to increase the production efficiency of crops through the economic use of resources. SSMZs may or may not be stable over temporal variability. However, technologies are available for the development of management zones, but spatial and temporal information is still under question (van Uffelen et al., 1997). In this case, yield mapping based on spatiotemporal variability could be an effective tool for site-specific crop management, which determines the effectiveness of field productivity as influenced by physical, chemical and biological processes (Long, 1998). However, yield mapping for SSCM is a challenging task because several biotic and abiotic factors, as well as interaction among them, affected the spatiotemporal yield within each specific year (Huggins et al., 1995; Khosla et al., 2010). Therefore, multi-sensor platforms such as satellite, airborne imagery or digital photography, etc. can be an effective approach to differentiate the high and low productive areas (Inman et al., 2008; Schmidhalter et al., 2008; Rab et al., 2009; Corwin, 2013).

0.2.5. Management zones

The most important step in SSCM is the development of management zones. Delineating the management zones is not easy because of complex interactions among factors that affect the agricultural crop yields. Site-specific management zones (SSMZs) describe the spatial and temporal variability of the factors influencing the variations in crop behavior, such as soil, biological, meteorological or topographic factors. These factors have great influence in the optimization of crop production, environmental impacts, and utilization of natural resources. There are many strategies for the development of SSMZs as followed: ECa survey directed to

soil sampling (Corwin et al., 2003)., mapping of soil analysis based on inherent soil properties (Kitchen et al., 1998; Chang et al., 2004)., soil and crop proximal sensors for the establishment of variable rate inputs (VRI) in the frame of VRT (Nawar et al., 2017; Barbanti et al., 2018)., phosphorus, potassium management, pH and organic matter zones rely on general soil analysis, ECa maps and soil elevation (Mallarino and Wittry, 2004)., nitrogen and manure management zones are developed based on nitric nitrogen (NO3-N), crop vegetation indices, spatiotemporal yield and soil properties such as soil texture, organic carbon, pH or ECa (Moshia et al., 2014; Moshia et al., 2015; Peralta et al., 2015; Basso et al., 2016)., lime and gypsum management zones originate from yield maps, soil tests, ECa maps, and sometimes farmer's knowledge (Corwin, 2013)., seeding rate management zones come from past yields, spatially and temporally, or could be from topsoil information (Gunzenhauser and Shanahan, 2011; Holmes, 2017)., and at the end, irrigation scheduling management zones are based on soil topography, soil, yield and ECa data (Bellingham, 2009; Hedley et al., 2010; Duncan, 2012; Ayankojo et al., 2019; Neupane and Guo, 2019).

0.2.6. Soil Spatial Variability

Managing the spatial variability based on soil, biological or climatic factors is also considered the main premise in SSCM, supporting the soil-plant relationship, minimizing the variable crop inputs and harmful environmental impacts (Bullock and Bullock, 2000; Di Virgilio et al., 2007; Maestrini and Basso, 2018a). Corwin and Lesch (2003) explained that the soil ECa survey directed to soil sampling is considered a reliable method for assessing the characteristic of soils variability. Various soil properties such as soil texture, organic matter, CEC, ECa, trace elements, NPK, topography, and climatic factors have showed their influence on yield and its associated traits (Hanks and Ritchie, 1991; Tanjii, 1990). However, spatial variability of soil is influenced by pedogenetic (a process of soil formation) and anthropogenic (caused by human activities) factors (Corwin et al., 2003). As a result, ECa variability is not always showing the same spatial pattern as that of yield, due to the complex interaction of soil properties, measured by soil ECa data, with crop yield (Corwin and Lesch, 2003).

0.3. Reason of PhD Research

Uniform field management practices may result in over dosages of crop inputs such as seed, fertilizers, pesticides and irrigation water, in some field parts. Furthermore, lack of the knowledge of spatiotemporal variability at field scale

results in reduced economic yields in certain parts of the field, and detrimental effects on the environment due to over dosages of crop inputs. Hence, this scenario may result in increased production cost, limitations in the available agriculture resources, and depletion of soil and ground water resources (Khosla et al., 2002; De Caires et al., 2015). Therefore, it is very important to increase the production efficiency of agricultural crops, improving the food quality, sustaining the finite resources and minimizing the detrimental effects on the environment (Corwin, 2005; Schrijver et al., 2016; Lindblom et al., 2017). The PA practices help in managing the spatial and temporal variability of crop and soil variables to enhance crop production efficiency under the finite resources scenario, and limit the detrimental environmental impacts (Lindblom et al., 2017). Data retrieving, computational clouds and artificial intelligence techniques have been already introduced into precision agriculture. However, the implementation of PA faces the challenge in farming due to the diversity and size of agricultural lands. Anyhow, modern farming practices are improving agriculture to support the precision agricultural concept (Blackmore, 2000; Fraisse et al., 2001; Johnson et al., 2003; Li et al., 2008; Georgi et al., 2018; Maestrini and Basso, 2018a; Scudiero et al., 2018; Toscano et al., 2019). However, these practices are widely known in modern agriculture, but their level of implementation is still low.

To achieve PA goals, we used precision agriculture practices, such as RS and SSCM zones, using integration of advanced technologies for improving the agricultural productivity and sustainability with minimum economic resources and environmental impacts. Moreover, supervised and unsupervised learning techniques have been applied on a big dataset of agricultural crops and converted into useful knowledge. This PhD work has provided a sustainable solution to the inherent problems of agricultural industry through using the advanced technologies and state-of-art processing a big dataset.

0.4. Research Objectives

The key objectives of the PhD research were: 1). Training: i) to the use of multi-purpose GIS software's namely Quantum GIS and ArcGIS which are very important tools to learn in the wide spectrum of PA approaches. We selected these software's based on economic cost, powerful inter-operable platform, multi-purpose analysis tools such as handling of big dataset, interpolation, mapping, geostatistical/cluster analysis, etc., configured with user friendly templates, open source (QGIS), best alternative to open source (ArcGIS), most advanced tools in computer based GIS technology i.e. PA ii) retrieving of spatial dataset using open source platforms, i.e.

USGS-Earth Explorer and Sentinels hub; spatial data pre-processing of crops, soil, ECa survey and remotely sensed platform; iii) creation of thematic maps through geostatistic approach; iv) hands-on use of equipment for multi-purpose geospatial analysis such as operation and calibration of the Geonics dual-dipole EM-38 electromagnetic induction conductivity meter, coupling EM38 to GPS, conducting an EM-38 survey, use of GPS and model based response surface sampling technique (ESAP software). 2). Application of remote sensing to assess the spatial variability of crop yields during growing seasons, such as winter cereals (durum and bread wheat) and spring dicots (sunflower and coriander), using satellite vegetation indices. 3). Detection of the critical growth period of surveyed crops through remotely sensed data. 4). Application of geostatistics on georeferenced crop yield and remote sensing data to study the spatial dependence (SpD) between their data distribution in terms of semivariogram 5). Investigating the spatiotemporal characteristics of crops over multiple years. 6). A conceptual approach to delineate the spatial variability of soil properties. 7). Validating the spatiotemporal behavior of crops as a function of soil variability within yield stability classes. 8). Examining the meteorological data during the growing season of crops, which affect crop productivity over each specified year.

Chapter 1

Assessing Multiple Years' Spatial Variability of Crop Yields Using Satellite Vegetation Indices

Abstract

Assessing crop yield trends over years is a key step in site specific management, in view of improving the economic and environmental profile of agriculture. This study was conducted in a 11.07 ha area under Mediterranean climate in Northern Italy to evaluate the spatial variability and the relationships between six remotely sensed vegetation indices (VIs) and grain yield (GY) in five consecutive years. A total of 25 satellite (Landsat 5, 7 and 8) images were downloaded during crop growth to obtain the following VIs: Normalized Difference Vegetation Index (NDVI), Enhanced Vegetation Index (EVI), Soil Adjusted Vegetation Index (SAVI), Green Normalized Difference Vegetation Index (GNDVI), Green Chlorophyll Index (GCI), and Simple Ratio (SR). The surveyed crops were durum wheat in 2010, sunflower in 2011, bread wheat in 2012 and 2014, and coriander in 2013. Geo-referenced GY and VI data were used to generate spatial trend maps across the experimental field through geostatistical analysis. Crop stages featuring the best correlations between VIs and GY at the same spatial resolution (30 m) were acknowledged as the best periods for GY prediction. Based on this, 2-4 VIs were selected each year, totalling 15 VIs in the five years with r values with GY between 0.729** and 0.935**. SR and NDVI were most frequently chosen (six and four times, respectively) across stages from mid-vegetative to mid-reproductive growth. Conversely, SAVI never had correlations high enough to be selected. Correspondence analysis between remote VIs and GY based on quantile ranking in the 126 (30 m size) pixels exhibited a final agreement between 64% and 86%. Therefore, Landsat imagery with its spatial and temporal resolution proved a good potential for estimating final GY over different crops in a rotation, at a relatively small field scale.

1. Introduction

Investigation of problems associated with agricultural yield, before harvesting, most commonly involves observing in-season growth variations, scouting areas at different fertility, and defining optimum soil sampling design according to needs of individual field. All this helps to increase the agricultural

economic yield. However, current traditional methods for estimating the crop yield during the growing season may lead to poor yield assessment and inaccurate area appraisal. These methods rely on the precise and detailed collection of crop data, which is cost-intensive and time-consuming (Dadhwal and Ray, 2000; Reynolds et al., 2000). In addition, extensive use of nitrogen (N) fertilizers poses a problem of growing concern in agriculture. Surplus N drains into groundwater affecting the quality of drinking water, or seeps into superficial water bodies determining eutrophication (Rütting et al., 2018). This scenario makes it necessary to adopt efficient crop production methods assuring minimum environmental impact and concurrent optimization of crop yields (Tilman, 1999). Remote sensing has proved to be an efficient technology in precision agriculture for estimating crop status during the growing season. This, specifically, consists in evaluating the relationship between spectral vegetation indices during growth and final crop yield (Taylor et al., 1997; Gitelson, 2016).

Crop yield varies spatially and temporally within a single field (Blackmore, 2003; Griffin et al., 2004), which makes it important to assess the spatial pattern of grain yield (GY) over the entire field in view of specific management practices (Blackmore, 2003). GY variation within a field depends on intrinsic characteristics as soil type, physical-chemical and topographic properties, and external characteristics as amount of applied fertilizers, irrigation, etc. (Hanna et al., 1982; Steiner et al., 2018). Spatial maps of crop yield have been extensively used to interpret the causes of yield variation across the field (Amado et al., 2007).

Identifying growth stages of any crop is very important for timely crop management decisions that maximize the final crop profitability. There are many scales used to identify crop growth and development of cereals (wheat), oilseed (sunflower) and grain crops (coriander). Mostly used scales are Feekes scale, Haun scale, Zadoks scale and BBCH scale. In this research paper, we used BBCH scale, commonly used in Europe (Botarelli et al., 1999). This is two-digit decimal scale and consists of one hundred stages, each allowing the description of well-defined development level of primary stages (0-9) and secondary stages (00-99) of monocotyledonous as well as dicotyledonous crops (Meier, 2001).

The principal growth stages along with their BBCH code for wheat crop are as follows (Meier, 2001): 0. Germination (00-09), 1. Leaf development (10-19), 2. Tillering (20-29), 3. Stem elongation (30-39), 4. Booting (41-49), 5. Heading (51-59), 6. Flowering (61-69), 7. Grain development (71-77), 8. Ripening (83-89), 9. Senescence (92-99). For sunflower (Lancashire et al., 1991): 0. Germination (00-09), 1. Leaf development (10-19), 3. Stem elongation (30-39), 5. Inflorescence emergence (51-59), 6. Flowering (61-69), 7. Fruit development (71-79), 8. Ripening (80-89), 9. Senescence

(92-99). For coriander (forming heads) (Feller et al., 1995): 0. Germination (00-09), 1. Leaf development (10-19), 4. Development of harvestable plant parts (41-49), 5. Inflorescence emergence (51-59), 6. Flowering (60-69), 7. Fruit development (71-79), 8. Ripening (81-89), 9. Senescence (92-99).

However, many issues in the spatial and temporal relationship between crop yields and vegetation indices (VIs) obtained from remote sensing need to be investigated, depending on crop stage and the specific management practice. To capture the distinguishing characteristics of an agricultural crop, it is advisable to use more vegetation indices, as each VI has a unique combination of wavebands that can be related to specific crop parameters and growth stages (Hatfield and Prueger, 2010).

Remotely sensed data can cover a large area to retrieve the spectral information in real time during crop growing period (Sadrykia et al., 2017). Landsat missions have been collecting and archiving imagery worldwide with multispectral sensors providing insights into plant response to solar radiation, opening the era of remote vegetation indices (VIs). Specific VIs, obtained by combining single wavebands of a multispectral image, offer the farming community clues to crop growth status in time to predict higher/lower productions in specific areas (Taylor et al., 1997; Mirik et al., 2006). However, various VIs have been developed at canopy scale (Hatfield et al., 2008), which are more sensitive to canopy reflectance, compared to individual bands (Qi et al., 1993).

We have selected six among the many VIs available at present (Table 1.3), which are commonly addressed in the literature, and could be helpful in estimating changes at canopy level of agricultural crops, and ultimate yield. Normalized Difference Vegetation Index (NDVI) was first proposed by Rouse et al. (1974). It is defined as the ratio between the difference and the sum of reflectance values in the near-infrared (RNIR) and red (RRED) spectrum, which is indicative of the photosynthetically active vegetation (Slayback et al., 2003; Tucker et al., 2005). NDVI is widely used to estimate crop biomass at different growth stages. Many scientists claim that NDVI is the best estimator for light interception, although its values fluctuate during crop cycle (Hatfield et al., 1984; Wiegand et al., 1992). In cultivated soils NDVI ranges from zero (bare soil) to 1; values of 0.6-1.0 indicate dense vegetation at peak growth stages (Militino et al., 2017).

Beside NDVI, various VIs have been developed to address crop growth status through specific relationship with chlorophyll, carotenoids or biomass (Sims and Gamon, 2003). These VIs provide information on biotic and abiotic stresses affecting crop yields (Zarco-Tejada et al., 2005). More recent VIs have been developed to counterbalance NDVI limitations, e.g. the interference of soil reflectance with sparse

canopy cover, and the low sensitivity to chlorophyll content in mature canopies. These VIs demonstrated higher performances in specific applications to precision agriculture (Mulla, 2013).

Enhanced Vegetation Index (EVI) has been developed to improve the sensitivity of canopy reflectance under high biomass regions, as it gives a more linear correlation with green leaf biomass that is directly related to final GY (Boegh et al., 2002). In addition to red and NIR bands, EVI utilizes a blue band compared to NDVI, which enhances vegetation appraisal through de-coupling of canopy reflectance signal and reducing the atmospheric influence (Rocha and Shaver, 2009). EVI ranges from -1 to +1 (Huete et al., 2002).

Soil background effects may create problems in the reflectance of crop canopy, so to overcome these effects in the application of VIs a Soil Adjusted Vegetation Index (SAVI) has been proposed (Huete, 1988) for applications in total biomass and crop yield prediction (Elwadie et al., 2005; Simões et al., 2005; Panda et al., 2010). SAVI involves an adjustment factor (L) in the NDVI equation to remove the soil noise, whose value depends on vegetation density (L=1, 0.5 and 0.25 for low, intermediate and high vegetation density, respectively). SAVI ranges from -1 to +1. The Green Normalized Difference Vegetation Index (GNDVI) is designed as a modification of NDVI, where the red band is substituted with a green band (Gitelson et al., 1996), which might be more useful for assessing the green biomass variations at canopy scale. GNDVI ranges from -1 to +1.

The estimation of chlorophyll concentration at leaf canopy involves the Green Chlorophyll Index (GCI), which is directly related to leaf area index and final GY. It ranges from 0 to 6 (Gitelson et al., 2003).

Lastly, the Simple Ratio (SR), also known as ratio vegetation index (RVI) (Jordan, 1969), is used to eliminate albedo effects in the atmosphere, as it is calculated by band ratio of light scattered in the NIR to light absorbed in the red reflectance (R_{red}). Hence, SR is close to 1 if the object gets similar reflectance in both red and NIR bands. For a green object, the value ranges from 0 to infinity (Pearson and Miller, 1972). SR, which is the simplest VI, owns nonetheless a higher sensitivity to high biomass and LAI values, compared to NDVI (Viña et al., 2011).

Many studies have successfully addressed various issues through remote sensing: leaf nitrogen content (Daughtry et al., 2000; Mulla, 2013), leaf area index (Huete et al., 2002; Gitelson et al., 2005), chlorophyll content (Plant et al., 2000), total biomass (Jordan, 1969), and final crop yield (Plant et al., 2000). Landsat satellite data at 30 m resolution have already been used to successfully predict crop yields (Basso et al., 2004; Kayad et al., 2016). The strength of the relationships between VIs and crop yield is the fundamental premise to this. However, crop spectral reflectance

varies with species and depends on the concentration of leaf pigments, soil moisture, biomass structure and ratio of light absorption to transmittance, management practices, pest and disease outbreaks during crop growth (Van Leeuwen and Huete, 1996; Hatfield et al., 2008).

Geostatistics encompasses a series of techniques of crucial importance in the assessment of spatial variability with both ground based and remotely sensed data (Journel, 1989). Owing to the discrete assessment of several crop traits, geostatistics serves to adapt them to the same grid size in order to compare them. In spatial studies, variograms are used as main geostatistical tool in the process of kriging. Kriging is one of the commonest techniques to estimate the prediction values from neighbouring actual values, a process known as interpolation (Woodcock et al., 1988; Isaaks and Srivastava, 1989). Therefore, geostatistics was seen a valuable tool in the perspective of studying the relationship between remote VIs and ground based crop features, as GY in this work.

Given the ample variation in the spectral composition of VIs, their variable performance at different growth stages of crops, and the resulting uncertainty, this study was intended to explore a significant number of remotely available VIs over a five-year period in a field hosting winter cereals and spring dicots alternating annually. Our specific objectives were to: (i) assess the spatial variability of the surveyed crop yields over five years; (ii) compare the behaviour of the targeted VIs during the growing season of each crop, in view of predicting final yield; (iii) select the best VIs in the five crops as cases for the study of spatial and temporal variability, and relationship with final grain yield.

1.2. Materials and Methods

1.2.1. Experimental site

The field site was located in the plain near Ravenna, Italy (44° 29′ 26″ N, 12° 07′44″ E, 0 m above sea level), a few kilometres from the Adriatic coast (Figure 1.1). An 11.07 ha experimental area was chosen within a larger field (ca. 25 ha) of the Agrisfera Cooperative. Soils in this area have a variable texture depending on changes in sediment dispersal patterns in response to fluctuating sea level (Amorosi et al., 2002). To cope with the limited elevation and shallow water table, a network of underground draining pipes discharging into a ditch on the north side serves the field. The climate falls in the Mediterranean North environmental zone (Metzger et al., 2005), with mild winter and a long growing season, although precipitation is mostly concentrated in the cold semester.

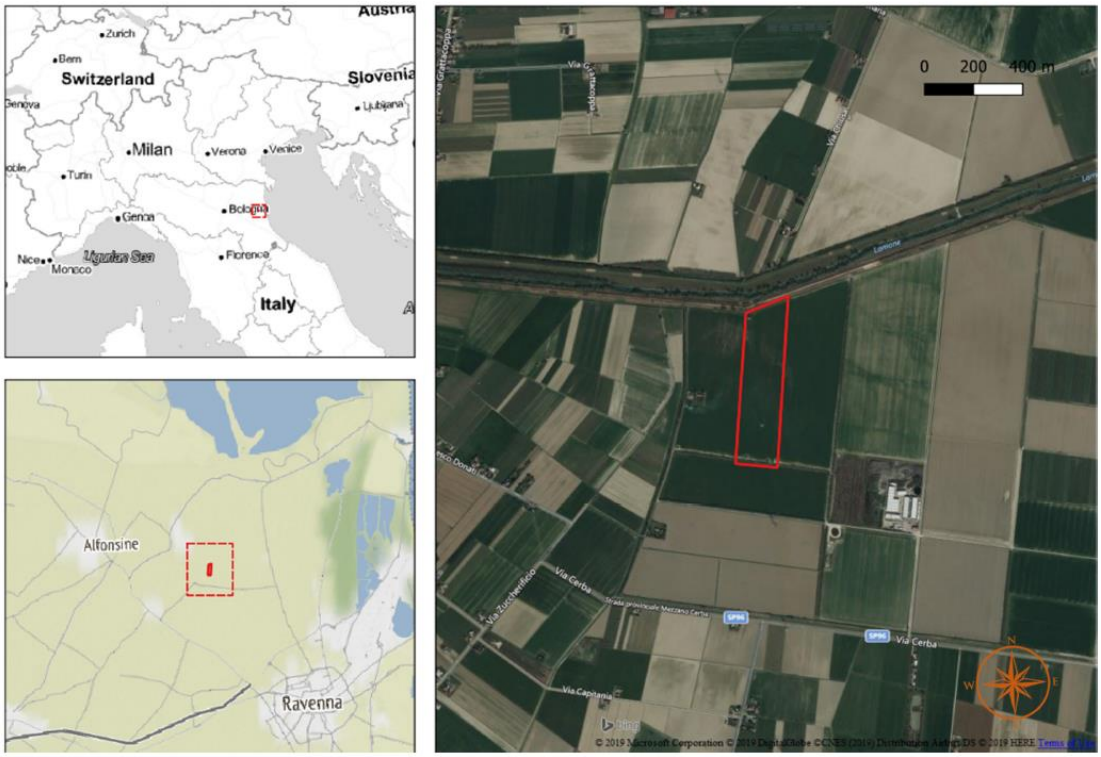

Figure 1.1. Study area location map. Detail framed by red trapezium, whose coordinates are: 44°29'35.05"N, 12° 7'41.86"E (NW corner); 44°29'37.33"N, 12° 7'50.05"E (NE corner); 44°29'14.71"N, 12° 7'46.31"E (SE corner); 44°29'15.52"N, 12° 7'38.81"E (SW corner).

1.2.2. *Field data collection*

Five crops were cultivated in a rotation system in the crop seasons 2010-2014: durum wheat in 2010 (DW 2010), sunflower in 2011 (SF 2011), bread wheat in 2012 (BW 2012), coriander in 2013 (CO 2013), and bread wheat in 2014 (BW 2014). Seeding and harvest dates, and the resulting crop cycle durations are reported in Table 1.1. Cultivation was based on the good practice for each specific crop, according to local conditions. Each year the field was ploughed in the summertime; harrowed in the autumn (the three years with DW or BW) or winter (SF and CO) for seedbed preparation.

At maturity, yield data were collected by a New Holland CR 9080 (CNH Industrial N.V., Basildon, UK) combine harvester using specific headers according to the crop (Figure 1.2). An average 6170 GY data points per year were registered in the 11.07 ha experimental area. Therefore, each GY pixel covered an average 18 m². The combine harvester was equipped with assisted guiding system based on real time kinematic GPS, yield mapping system consisting of a Pektron flow meter (Pektron Group Ltd, Derby, UK) and Ag Leader moisture sensor (Ag Leader Technology, Ames, IA, USA).

Figure 1.2. New Holland CR 9080

Spatial data of raw yield were saved through the Farm Works™ Mapping software (Figure 1.3) (Trimble Navigation Ltd., Sunnyvale, CA, USA), and exported to ESRI shape file format to be handled in QGIS 2.18.20. Yield data were filtered using Yield Editor Software to detect and remove outliers (Sudduth and Drummond, 2007), and adjusted at 13% moisture for DW and BW; at 9% moisture for SF and CO. The crop data of each year were intersected with polygon field boundary layer.

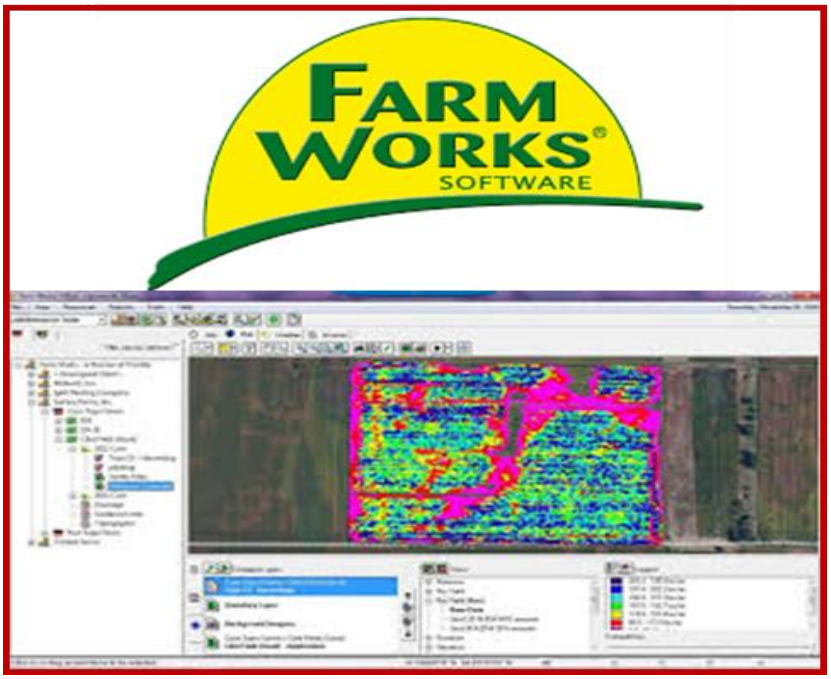

Figure 1.3. Software for yield data management by Trimble Navigation Ltd., Sunnyvale, California, USA

Table 1.1. Seeding and harvest dates, and crop cycle duration of cultivated crops.

Crop and Year	Botanical Name	Seeding	Harvest	Duration (d)
DW 2010	*Triticum turgidum* ssp. *durum* L.	30 October (2009)	10 July	253
SF 2011	*Helianthus annuus* L.	5 April	7 September	155
BW 2012	*Triticum aestivum* L.	14 October (2011)	1 July	261
C0 2013	*Coriandrum sativum* L.	11 April	10 July	90
BW 2014	*Triticum aestivum* L.	9 November (2013)	7 July	240

DW, durum wheat; SF, sunflower; BW, bread wheat; CO, coriander.

1.2.3. Imagery acquisition and processing

Remotely sensed data from Landsat missions were used, due to their frequency ensuring a dense time coverage in the investigated period. Landsat 5-Thematic Mapper (TM), Landsat 7-Enhanced Thematic Mapper Plus (ETM+) and Landsat 8-Operational Land Imager (OLI) have already been used in the monitoring of field crops over relatively small areas (6-11.5 ha) (Kumhálová et al., 2014; Rodriguez et al., 2014; Herbei and Sala, 2015).

Collected Landsat (LS) images covered the following growth periods: 1 February–30 June for DW 2010 and BW 2012 and 2014; 1 May-31 August for SF 2011; 1 May–15 July for CO 2013. Landsat remote imagery were downloaded through US Geological Survey (USGS)-Earth Explorer website, a largest remote data network, using Collection Level-1, Tier 1, Precision Terrain (LITP) platform. This is an inventory structure for data collection, containing the highest quality Level-1 data suitable for time-series data record. Moreover, it gives access to all data as originally acquired and has an average revisiting time of 16 days. Landsat data archive equipped with 30 m spatial resolution (SpR) was used for vegetation monitoring in the five years of the survey.

Table 1.2. Acquisition dates of Landsat satellite images and corresponding days after sowing (DAS) and growth stages (BBCH scale) in the five years.

Crop and Year	LS-Mission	Date	DAS	BBCH Stage	Description
DW 2010	LS-5 TM	13 March	134	31	Stem elongation (1st node visible)
		29 March	150	32	Stem elongation (2nd node visible)
		14 April	166	36	Stem elongation (6th node visible)
		30 April	182	43	Mid booting (flag leaf sheath initial swelling)
		7 May	189	55	Mid heading (half inflorescence emerged)
SF 2011	LS-5 TM	4 June	60	30	Beginning of stem elongation
		20 June	76	32	Two visibly extended internodes
		27 June	83	51	Inflorescence just visible amid young leaves
		22 July	108	67	Flowering decline (inner 3rd florets in bloom)
		14 August	131	75	Middle inflorescence seeds grey, at final size
BW 2012	LS-7 ETM+	17 March	155	33	Stem elongation (3rd node visible)
		26 March	164	36	Stem elongation (6th node visible)
		11 April	180	41	Early booting (flag leaf sheath extending)
		4 May	203	63	Flowering begun; anthers visible
		29 May	228	83	Early dough
CO 2013	LS-8 OLI	24 May	43	34	Main shoot reaching 30% of expected height
		9 June	59	55	First flowers of main inflorescence visible
		16 June	66	63	30% of flowers open
		25 June	75	71	First fruits formed
		2 July	82	81	Beginning of ripening (10% fruits ripe)
BW 2014	LS-8 OLI	8 March	119	32	Stem elongation (2nd node visible)
		31 March	142	37	Flag leaf just visible, still rolled
		25 April	167	55	Mid heading (half inflorescence emerged)
		18 May	190	77	Late milk
		3 June	206	85	Soft dough (grain content soft but dry)

DW, durum wheat; SF, sunflower; BW, bread wheat; CO, coriander; DAS, days after sowing.

Specifically, multispectral images were retrieved by selecting the most recent Landsat mission available for each investigated year: LS-5 (TM) was used for DW 2010 and SF 2011, LS-7 (ETM+) for BW 2012, and lastly LS-8 OLI for SF 2013 and BW 2014 (Table 1.2). Landsat satellite scenes selection was carried out by accurately evaluating clear sky conditions and the quality of pixels in the field, by using the available data and metadata for each Landsat product.

Raster spectral bands (DNs) were converted to surface reflectance values by using the Semi-Automatic Classification Plugin (Congedo, 2016) in QGIS by applying simple atmospheric correction under DOS1 method (Dark Object Subtraction 1) (Chaves, 1988; Lu et al., 2002). Although atmospheric correction for collection level-1 data is not univocally advised, it leads to an improvement in the results, and makes the surface reflectance comparable among multi-temporal images (Lu et al., 2002).

Corrected raster images were intersected with polygon field boundary (11.07 ha), resulting in 126 data points extracted from each remote imagery with 30 m SpR.

Crop stages at the respective dates were expressed with the BBCH scale that assigns a decimal code to the growth stages of mono- and di-cotyledonous plants (Lancashire et al., 1991). A total of 25 images were used, i.e., 5 dates × 5 years.

All VIs were calculated through the algebraic combinations of reflectance values of red, infra-red and green portions of the electro-magnetic spectrum (Basso et al., 2004), based on the formulas presented in Table 1.3.

Table 1.3. Vegetation indices used in this study, respective formulas and literary sources.

Index	Description	Formula	Source
NDVI	Normalized difference vegetation index	$(R_{NIR} - R_{Red})/(R_{NIR} + R_{Red})$	(Amado et al., 2007)
EVI	Enhanced vegetation index	$2.5(R_{NIR} - R_{red})/(R_{NIR} + 6R_{red} - 7.5R_{blue} + 1)$	(Militino et al., 2017)
SAVI	Soil adjusted vegetation index	$(R_{NIR} - R_{red})(1 + L)/(R_{NIR} + R_{red} + L)$	(Sims and Gamon, 2003)
GNDVI	Green normalized difference vegetation index	$(R_{NIR} - R_{green})/(R_{NIR} + R_{green})$	(Zarco-Tejada et al., 2005)
GCI	Green chlorophyll index	$(R_{NIR}/R_{green}) - 1$	(Mulla, 2013; Panda et al., 2010)
SR	Simple ratio	R_{NIR} / R_{red}	(Boegh et al., 2002)

R_{NIR}, reflectance in the near infrared band: R_{red}, reflectance in the red band: R_{blue}, reflectance in the blue band: R_{green}, reflectance in the green band: L, weighting coefficient = 0.25 (high vegetation density).

1.2.4. Analysis methods

Georeferenced GY and remote VI data were subjected to geostatistical analysis (ArcGIS software version 10.3) to study the degree of spatial dependence (DSpD) in data distribution. The spatial dependence (SpD) was calculated by means of empirical semivariogram, according to the following equation:

$$\gamma(h) = \frac{1}{2N(h)} X \sum_{i=1}^{N(h)} [Z(x_i) - Z(x_i + h)]^2 \quad (1)$$

Where, $\gamma(h)$ is the semi-variance at a specified distance, h represents lag distance between two paired points, $N(h)$ is the number of paired points at distance h, $Z(x_i)$ is the measured value at location x_i, and $Z(x_i + h)$ denotes the secondary value measured at locations $x_i + h$ separated by the given distance (h) (Goovaerts, 1997).

The experimental variogram was fitted by means of the spherical, exponential, linear and Gaussian models. The spherical model exhibited a goodness of fit that was not surpassed by the other models and was, therefore, chosen. The spherical model, thanks to a well-defined sill, easily-interpreted range and

mathematical simplicity, is considered one of the best models for soil or plant variability fitting (Clark, 1979; Woodcock et al., 1988; Isaaks and Srivastava, 1989; Maynou, 1998; Guedes Filho et al., 2010).

Directional sample variograms were also computed for the canonical directions 0, 22.5, 45, 90, 135 degrees. Resulting variograms exhibited similar shapes, leading to the conclusion that directional effects were negligible/absent. Therefore, there was no evidence of spatial anisotropy potentially leading to wrong interpretation in data analysis.

In the spherical model, the following equations are applied:

$$\gamma(h) = 0 \qquad \text{for} < h = 0 \tag{2}$$

$$\gamma(h) = C_0 + C\left(\frac{3h}{2a} - \frac{h^3}{2a^3}\right) \qquad \text{for } 0 < h \leq a \tag{3}$$

$$\gamma(h) = C_0 + C \qquad \text{for } h > a \tag{4}$$

Where: C_0 is the nugget, C_0+C is the sill, a is the range, and h is the separation lag distance (Isaaks and Srivastava, 1989).

Three parameters need to be defined while fitting the theoretical model to the experimental semivariogram: (i) nugget effect (C_0), representing the error or variation in the measurement at minimum sampling distance (h=0), i.e. the background effect; (ii) sill variance ($C_0 + C$), composed of C_0 (nugget variance) and C (structural variance), which is the maximum y-axis value increase with lag distance, and remains constant beyond distance h; (iii) SpD range (a), indicating the maximum limit at which data points are still spatially correlated and the semi-variogram reaches the sill value; beyond that limit no spatial auto-correlation can be demonstrated.

We classified the strength of SpD into three groups by calculating the percent nugget (C_0) to sill (C_0+C) ratio according to Cambardella et al. (1994): (i) < 25 %, indicating strong SD; (ii) 25-75 %, moderate SD; (iii) >75 %, weak SD.

Through semivariograms, spatial yield maps were produced by simple kriging with 10 m cell size to extrapolate the values to non-sampled field parts (Moral et al., 2010). Simple kriging was preferred over ordinary kriging because the mean value was known, which is the premise for a better estimate of the variance. Simple kriging is considered a realistic interpolation method: it provided highest R^2 and minimal error parameters among seven methods in environmental characteristics (Maynou, 1998; Xiao et al., 2016), and in the estimation of crop yield (Mckinion et al., 2010).

GY data referred to 1106 pixels (10 m cell size), and VI data referred to 126 pixels (30 m cell size) acquired in the 11.07 ha experimental field were submitted to

descriptive statistics including mean, median, minimum, maximum, standard deviation (SD) and coefficient of variation (CV). Kolmogorov-Smirnov test was applied to ascertain the normal distribution in the data sets.

Kriged maps of crop yield were aggregated at the same 30 m cell size as the SpR of satellite imagery (Kayad et al., 2016). Then, raster maps were converted into point data to assess the relationships between remote imagery and crop yields, i.e. between VIs and GY in each respective year, by means of Pearson's correlation (Shanahan et al., 2001). The best times/crop stages for the prediction of final yields were acknowledged as those featuring the highest correlations for all the indices averaged (Brian McConkey et al., 2004; Singla et al., 2018). The vegetation index showing the highest correlation with yield was selected from each date falling within these stages in each crop. When two VIs exhibited the same *r* value, both were selected. Based on this, a series of representative VIs were retained as study cases for each year, and further processed.

Geostatistics (ArcGIS software version 10.3) was applied on GY and selected VIs, in order to describe the data distribution of remote VIs and GY data in terms of semivariogram through the above described spherical model. The intrinsic variation in these two sets of variables was assessed based on their SpD across the field. Geostatistics also served in the analysis between original VI data and kriged GY data for the determination of correspondence levels and final agreement between them.

Spatial maps of remote VIs and GY were shown with the same 30 m cell size (Moral et al., 2010). A colour scale was chosen based on quantile classification for all maps produced in this study. All maps were georeferenced and co-registered in reference system of WGS 84/UTM zone 32N-EPSG: 32632.

The prediction accuracy of VI and GY data was assessed with the spherical model in terms of coefficient of determination (R^2) of model-predicted vs. actual observations (Robertson, 1998; Leopold et al., 2006), while mean absolute error (MAE) and root mean square error (RMSE) were calculated through kriged residuals (Pebesma, 2004). The mean relative error (MRE) and relative RMSE (RRMSE) were calculated as percent ratios on the average VIs and GY values, respectively. Maximum R^2 and minimal error parameters are associated with best model accuracy (Xiao et al., 2016).

After analysing the SpD within VIs and GY data, we investigated the correspondence between them. The correspondence levels were calculated as the proportion of pixels belonging to same remote imagery and crop yield class. To represent the relative similarity between them, remote imagery and crop yield data were classified from lowest to highest values into five classes (i.e., quintiles) of equal frequency over the entire field. Then, the correspondence levels and final agreement

(%) between each VI and GY were determined as described by Stępień et al. (2016): for a given pixel, if the class of VI quantile was the same as that of GY quantile, the correspondence was considered 'high' with value 1; if the class of VI and GY belonged to adjacent quantiles, the correspondence was considered 'medium' with value 0.5; if the class of VI and GY quantile were separated by more than one class, the correspondence was considered 'low' with value 0. Based on this, final agreement was calculated as the sum of pixel agreement scores, according to the formula:

$$F_a = \frac{(P_h \cdot 1.0) + (P_m \cdot 0.5) + (P_l \cdot 0)}{P_t \cdot 100} \quad (5)$$

Where: F_a = final agreement (%); P_h = number of pixels with high agreement; P_m = number of pixels with medium agreement; P_l = number of pixels with low agreement; P_t = total number of pixels

The coefficient of variation of F_a was also calculated as the standard deviation of correspondence levels in percent of their mean.

1.3. Results

1.3.1. Descriptive statistics of crop yields

Descriptive statistics of crop yields in the five years is reported in Table 1.4. In wheat, mean GY ranged between 4.26 and 5.91 t ha^{-1}. The lower GY was referred to DW 2010 and BW 2012 that showed the same mean data, whereas the higher GY was related to BW 2014. The two dicots (SF 2011 and CO 2013) were comparatively much less productive, attaining less than 2 t ha^{-1} mean GY. An ample variation in yield data was described by all crops, resulting in a standard deviation that, proportioned to GY, determined a CV value ranging between 23.2% (DW 2010) and 31.7% (CO 2013).

Table 1.4. Descriptive statistics of crop yields (t ha^{-1}) in the five years.

Crop and year	Mean	Median	Min.	Max.	SD	CV %	K-S
DW 2010	4.26	4.26	1.77	6.05	0.99	23.2	**
SF 2011	1.45	1.44	0.23	2.99	0.41	28.6	**
BW 2012	4.26	4.27	1.68	6.07	0.99	23.3	**
CO 2013	1.83	1.90	0.71	2.86	0.58	31.7	**
BW 2014	5.91	5.81	2.50	9.08	1.66	28.2	**

DW, durum wheat; SF, sunflower; BW, bread wheat; CO, coriander; Min., minimum; Max., maximum; SD, standard deviation: CV, coefficient of variation: K-S, Kolmogorov-Smirnov test for normal distribution; **, significant at $P \leq 0.01$.

1.3.2. Descriptive statistics of remote indices

The five years' remote indices are described in table 1.5. The complete descriptive statistics of each year's data are provided in the supplementary materials at the end of the thesis (Table S1.1. for DW 2010, Table S1.2 for SF 2011, Table S1.3 for BW 2012, Table S1.4. for CO 2013, and Table S1.5 for BW 2014).

Table 1.5. Mean value of remote vegetation indices, and Pearson's correlations (r) with crop yields in the five years. VIs with best correlations with GY are highlighted.

Crop and year	BBCH stage	NDVI		EVI		SAVI		GNDVI		GCI		SR	
		mean	***r***	**mean**	***r***	**mean**	***r***	**mean**	***r***	**mean**	***r***	**mean**	***r***
DW 2010	31	0.29	0.843**	0.31	0.755**	0.17	0.764**	0.21	0.767**	0.53	0.764**	1.72	0.762**
	32	0.29	0.814**	0.33	0.795**	0.19	0.783**	0.23	0.778**	0.60	0.774**	1.72	0.788**
	36	**0.59**	**0.878****	0.49	0.816**	0.30	0.818**	0.39	0.822**	1.33	0.816**	2.93	0.816**
	43	**0.71**	**0.878****	0.66	0.819**	0.40	0.822**	0.49	0.826**	2.06	0.823**	4.14	0.825**
	55	0.66	0.294**	0.73	0.444**	0.44	0.454**	0.51	0.400**	2.10	0.431**	4.01	0.405**
SF 2011	30	0.47	0.395**	0.51	0.509**	0.32	0.475**	0.37	0.429**	1.19	0.446**	2.42	0.536**
	32	0.66	0.614**	0.90	0.707**	0.52	0.700**	0.53	0.688**	2.33	0.687**	4.17	0.684**
	51	0.70	0.736**	0.76	0.745**	0.49	0.749**	**0.55**	**0.751****	2.49	0.748**	4.53	0.742**
	67	0.52	0.672**	0.54	0.725**	0.34	0.716**	0.40	0.712**	1.39	0.718**	**2.81**	**0.729****
	75	0.28	0.317**	0.24	0.375**	0.16	0.351**	0.22	0.341**	0.57	0.320**	1.62	0.459**
BW 2012	33	0.47	0.793**	**0.45**	**0.801****	0.25	0.788**	0.33	0.767**	1.00	0.766**	**2.28**	**0.801****
	36	0.54	0.710**	**0.34**	**0.854****	0.18	0.852**	0.14	0.838**	0.60	0.852**	**1.89**	**0.854****
	41	0.52	0.783**	0.30	0.773**	0.10	0.742**	-0.73	0.698**	0.21	0.639**	1.21	0.631**
	63	0.80	0.870**	0.11	0.611**	0.45	0.586**	0.53	0.519**	2.61	0.717**	4.87	0.760**
	83	0.51	0.307**	0.54	-0.273ns	0.28	-0.317ns	0.32	-0.332ns	1.05	-0.324ns	2.33	-0.294ns
CO 2013	34	0.08	0.555**	0.27	0.268**	0.08	0.377**	0.11	0.213**	0.24	0.214**	1.17	0.555**
	55	0.33	0.800**	0.43	0.480**	0.28	0.805**	0.37	0.793**	1.16	0.806**	2.01	0.812**
	63	0.62	0.856**	**0.59**	**0.920****	0.43	0.917**	0.60	0.907**	3.06	0.911**	3.34	0.915**
	71	**0.68**	**0.902****	0.64	0.861**	0.53	0.861**	0.67	0.861**	4.19	0.866**	5.86	0.868**
	81	0.65	0.914**	0.63	0.886**	0.45	0.879**	0.62	0.912**	3.36	0.927**	**4.52**	**0.932****
BW 2014	32	0.69	0.886**	0.45	0.844**	0.41	0.844**	0.60	0.849**	3.11	0.843**	5.05	0.845**
	37	0.79	0.932**	0.59	0.922**	0.61	0.925**	0.59	0.930**	2.97	0.925**	**7.49**	**0.935****
	55	**0.84**	**0.926****	0.78	0.873**	0.57	0.870**	0.72	0.879**	5.13	0.881**	6.26	0.873**
	77	0.81	0.909**	0.59	0.927**	0.49	0.925**	0.65	0.918**	**3.85**	**0.934****	**4.78**	**0.934****
	85	0.40	-0.681ns	0.38	0.562**	0.28	0.167ns	0.40	-0.482ns	1.43	-0.404ns	2.43	-0.540ns

DW, durum wheat; SF, sunflower; BW, bread wheat; CO, coriander; ns, non-significant; **, significant at $P \leq 0.01$.

In DW 2010, the six VIs in the five growth stages ranging from beginning of stem elongation to heading (Table 1.2) outlined the mean values reported in Table 1.5. Mean values augmented until a peak at BBCH stage 43-55. Mean and median values were always very close, never diverging by more than 5%. VI variation was more contained than GY variation in the same year (Table 1.4): average CV was 12.3%, and highest CV reached 23.9%. Lastly, data were more often normally distributed (non-significant Kolmogorov-Smirnov test in 23 cases out of 30).

In SF 2011, the six VIs in the five growth stages ranging from beginning of stem elongation to seed ripening (Table 1.2) exhibited the mean values reported in Table 1.5. Mean values increased until a peak at approximately BBCH stage 51 (inflorescence just visible), although EVI staged higher value at BBCH stage 30. Mean and median values never diverged by more than 6%. VI variation was more contained than GY variation in the same year (Table 1.4): average CV was 11.2%, and highest CV was 20.5%. Data were almost equally divided between normally distributed (17 cases out of 30) and non-normally distributed (the remaining 13 cases).

In BW 2012, the six VIs in the five growth stages ranging from mid-stem elongation to early dough ripening (Table 1.2) staged the mean values reported in Table 1.5. Mean values increased until a peak at BBCH stage 63 (anthesis), except EVI that showed a very low value at this stage and peaked at BBCH stage 83 (early dough). Mean and median values sometimes diverged, especially at BBCH stage 41. Data variation was also fluctuating: average CV was 31.9%, but CV values above 100% were also recorded. Lastly, data were normally distributed only in 2 cases out of 30.

In CO 2013, the six VIs in the five growth stages ranging from mid-stem elongation to beginning of ripening (Table 1.2) showed the mean values reported in Table 1.5. Mean values increased until BBCH stage 71 (fruiting). Mean and median values never diverged by more than 4%. VI variation was more contained than GY variation in the same year (Table 1.4): average CV was 9.4%, and highest CV was 22.5%. Despite this, data were normally distributed only in 5 cases out of 30.

In BW 2014, the six VIs in the five growth stages ranging from early stem elongation to soft dough ripening (Table 1.2) featured the mean values reported in Table 1.5. Mean values increased until BBCH stage 55 (heading). Mean and median values were generally similar; only in three cases they diverged by 10-13%. VI variation was more contained than GY variation in the same year (Table 1.4): average CV was 13.2%, and highest CV was 30.2%. Nonetheless, data were normally distributed only in 3 cases out of 30.

1.3.3. Correlations and choice of representative vegetation indices

In this experiment, Pearson's correlations between VIs and GY in the five years are reported in Table 1.5. High, statistically significant *r* values were generally obtained, indicating that remote indices across variable growth stages were aligned with final yields. We visually checked all correlations (graphs not reported in MS) to spot if any cloud of data outlined a curvilinear relation, finding none.

At growth stages of incipient senescence (BBCH>80), VIs were insignificantly/negatively correlated with GY (BW 2012 and 2014), because senescence encourages the breakdown of pigments that influence the reflectance properties of leaf canopy.

Overall, the three wheat crops (DW 2010, BW 2012 and 2014) staged *r* values above 0.700 in the average of the six VIs at BBCH stages not exceeding 50, i.e. before heading (Table 1.5). Afterwards, the *r* values sharply declined in DW 2010 (at BBCH 55, average *r* = 0.405), whereas in BW 2012 and 2014 they remained quite high until the mid-60's and mid-70's BBCH stages, respectively. Owing to the morph-physiological similarity between durum and bread wheat, it is sensed that the different behaviour was due to different ambient conditions during the reproductive phase in 2010 vs. 2012 and 2014.

In contrast to wheat, the two dicot species (SF 2011 and CO 2013) staged *r* values above 0.700 in the average of the six VIs at BBCH stages > 50, i.e. during the reproductive phase (Table 1.5). SF 2011 maintained *r* values above 0.700 until the mid-reproductive phase (BBCH 67), whereas CO 2013 remained well above this threshold until later stages (BBCH 81).

Based on the procedure described in sub-section 2.4, the 2-4 VIs with best correlations with GY (highlighted in Table 1.5) were selected each year as representative study cases. They covered growth stages from BBCH 33 to BBCH 81. SR and NDVI were the two indices most frequently chosen: six and four times, respectively. At the opposite end, SAVI never exhibited correlations high enough to be included in the list.

1.3.4. Spatial variability in crop yields

Analysis of the spherical semivariogram fitted to GY data is reported in Table 1.6. The lag distance was between 6.79 and 9.97 m, (data omitted in Table 1.6), depending on a particular crop of the year. SF 2011 was the crop showing the strongest background effect (C_0) on total (C_0+C) variance, associated with a high CV (Table 1.4). Compared to this, the very low C_0 weight on C_0+C indicates almost no discontinuity in the other four crops' spatial structure. The five crops exhibited a sill comprised between 0.92 (DW 2010 and BW 2012) and 1.09 (CO 2013), meaning a quite similar total variance. However, the

range of the SpD varied amply, being comprised between 65.90 m (BW 2012) and 99.87 m (CO 2013). Finally, the proportion between the two components, nugget to sill variance, varied considerably between SF 2011 where C_0 represented 34% of C_0+C, and the other four crops where C_0 represented 0-2% of C_0+C. As a result, SF 2011 can be considered a case of moderate SpD, whereas the other four crops featured strong SpD (Cambardella et al., 1994).

Table 1.6. Parameters of the spherical model used to fit the experimental semivariograms of crop yields, and model performance in the five years.

Crop and year	C_0	C_0+C	a (m)	SpD	R^2	MAE	RME (%)	RMSE	RRMSE (%)
DW 2010	0	0.92	66.96	S	0.98**	0.09	2.2	0.14	3.3
SF 2011	0.35	1.02	73.59	M	0.71**	0.15	10.6	0.22	15.5
BW 2012	0	0.92	65.90	S	0.98**	0.09	2.2	0.14	3.3
CO 2013	0.02	1.09	99.87	S	0.99**	0.05	2.6	0.07	3.6
BW 2014	0.007	1.08	85.89	S	0.99**	0.13	2.2	0.18	3.1

DW, durum wheat; SF, sunflower; BW, bread wheat; CO, coriander; C_0, nugget effect; C, structural variance; C_0+C, sill variance; a, range; SpD, spatial dependence (S, strong; M, moderate); **, significant at $P \leq 0.01$; MAE, mean absolute error; MRE, mean relative error; RMSE, root mean square error; RRMSE, relative root mean square error.

The performance of the spherical model in the 5 years was generally good (Table 1.6). R^2 was always highly significant, ranging between 0.71 and 0.99, while the two error terms (MAE and RMSE) were low. This is especially true with respect to GY means (Table 1.4), resulting in relative error terms (MRE and RRMSE) that were between 2.2% and 10.6% (MRE), and between 3.1% and 15.5% (RRMSE).

Yield maps exhibited a quite similar pattern in the five years, as shown in Figure 1.2. The north side of the field always featured a lower GY than the south side. Especially the three years with wheat (DW 2010, BW 2012 and 2014) behaved in a similar way with lowest yield rank in the north-central portion of the field, and highest yield rank in the south – southwestern portion. Compared to this, the two spring sown crops (SF 2011 and CO 2013) exhibited a slightly wider area of low GY in the north portion of the field. These two crops also featured higher CV's (Table 1.4), i.e. higher yield variation than the three wheat crops.

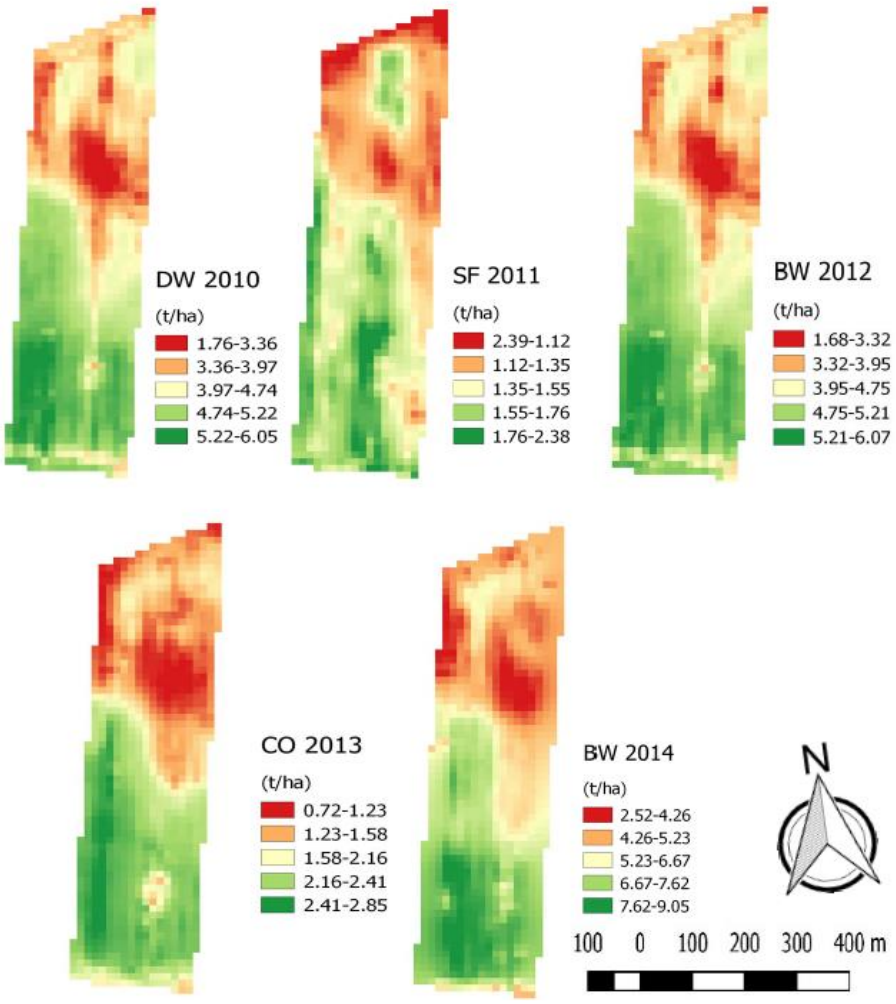

Figure 1.2. Spatial variability maps of crop yields in the five years with 10 m cell size (1106 pixels in the 11.07 ha field).

1.3.5. *Spatial variability in remote vegetation indices*

Analysis of the spherical semivariogram fitted to VI data is reported in Table 1.7. The lag distance was between 8.17 and 15.30 m (data omitted in Table 1.7), depending on specific VI, crop and stage. The nugget (C_0) was always nil, indicating continuous SpD of data over distance (Journel, 1989). The sill (C_0+C) was comprised between 1.18 (NDVI in BW 2014 at BBCH stage 55) and 1.42 (GNDVI in SF 2011 at BBCH stage 51). The range was comprised between 108.84 m (EVI in BW 2012 at BBCH stage 36) and 154.25 (NDVI and SR in CO 2013 at the respective BBCH stage 71 and 81). Finally, owing to nil nugget effect, the SpD was always strong, i.e. 100% of the sill was associated with the structural component (C).

The performance of the spherical model in the 15 cases was good under all viewpoints (Table 1.7). R^2 was always ≥0.95, and the two error terms (MAE and RMSE)

were low, especially with respect to mean VI values (Table 1.5). In fact, the relative error terms (MRE and RRMSE) were comprised between 0.6% and 5.6% of the mean.

In Figure 1.3, remote VI maps and the respective GY maps are depicted at the same cell size (30 m). A palette of five colours indicates values ranging from very low (red) to very high (dark green), passing through low (orange), medium (yellow) and high (light green). The 15 VIs, whose choice was based on their correlations with yield (Table 1.5), also from a spatial viewpoint described a pattern across the study area consistent with crop yield pattern: lower values in the north portion of the field, and conversely higher values in the south – southwestern portion.

Some VIs at specific growth stages evidenced sharp differences between the two areas, as in the case of EVI and SR at BBCH 36 in BW 2012. Some other VIs depicted faded differences, as SR at BBCH 67 in SF 2011. However, spatial maps visually demonstrate that a small number of high remote VIs were associated with low final GY, and vice versa.

Table 1.7. Parameters of the spherical model used to fit the experimental semivariograms of remote vegetation indices, and model performance in the five years.

Crop and Year	BBCH Stage	C_0	C_0+C	a (m)	SpD	R^2	MAE	RME (%)	RMSE	RRMSE (%)
						NDVI				
DW 2010	36	0	1.32	142.50	S	0.99**	0.006	1.0	0.009	1.5
	43	0	1.23	142.50	S	0.99**	0.007	1.0	0.010	1.4
						GNDVI				
SF 2011	51	0	1.42	149.43	S	0.99**	0.004	0.7	0.005	0.9
						SR				
	67	0	1.27	115.97	S	0.98**	0.050	1.8	0.070	2.5
						EVI				
	33	0	1.29	149.43	S	0.99**	0.006	1.2	0.007	1.6
BW 2012	36	0	1.23	108.84	S	0.99**	0.011	3.2	0.019	5.6
						SR				
	33	0	1.25	147.08	S	0.99**	0.016	0.7	0.020	0.9
	36	0	1.28	115.05	S	0.99**	0.037	2.0	0.060	3.2
						EVI				
	63	0	1.38	149.43	S	0.99**	0.005	0.8	0.007	1.2
CO 2013						NDVI				
	71	0	1.31	154.25	S	0.98**	0.006	1.0	0.010	1.5
						SR				
	81	0	1.35	154.25	S	0.99**	0.038	0.8	0.060	0.8
						SR				
	37	0	1.25	134.67	S	0.99**	0.069	0.9	0.14	1.9
						NDVI				
BW 2014	55	0	1.18	113.91	S	0.95**	0.004	0.5	0.005	0.6
						GCI				
	77	0	1.32	149.43	S	0.99**	0.025	0.6	0.050	1.3
						SR				
	77	0	1.32	149.43	S	0.99**	0.030	0.6	0.060	1.3

DW, durum wheat; SF, sunflower; BW, bread wheat; CO, coriander; C_0, nugget effect; C, structural variance; C_0+C, sill variance; a, range; SpD, spatial dependence (S, strong) **, significant at $P \leq 0.01$; MAE, mean absolute error; MRE, mean relative error; RMSE, root mean square error; RRMSE, relative root mean square error.

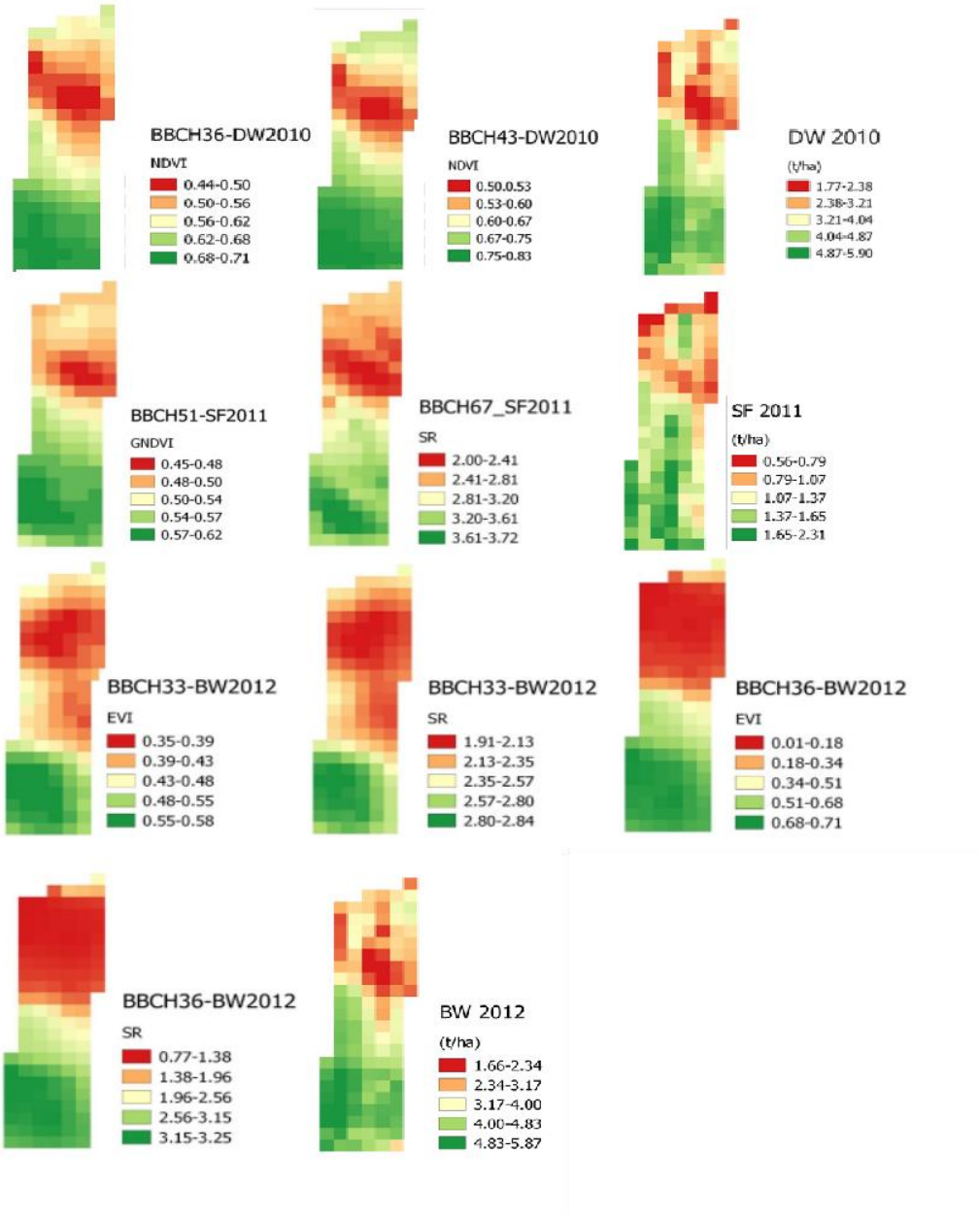
BBCH36-DW2010
NDVI
0.44-0.50
0.50-0.56
0.56-0.62
0.62-0.68
0.68-0.71
BBCH43-DW2010
NDVI
0.50-0.53
0.53-0.60
0.60-0.67
0.67-0.75
0.75-0.83
DW 2010
(t/ha)
1.77-2.38
2.38-3.21
3.21-4.04
4.04-4.87
4.87-5.90
BBCH51-SF2011
GNDVI
0.45-0.48
0.48-0.50
0.50-0.54
0.54-0.57
0.57-0.62
BBCH67_SF2011
SR
2.00-2.41
2.41-2.81
2.81-3.20
3.20-3.61
3.61-3.72
SF 2011
(t/ha)
0.56-0.79
0.79-1.07
1.07-1.37
1.37-1.65
1.65-2.31
BBCH33-BW2012
EVI
0.35-0.39
0.39-0.43
0.43-0.48
0.48-0.55
0.55-0.58
BBCH33-BW2012
SR
1.91-2.13
2.13-2.35
2.35-2.57
2.57-2.80
2.80-2.84
BBCH36-BW2012
EVI
0.01-0.18
0.18-0.34
0.34-0.51
0.51-0.68
0.68-0.71
BBCH36-BW2012
SR
0.77-1.38
1.38-1.96
1.96-2.56
2.56-3.15
3.15-3.25
BW 2012
(t/ha)
1.66-2.34
2.34-3.17
3.17-4.00
4.00-4.83
4.83-5.87

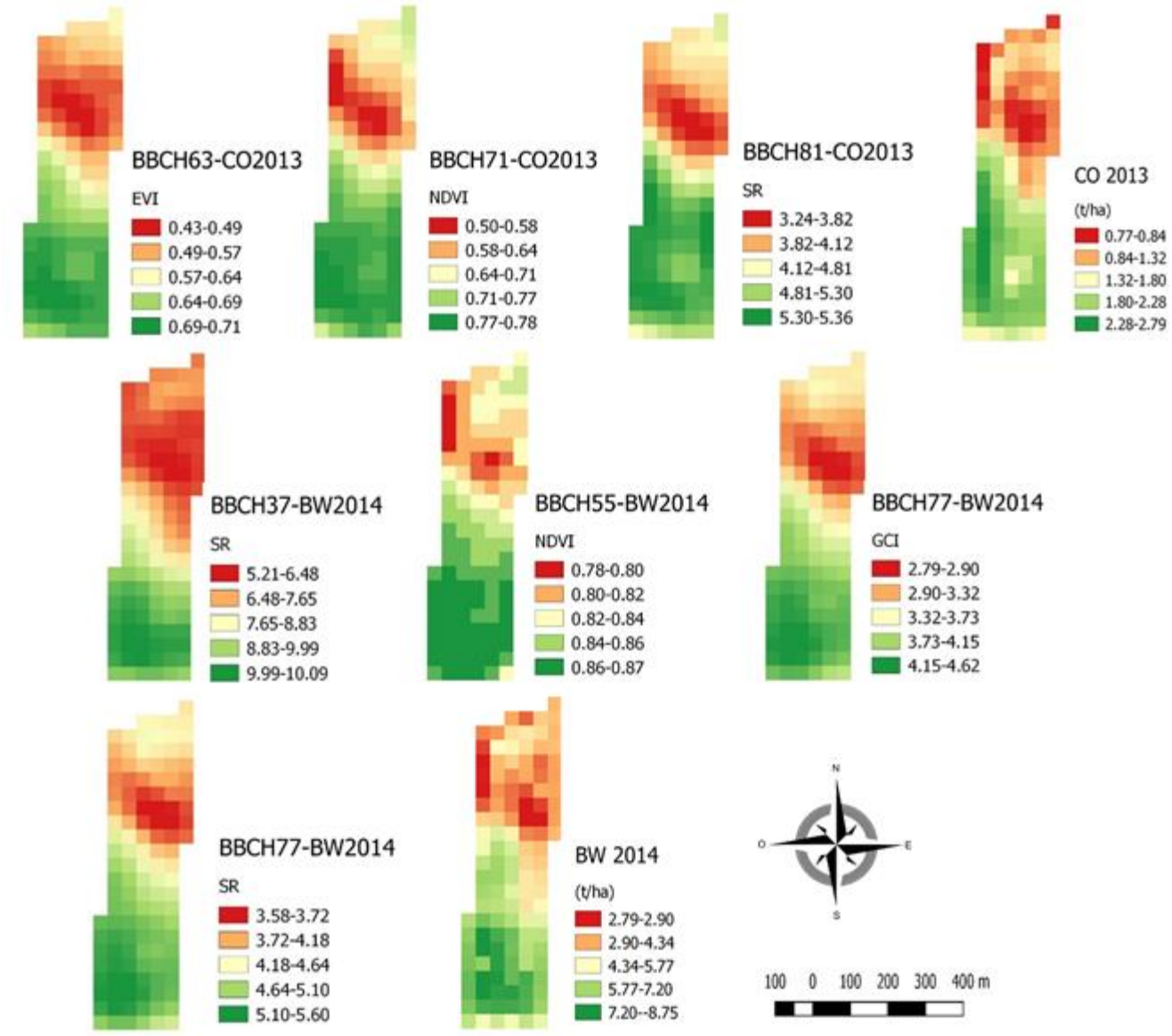

Figure 1.3. Spatial variability maps of remote VIs and crop yields with 30 m cell size.

1.3.6. Correspondence between remote vegetation indices and crop yields

The apparent similarity in spatial pattern and geostatistical structure between VIs and GY is the premise for assessing the correspondence between remote indices and crop yields at the same pixel level (Table 1.8). In the 15 cases, high correspondence ranged between 42% and 72%, medium correspondence between 27% and 50%, and low correspondence between 1% and 16%. The resulting F_a ranged between 64% and 86%. Highest agreement was observed in BW 2014 (average of 4 VIs, 83%); lowest in SF 2011 (average of two VIs, 65%).

Table 1.8. R^2, correspondence levels, final agreements and respective coefficients of variation between VIs and GY.

Crop and year	BBCH stage	R^2	Correspondence level (%)			F_a (%)	CV (%)
			high	medium	low		
				NDVI			
DW 2010	36	0.77**	53	41	6	73	41.9
	43	0.77**	51	42	7	72	43.6
				GNDVI			
SF 2011	51	0.56**	42	47	11	65	50.6
				SR			
	67	0.53**	44	40	16	64	56.4
				EVI			
	33	0.49**	40	50	10	65	49.9
BW 2012	36	0.73**	49	41	10	70	47.1
				SR			
	33	0.64**	43	48	9	67	47.3
	36	0.73**	48	43	9	70	46.2
				EVI			
	63	0.85**	53	43	4	75	38.6
CO 2013				NDVI			
	71	0.81**	58	36	6	76	39.6
				SR			
	81	0.87**	71	26	3	84	31.9
				SR			
	37	0.87**	70	30	0	85	27.1
				NDVI			
BW 2014	55	0.86**	59	38	3	78	36.0
				GCI			
	77	0.87**	67	30	3	83	31.9
				SR			
	77	0.87**	72	27	1	86	27.5

DW, durum wheat; SF, sunflower; BW, bread wheat; CO, coriander; F_a, final agreement; CV., coefficient of variation; **, significant at $P \leq 0.01$ (n=126).

1.4. Discussion

The CV data related to mean GY in the five years (Table 1.4) denote high yield variation, based on a CV threshold of 20% indicating high variation in field attributes (Gomes, 1985). This was a favourable circumstance in the present study, allowing us to appraise crop behaviour under conditions of sizeable spatial variability. Despite high CV, median GY in the five years was quite close to mean GY, differing from this latter by no more than ±4%. However, in all five years GY data were not normally distributed

(significant Kolmogorov-Smirnov test), although normality is not a prerequisite for kriging interpolation (Goovaerts, 1997).

In general, crop yield variation reflects the interactions among soil-related factors or topography (Kravchenko and Bullock, 2000). Moreover, variation within the same plant genus (e.g., wheat) may be due to several factors as growth response to the amount of rainfall during specific crop stages, owing to the fact that wet years favour biomass accumulation thanks to higher soil water availability (Guedes Filho et al., 2010).
The similar spatial patter exhibited by yield maps across the five years (Figure 1.2) is echoed in a previous survey on a narrower portion (4.15 ha) of the same field (Barbanti et al., 2018). In that work, soils in the northern part were shown to be quite sandy and poor in organic matter. It is evinced, therefore, that under rainfed cultivation the two spring crops (SF and CO) may have suffered stronger drought during the reproductive stage in the summer time, compared to the three wheat crops sown in the autumn and maturing in the springtime.

High values of the six VIs in the respective scales indicate healthy, well growing crops. However, high VI values alone are not always good predictors for high GY, because higher canopy biomass prior to grain filling only contributes to good growth status, possibly due to adequate water availability, which is not always a prerequisite for maximum grain production (Benedetti and Rossini, 1993).

Notwithstanding this, the good correlations between VIs and GY (Table 1.5) are a remarkable outcome, considering that mono-cotyledonous (DW and BW) and di-cotyledonous (SF and CO) crops have different reflectance properties due to differences in leaf mesophyll cells and structure of front and back leaf side (Woolley, 1971). In other works, this has resulted in remote VIs behaving crop specifically according to leaf canopy structure (Viña et al., 2011).

The different relationships between VIs and GY in winter wheat (DW 2010, BW 2012 and 2014) vs. the two spring dicots (SF 2011 and CO 2013), consisting in the former crop showing better correlations in the vegetative phase, and the latter two crops in the reproductive phase (Table 1.5), is at least partially associated with the time elapsed from seeding to the stage at which good correlations were found. In fact, wheat is cultivated as winter crop while sunflower and coriander can only be cultivated as spring crops in the specific climate (Metzger et al., 2005). It results that wheat cycle lasted an average 251 days from seeding to harvest, while sunflower cycle lasted 155 days, and coriander cycle only 90 days (Table 1.1). Wheat scored the best correlations in the three years combined (Table 1.5) between 120 DAS (BBCH 32 in BW 2014) and 180 DAS (BBCH 41 in BW 2012)

(Table 1.2). Sunflower scored the best correlations from 83 to 108 DAS, and coriander from 59 to 82 DAS (Table 1.2). Thus, the two dicots had been living for a shorter time, although they had reached a more advanced stage (Table 1.2). It is perceived, therefore, that the long time passed when the first VIs were acquired in wheat may have served the plant to better sense the environmental differences within the field, and translate them into a spectral response in agreement with the final yield. The two spring dicots featuring a shorter cycle, also necessitated a certain amount of time to experience the same differences, and good correlations between VIs and GY were achieved at later stages. However, we have not found other works addressing this point, meaning that these findings are not echoed in the literature, to our best knowledge. Therefore, further evidence is needed to corroborate this hypothesis.

All the VIs acquired in these two time frames specific for wheat and spring dicots performed in a similar way. Assuming r = 0,700 as the threshold for good correlation, NDVI, GNDVI, GCI, SR and EVI fell below this value only once (Table 1.5). However, even in that case NDVI, GNDVI, GCI, SR decreased to levels slightly lower than this threshold (r between 0.631 and 0.698, depending on VI), whereas EVI plummeted to r = 0.480 in CO 2013 at BBCH 55 (Table 1.5). Compared to them, SAVI never fell below this threshold. Therefore, the choice of the best VI was not so critical within a suitable time frame, despite relevant differences in spectral composition and calculation formula.

Several works were found similar to our study, i.e. remote VIs successfully estimated spatial crop yields, Labus et al. (2002) found a strong relationship (R^2=75.3%) between NDVI and wheat yield. Herbei and Sala (2015) studied the relationship between growth stages and VIs in sunflower, and found a maximum correlation with NDVI (R^2 >0.97) at flowering, followed by a decline at maturity. Plant et al. (2000) explained that NDVI is sensitive to canopy reflectance decreasing its correlation with cotton yield over a small field area. Yields of wheat, maize, rice, sugarcane and soybean were also successfully estimated by means of NDVI (Prasad et al., 2006; Pinheiro Lisboa et al., 2018; Singla et al., 2018). After positive achievements with NDVI, other VIs proved also effective in the estimation of different crop yields (Basso et al., 2004; Zarco-Tejada et al., 2005; Hatfield et al., 2008; Kumhálová et al., 2014; Kayad et al., 2016; Kuiawski et al., 2017; Domínguez et al., 2017).

The good performance of the spherical model in fitting GY experimental semivariograms (Table 1.6) is consistent with the equally good performance of the same model in fitting VI experimental semivariograms (Table 1.7). The higher sill values in the model structure of VI semivariograms is assumed to indicate a higher percentage of

canopy cover, because young plants have less contrast in reflected light spectra resulting in lower sill variance (Cohen et al., 1990). However, at growth stages > BBCH 30, as in our 15 cases (Table 1.7), full canopy cover is normally achieved, resulting in a random variation of sill data. Additionally, VI ranges largely exceeded GY ranges (Table 1.6), indicating a farther reaching SpD of VI vs. GY data. This, in turn, supports the adoption of the 30 m Landsat resolution also for GY data to be compared (Cohen et al., 1990). Lastly, geostatistical analysis indicates a strong SpD of VIs over distance (h), and the same was shown in GY data. In both cases, this is the premise for a continuous appraisal of the investigated traits over field surface.

In accordance with the similarities shown in spatial pattern and geostatistical analysis, final agreement between remote indices and crop yields at pixel level (Table 1.8) was, unsurprisingly, related to the R^2 values between VIs and GY obtained from the *r* values reported in Table 1.5. More surprisingly, F_a data appeared to be adversely related to F_a coefficient of variation (Table 1.8). In other words, very good agreement was obtained when the variation among the three correspondence levels (high, medium, low) was limited, as in the case of SR at BBCH stage 37 and 77 in BW 2014 (F_a, 85-86% with respective CV, 27.1-27.5%). Conversely, a modest agreement was obtained when strong variation occurred among the three correspondence levels, as in the case of SR at BBCH stage 67 in SF 2011 (F_a, 64% with CV, 56.4%). In theory, F_a and CV are reciprocally independent, i.e. high F_a could also be obtained with high CV, and vice versa. This finding is of non-univocal interpretation and, to our knowledge, has not been reported so far in the literature.

Several reasons can explain why VI ranking into quintiles does not fully match the same ranking of GY data. Water availability, nutrient uptake, crop management practices, weather conditions, pests and diseases, etc., can influence growth status and final yield to a different extent: resilience can be shown when a crop withstands unfavourable growth conditions (low VI values), attaining a fairly good yield. Conversely, rigidity is shown when slightly unfavourable growth conditions (relatively high VI values) result in poor yield. This latter case is also determined by the fact that GY may be reduced also when above-ground biomass is not significantly reduced.

An overall F_a of 74% (Table 1.8) is nevertheless a good outcome: it means that almost ¾ of the 126 cells belong to the same VI and GY quintile, despite ample variation in both VI and GY data.

There is still no general consensus in the use of rank comparison between spatially variable GY and remotely sensed VIs. In soybean (Kuiawski et al., 2017), the combined

SR and SAVI, together with soil elevation concurred to delineate management zones reflecting significant differences in final yield and soil properties. More generally, in winter cereals (barley and wheat), NDVI from Landsat as well as higher resolution satellites (QuickBird and WorldView-2) proved effective in describing yield spatial variability, especially at the onset of the reproductive stage (Kumhálová and Matějková, 2017). The same happened in winter oilseed rape with the Enhanced Moisture Stress Index (Domínguez et al., 2017). No other hint of rank comparisons between VIs and GY can be found in the literature, to our best knowledge.

The relationships (r and R^2 values) between VIs and final GY in the three cited sources (Domínguez et al., 2017; Kuiawski et al., 2017; Kumhálová and Matějková, 2017) are no better, in general, than those found in the present study (Table 1.8). In this light, the above discussed data of F_a (Table 1.8) may be considered encouraging, and set the premise for a larger use of remote (satellite) imagery in the interpretation and subsequent management of crop spatial variation.

1.5. Conclusions

Landsat satellite imagery with its spatial and temporal resolution exhibited a good potential for estimating the final GY over different crops in a chronological rotation, at a relatively small field scale (11.07 ha). This is further stressed by the circumstance that the spatial resolution provided by the Landsat system (30 m) was shown sufficient to characterize crop variation across a field of moderate extension. This sets the premise for a wider use of satellite data in yield predictions during the growing season, beside their role in supporting site specific management of crop practices.

Simple ratio and NDVI were the two VIs most frequently selected as best indices, compared to EVI, SAVI, GNDVI and GCI across stages ranging from vegetative (BBCH ~30's) to reproductive phase (BBCH ~70's). In contrast to this, SAVI never exhibited correlations with yield high enough during these stages, to be included among best VIs. Pixel level study demonstrated a generally good agreement between the five classes of VIs, on one side, and those of GY, on the other side.

Beside these 15 cases showing the best correlations with yield, two specific time frames were identified for winter wheat and the two spring dicots, showing high and consistent correlations between all remote indices, in general, and final yields. Based on our data, this sets the premise for a reliable use of VIS in yield predictions. Outside these time frames, the relationships between VIs and GY are less consistent, and subjected to factors of difficult interpretation.

Chapter 2

Soil and Weather Factors Drive Spatio-temporal Variability of Yields in a Crop-Rotation Field under Uniform Management

Abstract

Spatial variability in crop yield within agricultural lands is the premise for site specific crop management (SSCM) intended as means to enhance the crop output while reducing unneccessary costs and minimizing the environmental impact. In this study, standardised crop yields over five year (2010-2014) were used to characterize the spatio-temporal field variability covering 11.07 ha area under rainfed conditions, cultivating winter cereals and spring dicots in a crop rotation system. The interpolated yield for each crop was classified into spatial and temporal variability across the field. Then, standardised yield maps were produced over single and multiple crops. Yield stability classes (YSCs) were produced over multiple crops based on the information of spatio-temporal characteristics within field, each class identified by specific features that can be managed in a site specific way. These classes were as followed: high yielding and stable (HYS, relative yield > 100 %; CV < 30 %), low yielding and stable (LYS, relative yield < 100 %; CV < 30 %), and unstable class (unstable, CV > 30 %). After that, we evaluated the YSCs by following the statistical simple correlations between stable soil properties and spatiotemporal yield within YSCs, and as a function of the differences in soil properties among the three classes. In addition, we investigated the weather data within growing season of each crop for evaluating the temporal yield variability within years. Results demonstrate that spatial variability maps were more consistent with YSCs map than the temporal stability map. However, unstable class was found to be slightly more productive than the LYS class, but inconsistent over time. For the YSCs, the proportion of the three respective classes was 46, 30 and 24 %. Preliminary correlation analysis showed that relative yield variability within YSCs was fairly positively correlated with stable soil properties. Moreover, YSCs were also found to be relatively consistent vs. soil properties. Lower values of soil ECa, in the average, were found consistent with HYS, whereas higher ECa values were found inconsistent with LYS and unstable class yield. More specifically, the higher values of sand and ECa under unstable class did not significantly influence crop yields, resulting in a slightly higher relative yield (83 %) attained by unstable vs. the LYS class (80 %). Weather data showed an erratic behaviour

among the growing seasons of the surveyed crops, supporting the yield variability among years. Consequently, establishing YSCs based on spatial and temporal variability of crop yields may be considered the best approach for delineating the SSCM zones, as it comprises all the factors influencing crop yield.

2. Introduction

Precision agriculture has a great potential to increase crop growth and final yield at minimum cost and detrimental environmental impacts through the application of variable crop inputs (Basso et al., 2017). Variable crop inputs at right time and place to a particular area, where yield is consistently high or low over time than average, based on previous field history to input response, is highly encouraged in today's agriculture. Therefore, it is necessary to manage the areas within field through the observation of temporal behaviour of crops, in-season weather conditions, and determine soil nutrient status for optimizing the crop productivity and sustaining the finite natural resources (Blackmore, 2000; Maestrini and Basso, 2018a). However, soil properties significantly affect crop yield, but their interaction with yield depending on the interaction between soil physical-chemical properties and other external factors such as meteorological, topographic, anthropogenic factors and living entities within soil (Sys et al., 1991; Corwin et al., 2003). Bullock and Bullock (2000) stated that it is very important to adopt the most efficient methodology to characterize the spatial variability of soil for site specific crop management (SSCM). Apparent soil electrical conductivity (ECa) directed to soil sampling has been proved one of the most reliable method to characterize the field variability inflenced by soil properties and other external factors (Corwin and Lesch, 2003). However, ECa has not shown always consistent results with crop yield due to complex interactions of ECa with soil data and other external sources (Corwin et al., 2003).

Variation of climatic factors, i.e. precipitation and temperature, has been found paramount to influence the variability in rainfed conditions over each year (Iizumi and Ramankutty, 2015; Asfaw et al., 2018). Currently, enough attention is being paid to minimize the uncertainty of crop yield within seasons (unstable zones) caused by the erractic pattern of climate variables, namely precipitation. Several factors combine to aggravate the situation of low yielding areas such as: a reduction in winter rainfall hampering soil moisture profile to be fully recharged, or on the contrary excess winter rainfall restricting rooting, flowering or heading stage are more susceptile to water deficit as compared to excess rain, lack of spring rain, very low radiation at the time of

fertilization of the flowers, and finally inadequate frost hardening of wheat associated with very severe cycles of frost and thawing (Brisson et al., 2010). Impacts of climate on crop yield also depend on latitude and topography of the area, as well as irrigation practices. According to the 5th Report of the Intergovernmental Panel on Climate Change (Field et al., 2014), as compared to the 20th century, average annual temperature will increase by more than 2 degree in South Asia in the middle of 21st century. Acoording to an estimation, increasing temperature will exceed 3-6 degree under high CO_2 emission in the 21st century, whereas less than 2 or upto 3 degree under low emission scenario. However, the rate of increasing temperature will be higher under Himalaya regions as compared to global rate. Increasing temperature may influence the occurrence of precipitation, and ultimately availability of water to crop plants (Mishra et al., 2014). Crop yields can be increased through the application of irrigation water or precipitation during growing season. However, precipitation has more impact on grain yield than temperature (Kang et al., 2009). We should shorten the growing season of cultivated crops through changing the sowing time of crops in current changing environment, for enhancing crop adaptation to changing external conditions. However, it is very important to observe the climatic variables during growing season of crops to provide the insight for farmers to think critically about the selection of varieties, sowing time, plant population and dosages of fertilizers for crop cultivation (Cuculeanu et al., 2002; Barbanti et al., 2012; Asfaw et al., 2018).

Furthermore, biotic (living entities) and abiotic stresses (non-living entities) are also equally contributing to affect crop growth and development, and ultimately yield. The impact of living entities such as insects, molluscs, higher animal, fungi, bacteria, virus and nematodes may or may not be advantageous to plant health, but it depends on the interaction between them (Higley and Peterson, 2001; Flynn, 2003; Dresselhaus and Hückelhoven, 2018). Shrestha et al. (2012) explained that sudden changes in climatic variables have shown greater influence on occurrence of insect pests, diseases and water availability during the growing season. Among abiotic stress, low water availability, heat, high salinity, flooding, high or low temperatures, hypoxia/anoxia, and nutrient deficiency have shown their influence on crop productivity (Mariani and Ferrante, 2017; Schlenker and Roberts, 2008), depending on crop genotype adaptation capabilities (Zandalinas et al., 2018; Dresselhaus and Hückelhoven, 2018).

The field area of this study, 11.07 ha located near Ravenna, Italy, was managed in 3 separate fields from 1976 to 2005: north part of the field was cultivated with peach orchard and vineyard, whereas the lower two fields were cultivated with grain crops. In

2006, a contractor modified the field into a single management unit and started the cultivation as a traditional farming in vertical position. However, this research work highlights the current status of field productivity based on spatio-temporal yield over five years data, and guidelines for field management practices in site speciifc way.

Many past studies demonstrated the different methods for delineating the SSCM within same piece of land. Stafford et al. (1998) concluded that yield maps play an important role in precision agriculture for making site specific decisions. Using a yield map based on spatio-temporal characteristics is important for field management guidelines to enhance the agricultural commodities (Amado et al., 2007). Lark and Stafford (1996a & b) produced management zones (MZs) using multiple years' yield data through unsupervised fuzzy clustering method. Swindell (1997) analyzed the spatial variability based on several crop harvest index over single year. Fraisse et al. (1999) contributed by adding topographical and soil EC data through unsupervised cluster analysis. Basnet et al. (2003) used several years'standardised yield to define the MZs through overlapping similar grid resolutions. Da Silva (2006) determined the homogenous zones based on spatio-temporal yields of irrigated maize over three years. Jaynes et al. (2005) defined the MZs using several years' temporal yield of soybean, soil elevation and apparent soil ECa. Maestrini and Basso (2018b) went further and developed MZs based on spatio-temporal yield of maize, soybean, wheat and cotton over multiple years through considering the topography, crop vegetation indices and climatic factors within season. Hereafter, we delineated the yield stability classes (YSCs) based on spatio-temporal yield over five years' in a similar way as described by (Blackmore, 2000; Panneton et al., 2001; Panneton and Brouillard, 2002; Blackmore et al., 2003). Furthermore, we analyzed the crop spatio-temporal variability based on simple correlations and statistical differences of spatial soil data within YSCs; and additionally we examined the meteorological data trends during growing seasons of crops, which influence the temporal yield behaviour over each specific year (unstable zones).

The key objectives of present research were to: i). Characterize the spatio-temporal patterns of yield in rainfed conditions under crop rotation and uniform management; ii). Follow the protocol of apparent ECa survey directed to soil sampling for examining the spatial variability of general soil physical-chemical properties within field; iii). Investigate the crops' spatio-temporal variability as a function of simple correlations and statistical differences of stable soil properties within yield stability classes; iv). Examine the meteorological data during growing seasons of surveyed crops, which affect the temporal yield varaiability across years.

2.1. Materials and Methods

2.1.1. *Study site description*

A 11.07 field area of the Agrisfera Cooperative, located in the Mediterranean North environmental Zone (Metzger et al., 2005), was chosen as experimental field near Ravenna, Italy (Figure 2.1). This site is located at N 44° 29′ 26″, E 12° 07′ 44″ and 0 m above sea level, showing flat landmass with predominantly sandy to clayey soil texture (up to 60 cm depth), depending on sub-field position. The field was managed in a chronological rotation with winter cereals, namely Durum Wheat 2010 (DW 2010) and Bread Wheat 2012 and 2014 (BW 2012 & 2014), and spring dicots, namely Sunflower 2011 (SF 2011) and Coriander 2013 (CO 2013). Cultivation was based on the good agronomic practices for each specific crop, according to local conditions.

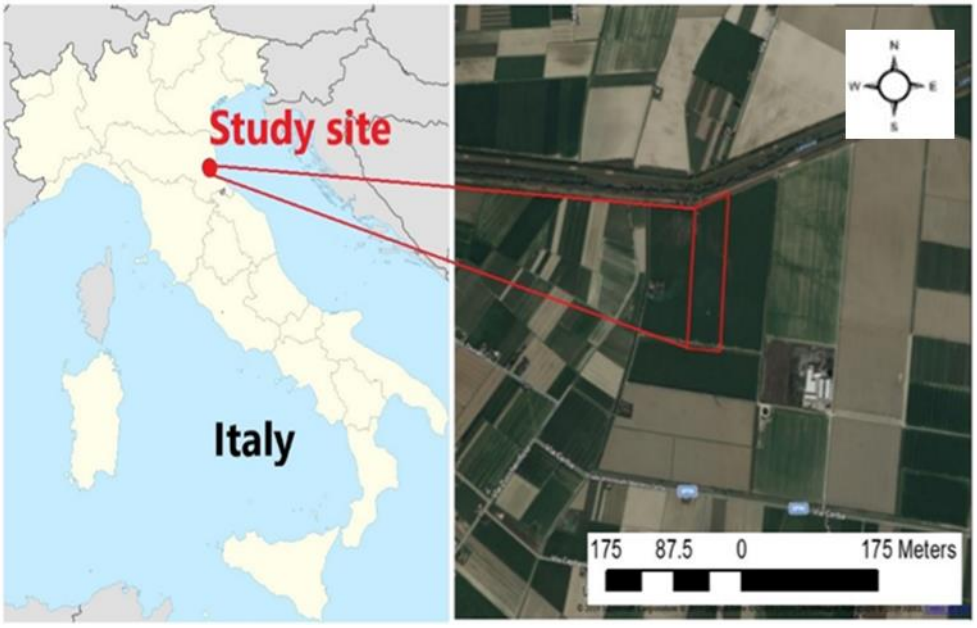

Figure 2.1. Study site location in northern Italy

2.1.2. Crop data collection and management

Five years' crop data were collected by a New Holland CR 9080 (CNH Industrial N.V., Basildon, UK) combine harvester using specific headers according to the crop. The combine was equipped with assisted guiding system based on real time kinematic GPS, yield mapping system consisting of a Pektron flow meter (Pektron Group Ltd, Derby, UK) and Ag Leader moisture sensor (Ag Leader Technology, Ames, IA, USA).

All raw yield data were processed for each crop, removing the data points that were beyond our projection (Blackmore, 1999). Resulting from this, an average 6170 GY data points were archived each year in the experimental area. The sowing and harvesting dates were: DW 2010, Oct. 30 (2009) – Jul. 10; SF 2011, Apr. 5 – Sep. 7; BW 2012, Oct. 14 (2011) – Jul. 1; CO 2013, Apr. 11 – Jul. 10; BW 2014, Nov. 9 (2013) – Jul. 7. For each crop, standardised crop yield was used for comparison among years, by removing the yield units (t/ha) and replacing them with relative percentage (%) giving 100 % to field average yield, and calculated as follows:

$$S_i = \left(\frac{y_i}{\bar{y}}\right) \times 100 \quad (1)$$

Where, S_i=standardised yield (%) at point i within field, y_i=yield at point i (t/ha), and $\bar{y}$=mean yield of all data points of that year.

Then, we employed the geostatistical analysis (ArcGIS version 10.3) on standardised crop data of each year for 3 purposes: i) to examine the degree of spatial dependence (SpD) in term of semivariogram between crop yields over five years, ii) to produce the continuous grid points over entire field before mapping, iii) to allow the calculations between years to be carried out in a excel sheet using the data from coincident grid points for spatial and temporal maps. The semivariogram is a function of dissimilarity between measured data points from each other over a distance (h). The SpD was calculated according to following equation:

$$\gamma(h) = \frac{1}{2N(h)} X \sum_{i=1}^{N(h)} [Z(x_i) - Z(x_i + h)]^2 \quad (2)$$

Where, $\gamma(h)$ is semi-variance, h represents a lag distance between two data points, $N(h)$ is the number of paired points at distance (h), $Z(x_i)$ and $Z(x_i + h)$ are measured values at two separate locations namely (x_i), $(x_i + h)$ over defined distance.

To describe the semivariogram properties, 3 parameters are necessary to be defined: nugget (C_0), measurement errors at 0 distance (h=0) that could not be identified; sill ($C_0 + C_1$), the maximum value at y-axis that increases with increasing lag distance (h) and remains constant at higher distance; range (a), maximum value at which data points still correlated and semivariogram touches the maximum sill value at y-axis; beyond that maximum distance there is no more spatial correlation. We calculated the degree of spatial dependence (DSpD) as given by Cambardella et al. (1994): < 25 %, indicating strong SD; (ii) 25-75 %, moderate SD; (iii) >75 %, weak SD.

Iterative cross validation technique was used to choose the best fitting semivariogram model among Circular, Spherical, Exponential, Gaussian and Stable one, based on the highest coefficient of determination (R^2) and minimum mean absolute error (MAE) (Xiao et al., 2016). The maximum R^2 and minimum errors is the criteria for

choosing a best-fitting interpolation model (Cornell & Berger, 1987; Dashtpagerdi et al., 2013). Standardised maps over single crop were produced by simple kriging (SK) with 10 m cell size, giving 22 columns and 70 rows, through best fitting semivariogram models (Moral et al., 2010). Simple kriging is an interpolation method providing maximum R^2 and minimal error parameters (Maynou, 1998; Xiao et al., 2016). Based on these principles, each map was obtained with 1156 regular grid points having 100 % field average yield, hence each sampling point could be compared to mean yield of all data points within field to identify how much the yield points in the field differ from the 100 % field average. For multiple crops, a spatial variability map was produced by simply calculating the interpolated yield at each point from standardised data, laid over the same grid over the five years:

$$\bar{S_i} = \frac{\sum_{t=1}^{n} Si_I}{n} \quad 3$$

Where, $\bar{S_i}$= mean of interpolated S_i (%), S_i= interpolated standardised GY (%) at point i over n years.

For multiple crops, a temporal variability map was produced to assess the stability of GY over the five years, demonstrating how much GY varied at each single point over time. In this case, we calculated the coefficient of variation (CV) of each grid point from standardised crop data over the 5 years (Blackmore, 2000):

$$CVS_i = \frac{\left(\sum_{t=1}^{t=n} s^2 i_t - \left(\sum_{t=1}^{t=n} s^2 i_t\right)^2\right)^{0.5}}{\frac{n(n-1)}{\bar{S_i}}} \times 100 \quad 4$$

Where, CVS_i= interpolated standardised CV (%) at point i over n years.

For the threshold level of spatial maps over single and multiple crops and temporal map over multiple crops, the four class boundaries were assigned based on the natural break classification technique in which the data values are arranged in order and grouped together based on statistically adjacent data points. Two classes were defined at either side of the 100 % field average for spatial maps, whereas four classes were produced for temporal map defined between 2-73 % CV. With this method, each class showed a relatively large difference as compared to another, which in turn minimizes the standard deviation (SD) within the data of each class.

2.1.3. Spatio-temporal yield variability analyses

The YSCs were produced through combining both spatial and temporal maps over the five consecutive years. Three YSCs were produced as followed: high yielding and

stable (HYS), low yielding and stable (LYS), and unstable. Each class derived from the spatio-temporal data set of multiple crops (equations 3 & 4), with 3 years winter cereals (bread and durum wheat) and 2 years spring dicots (sunflower and coriander), by applying the combinational logic statement (Blackmore, 2000). A GY point was considered to belong to a particular class if both conditions shown in table 2.1 were fulfilled.

Table 2.1. Yield stability classes and their logical statement

Yield stability classes	Multiple crops	
	Logic 1	**Logic 2**
HYS	s_i>100	CVs_i<30
LYS	s_i<100	CVs_i<30
Unstable	-	CVs_i>30

HYS, high yielding and stable; LYS, low yielding and stable; s_i, interpolated standardised grain yield at point (i); CVs_i, interpolated standardised coefficient of variation at point (i).

Logic 1 indicated whether GY point was above or below the mean yield of all points in the field (100 % field average), whereas logic 2 defined the stability of the yield at that GY point over the five years, by comparing the CV with a given threshold (30 %) within field.

All georeferenced maps and data anaylsis were carried out by ArcGIS software under the reference system WGS 84/UTM zone 32N-EPSG: 32632

2.1.4. Soil characterization

For soil analysis, a procedure developed by Corwin and Lesch (2003, 2005) was used for ECa directed to soil sampling. Soil ECa survey was conducted by using mobile based electrical resistivity (ER) over the 11.07 ha field area (Figure 2.2). The fixed ER electrodes were adjusted to measure ECa to a depth of 0.60 cm. The raw ECa data points were projected to Universe Transverse Mercator (UTM) reference system in the EPSG: 32632 with 32° N by using ArcMap version 10.3. Then raw ECa data were cleaned and total 2651 points (dS/m) were obtained across the field. After ECa survey, the ESAP-95 version 2.01 statistical software developed by Lesch et al. (2000) was used to determine the variable positions where soil cores were taken based on ECa measurements. Twenty soil sampling positions (Figure 2.2) were chosen using model based response surface (ESAP software) sampling type (Lesch et al., 1995). Sampling positions were searched out through GeoGIS mobile-based GPS Stonex version 14.097. Soil cores from the 20 sites were taken with a drilling rig from 0-60 cm depth with the increment of 30 cm: 0-30 and

30-60 cm. Soil samples were collected in muslin cotton bags then air-dried at 40 °C, and sieved with 2 mm diameter mesh.

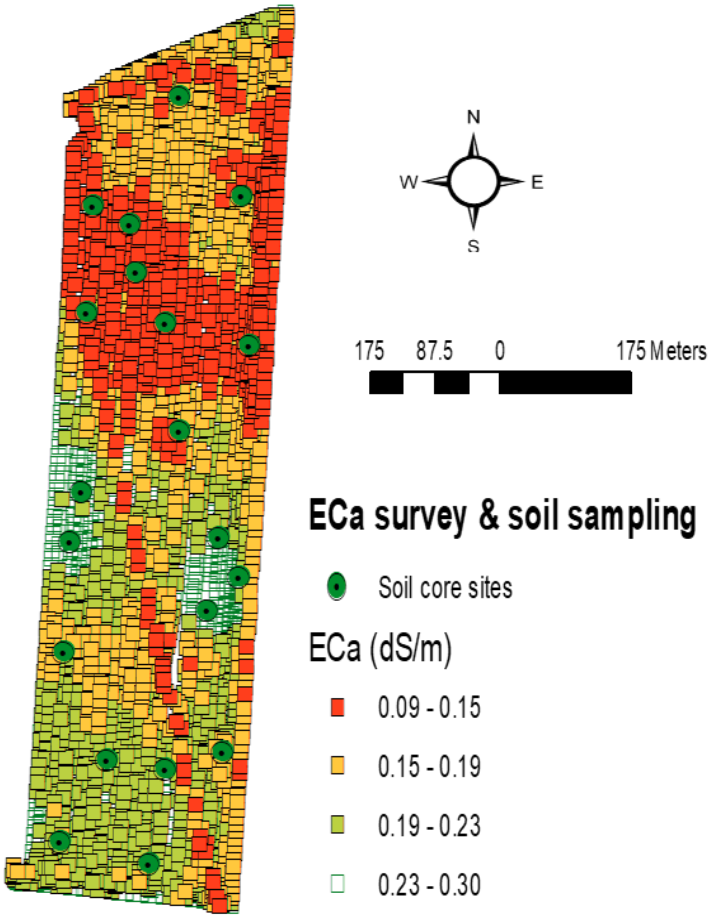

Figure 2.2. Map of extensive soil ECa survey and 20 soil sampling sites. Positions of soil sampling are indicated by green circle.

2.1.5. Soil physio-chemical analysis

In lab, sieved soil (200-250 g) was taken from 20 designated sampling sites for the analysis of general soil properties: soil texture (sand, silt and clay), pH, total carbonate ($CaCO_3$), total organic carbon (C), total nitrogen (N), available P (Olsen), exchangeable cations (K, Ca, Mg, Na), cation exchange capacity (CEC), and soil electrical conductivity (ECe). Soil analysis was determined by using the analytical methods of the Italian protocol for soil analysis (D.M. 13/09, 1999), apart from CEC that was measured by cobalt hexamine trichloride method (Orsini and Rémy, 1976), and C and N by dry combustion method (CHNS-O mod. EA 1110, Thermo Scientific GmbH, Dreieich, Germany), by means of acetanilide as a standard for C and N concentration.

2.1.6. Evaluation of spatio-temporal YSCs

Simple correlations were calculated between spatiotemporal yield variability (within YSCs) and stable soil properties (soil texture, CEC, standardised ECa). Correlation between soil properties, soil properties and ECa, and between spatiotemporal yield and ECa were also determined. Thereafter, we went further and determined whether historical spatio-temporal yield (within YSCs) could effectively describe the statistical differences of stable soil properties using one-way analysis of variance. Once the soil data (avg. depth 0-60 cm) were classified to each of the three YSCs, then differences were evaluated in the same way as described by Li et al. (2008) and Scudiero et al. (2018). In addition, we examined the in-season weather data during the growing season of the surveyed crops to evaluate the temporal yield variability within years. To do so, five years' meteorological data of Agrisfera Cooperative Farm, Ravenna Italy, was obtained from the Hydro-meteorological Services of the Emilia-Romagna region. We investigated the wet and dry periods from initial to late developmental stages, Feekes growth scale by Large (1954), during growing period of each crop, by computing crop evapo-traspiration (ETc) according to Allen et al. (1998), and its balance with precipitation (P). We also observed the total precipitation and average temperature trends on monthly basis during cropping period according to Bagnouls and Gaussen (1953). Many past studies demonstrated that climatic variables such as moisture levels, drought periods, precipitation and temperature trends significantly influence the temporal yield stability within growing season of the specific year (Homdee et al., 2016; Barbanti et al., 2012; Frieler et al., 2017; Mkonda and He, 2017; Asfaw et al., 2018; Kukal and Irmak, 2018; Mohsenipour et al., 2018; Maestrini and Basso, 2018a; Shiru et al., 2018; Tian et al., 2018).

2.2. Results and Discussion

2.2.1. Descriptive statistics of crop yields

Table 2.2 summarizes the differences between crop yield traits (mean, minimum, maximum, coefficient of variation (CV), kurtosis and skewness) over the five years. Crop yield varied greatly in minimum and maximum level during the study period. However, the largest min.-max. range (183) was found in BW 2012, whereas the tightest range (143) was shown in DW 2010. During the study period, the CV was high, ranging from 29 % for DW 2010 to 38 % for SF 2011 and CO 2013 (Blackmore, 2000; Gomes, 1985). These variations might be due to the influence of soil edaphic (physiochemical properties), anthropogenic (human activity influencing environment), biological (living entities),

meteorological (short-term climatic conditions) factors, as well as interactions among them (Yang et al., 1998; Kravchenko & Bullock, 2000). Lastly, the five years' yields were shown to be non-normally distributed, as the significant Kolmogorov-Smirnov test demonstrates.

Table 2.2. Descriptive statistics of standardised crop yield

Crop yields (relative %)	Mean	Min.	Max.	CV	Kurtosis	Skewness	K-S
DW 2010	100	13	156	29	-0.1	-0.6	*
SF 2011	100	12	190	38	-0.7	0.2	*
BW 2012	100	14	197	32	0.1	-0.1	**
CO 2013	100	19	181	38	-1.0	-0.3	*
BW 2014	100	21	178	33	-0.9	-0.2	*

DW, durum wheat; SF, sunflower; BW, bread wheat; CO, coriander; Min., minimum; Max., maximum; CV, coefficient of variation; K-S, Kolmogorov-Smirnov test for normal distribution; **, significant at $P \leq 0.05$; *, significant at $P \leq 0.01$.

2.2.2. Geostatistics

The spatial behavior of crop yields was evaluated in terms of semivariogram along with their model fitting (Table 2.3). DW 2014 showed a zero nugget effect followed by SF 2011 (0.01) and DW 2010 (0.03). Zero nugget effect indicates a high spatial continuity between data points. All crops exhibited a sill variance (C_0+C) ranging from 0.92 to 1.17, indicating a relatively similar total variance. However, the range of SpD varied enough, starting from 64 to 121 m. High range described the continuity between dataset to a maximum limit, whereas continuity disappeared very fast in the case of low range of data points. The degree of SpD explained the nugget to sill ratio: values less than 25 % indicate strong spatial continuity in their data distribution (Cambardella et al., 1994). Based on this, crop data showed 'strong' continuity in their SpD, except BW 2012. The results of semivariogram model fitting (R^2 and MAE) confirmed the good performance over the analyzed empirical data (Maynou, 1998; Xiao et al., 2016; Bhunia et al., 2018).

Table 2.3. Analysis of semivariogram parameters of standardised crop yields

Crop yields	Model	C_0	C_0+C	a (m)	C_0/ C_0+C (%)	DSpD	R^2	MAE
DW 2010	Stable	0.03	1.05	64	2.5	S	0.91	5.46
SF 2011	Exponential	0.01	1.01	38	1.0	S	0.92	7.51
BW 2012	Exponential	0.31	1.17	121	26.5	M	0.86	5.39
CO 2013	Stable	0.13	0.96	66	13.5	S	0.90	7.58
BW 2014	Stable	0.00	0.92	51	0.00	S	0.95	5.13

DW, durum wheat; SF, sunflower; BW, bread wheat; CO, coriander; C_0, nugget; C, partial sill; C_0+C, sill; a, range; C_0/ C_0+C, SpD; DSpD, degree of spatial dependence; S, strong; M, moderate.

2.2.3. Yield maps and spatio-temporal variability

Standardised GY maps were produced over single and multiple crops showing four classes either above or below the field average (Figure 2.3), namely: high yielding (HY), above average (AA), below average (BA) and low yielding (LY). For single crops, the upper and lower limits and their ranges were indicated in Table 2.2. Compared to single crops, in multiple crops a higher minimum (27) and lower maximum (148) relative yield were found, resulting in a narrower range (121). It can be seen that single-crop spatial variability maps and multiple-crop yield stability map were relatively consistent (Figure 2.3). This information indicates that low yield was found in the north part of the field, which covered an area of approximately 2.8 ha out of 11.07. Importance of stability becomes increased over multiple crops as compared to single crop. However, spatial variability maps were influenced more by high GY values than consistent changes over certain field parts (temporal yield).

Compared to the spatial variability maps for the single and multiple years, the temporal stability map that was produced by calculating the CV at each of the standardised grid points over multiple crops (Figure 2.3) indicated good stability in the five years over an area of 8.26 ha (76 %), while a 2.8 ha (24 %) area was seen unstable. This area can be considered significant for crop management practices, as it covers almost one fourth of the field surface. We observed that unstable portion of the field gave high yield as compared to LYS (Table 2.7). Therefore, this part of the field can be sufficiently productive as to non-significantly affect the overall crop yields, but it showed uncertainty over time, depending on management practices and, especially, in-season weather conditions.

Yield stability map depicts the features of spatio-temporal maps (Figure 2.3). The threshold level of each of the three YSCs were based on the logical statement (Table 2.1). All data points (1156) were converted to excel sheet to identify these three classes, HYS,

LYS and unstable, which were identified and exported by applying the logical statement (Table 2.1). The two yield stability classes HYS and LYS were shown stable and more reliable, consistently indicating the size and position of spatio-temporal variability across the field as compared to unstable class which changed over time and space. The YSCs identified the southern and northern part of the field to be consistently high and low yielding area, respectively. Therefore, they could be managed separately for maximizing the crop productivity in a site specific manner.

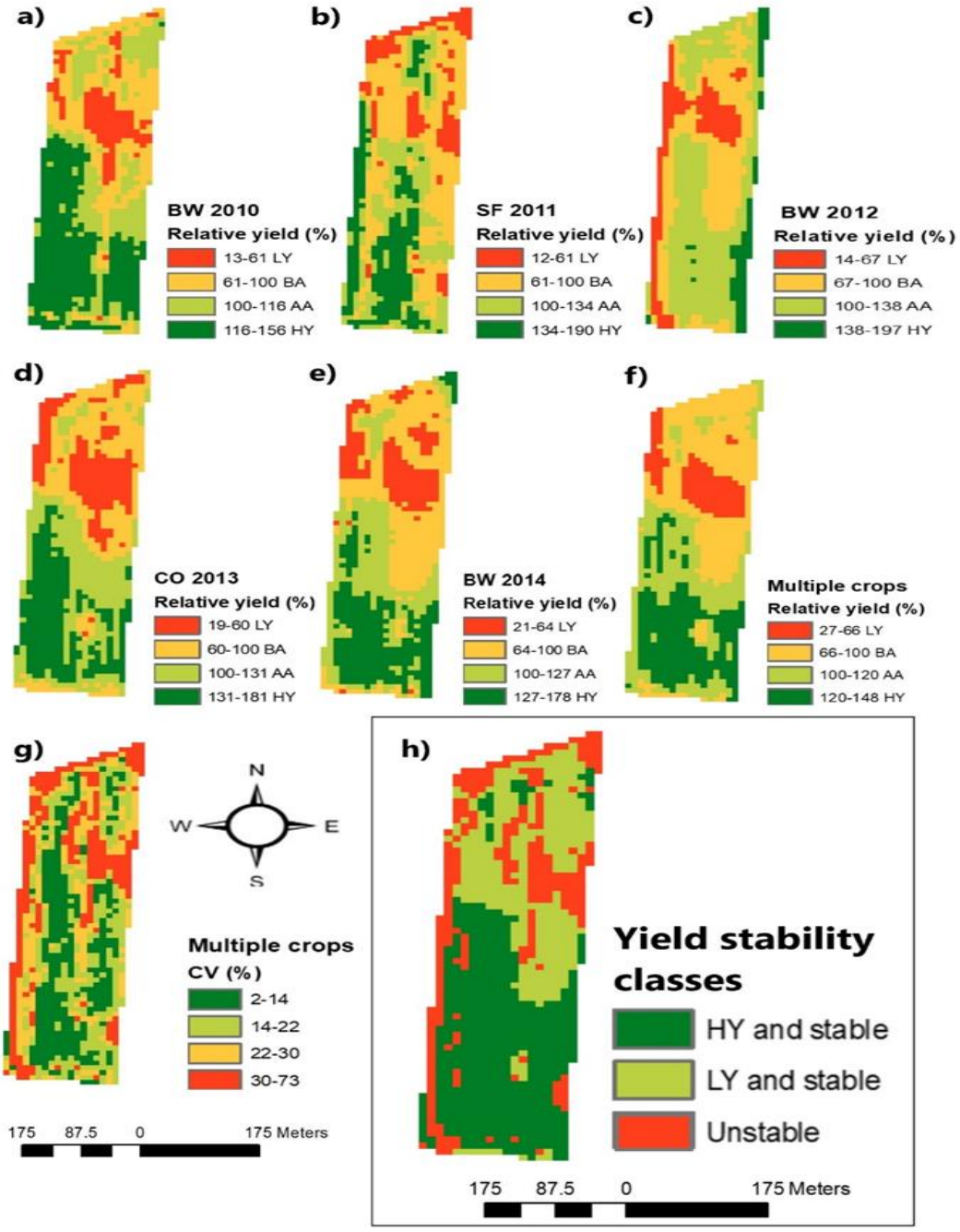

Figure 2.3. Consolidated spatio-temporal yield maps: LY, low yielding; BA, below average; AA, above average; HY, high yielding; **a** (spatial variability map of DW 2010); **b (**spatial variability map of SF 2011); **c** (spatial variability map of BW 2012); **d** (spatial variability map of CO 2013); **e** (spatial variability map of BW 2014); **f** (spatial variability map over 5 years' multiple crop); **g** (temporal variability map over 5 years' multiple crop); **h** (yield stability classes over spatiotemporal variability over 5 years' multiple crops).

2.2.4. Yield data distribution within spatio-temporal yield stability classes

Data distribution within the classes of spatio-temporal maps is shown in Table 2.4.

For spatial variability, in DW 2010 GY data distribution was found more skewed towards high yielding class, i.e. more grid points belonged to classes above average than below average. However, more grid points were found in above average yield in BW 2012, CO 2013 than below average class. Finally, more yield grid points were found under below average class than above average and high yielding classes, respectively, in case of SF 2011, DW 2014 and spatial map of multiple crops. The differences between the GY points over single and multiple crop maps highlight the circumstance that class limits are not coincident between single and multiple dataset. Both single and multiple crop distribution have units of percentage.

For temporal variability, CV limits range from 2 to 73 %. Based on this, out of 1156 data points, 334 points (29 % or 3.3 ha) were in the highly stable class (2-14 % CV), 310 points (27 % or 3.1 ha) were in the medium stable class (14-22 % CV), 310 points (27 % or 3.1 ha) in the lowly stable class (22-30 % CV), whereas 277 data points (24 % or 2.8 ha) were found in the unstable class (30-73 % % CV). Data distribution within each class is skewed towards lower stability class, except unstable class.

For yield stability classes, 527 data points (46 % or 5.3 ha) were found in HYS class, 352 (30 % or 3.5 ha) were grouped into LYS, and 277 points (24 % or 2.8 ha) were classified as unstable. No data point was found outside the three yield stability classes.

Table 2.4. Grain yield and CV data distribution within each class of spatio-temporal and yield stability classes

Variables	Relative yield (avg. 100 %) or CV	Yield or CV classes	Grid points
DW 2010	13-61	LY	134
	61-100	BA	317
	100-116	AA	301
	116-156	HY	404
SF 2011	12-61	LY	161
	61-100	BA	439
	100-134	AA	293
	134-190	HY	263
BW 2012	14-67	LY	176
	67-100	BA	374
	100-138	AA	506
	138-197	HY	100
CO 2013	19-60	LY	213
	60-100	BA	323
	100-131	AA	335
	131-181	HY	285
BW 2014	21-64	LY	176
	64-100	BA	387
	100-127	AA	304
	127-178	HY	289
Spatial map	27-66	LY	135
	66-100	BA	402
	100-120	AA	325
	120-148	HY	294
Temporal map (CV data)	2-14	Highly stable	334
	14-22	Medium stable	310
	22-30	Lowly stable	325
	30-73	Unstable	277
Yield stability classes		HYS	527
		LYS	352
		Unstable	277

DW, durum wheat; SF, sunflower; BW, bread wheat; CO, coriander; CV., coefficient of variation; LY, low yielding; BA, below average; AA, above average; HY, high yielding; HYS, high yielding and stable; LYS, low yielding and stable.

2.2.5. Spatial variability of general soil properties

Table 2.5 shows the physical-chemical soil properties depicting two depths that influence soil ECa and crop yield variability. The soil properties, namely sand, $CaCO_3$, C, N, C:N ratio, P, K, Ca, CEC and EC_e decreased in the deeper (30-60 cm) vs. shallower (0-30 cm) soil layer, whereas silt, clay pH, Mg were increased with depth. However, silt and

clay reached in average 38.2 and 12.1 % at 30-60 cm depth, respectively, while sand attained 52.7 % at 0-30 cm depth. The pH range was 8.02-8.67, which demonstrates the alkaline characteristics of the soil. The highest organic carbon (6.56 g/kg) was observed in the top soil (0-30 cm). The CEC value decreased from 11.8 to 9.34 with depth increment (30-60 cm vs. 0-30 cm), while EC decreased from 178 to 160 with the same depth increment. Overall, the soil physical-chemical properties showed a variation (CV) ranging from only 0.4 % of pH up to 34.0 % of silt, affecting crop behaviour and final yield to a potentially different degree.

Table **2.5.** Descriptive statistics of soil physical-chemical properties for two depths (0-30 & 30-60 cm).

Soil traits	Mean	Min	Max	SD	CV (%)	Kurtosis	Skewness
Depth 0-30 cm							
% sand	52.7	32.3	77.9	15.8	29.9	-1.5	0.2
% silt	36.3	16.5	53.1	12.3	34.0	-1.5	-0.1
% clay	11.0	5.57	17.4	3.70	33.5	-1.4	-0.2
pH	8.02	7.78	8.39	0.04	0.46	0.0	0.7
CaCO3 (g/kg)	185	142	218	4.63	2.50	-0.8	0.0
C (g/kg)	6.56	3.79	9.35	0.37	5.69	-1.0	0.0
N (g/kg)	0.82	0.51	1.06	0.04	4.65	-0.9	-0.4
C:N	7.94	6.84	10.3	0.84	10.6	1.9	1.2
P (mg/kg)	6.45	3.80	9.60	0.37	5.78	-0.8	0.3
K (cmol+/kg)	0.17	0.09	0.36	0.01	7.83	5.4	2.0
Ca (cmol+/kg)	8.51	5.46	11.0	0.40	4.65	-1.2	-0.4
Mg (cmol+/kg)	0.70	0.28	1.05	0.06	8.25	-1.4	-0.4
Na (cmol+/kg)	0.07	0.03	0.16	0.01	9.08	3.7	1.3
CEC (cmol+/kg)	11.8	7.09	15.6	0.55	4.67	-0.8	-0.3
EC (μS/cm)	178	120	209	5.56	3.13	0.0	-0.8
Depth 30-60 cm							
% sand	49.7	30.1	75.7	15.5	31.2	-1.5	0.4
% silt	38.2	18.1	53.8	12.5	32.8	-1.6	-0.3
% clay	12.1	4.3	16.2	3.54	29.4	-0.2	-0.8
pH	8.67	8.39	9.02	0.03	0.37	0.8	0.5
CaCO3 (g/kg)	179	153	205	3.12	1.75	0.0	0.0
C (g/kg)	5.54	2.96	7.41	0.30	5.39	-0.9	-0.5
N (g/kg)	0.73	0.45	0.93	0.04	5.00	-1.3	-0.5
C:N	7.56	6.45	8.08	0.36	4.77	3.8	-1.4
P (mg/kg)	6.32	3.40	10.2	0.47	7.41	-0.5	0.6
K (cmol+/kg)	0.13	0.07	0.27	0.01	7.88	2.9	1.2
Ca (cmol+/kg)	8.24	5.35	10.3	0.39	4.69	-1.4	-0.5
Mg (cmol+/kg)	0.73	0.30	1.12	0.06	8.66	-1.4	-0.3
Na (cmol+/kg)	0.07	0.04	0.13	0.01	8.47	1.3	1.3
CEC (cmol+/kg)	9.34	5.09	13.2	0.54	5.83	-1.0	-0.2
EC (μS/cm)	160	136	187	2.76	1.73	0.1	0.2

Min, minimum; Max, maximum; CV, coefficient of variation.

To cover the whole soil depth, Table 2.6 reports the averaged values of soil physical-chemical properties (0-60 cm) collected at the experimental field from the 20 positions. Exchangeable magnesium (Mg) and silt showed greater degree of spatial variability over the study area, as these contents exhibited the highest coefficient of variation (37.2 and 33.4 %), followed by clay and sand contents (31.1 and 30.2 %),

respectively. Exchangeable sodium (Na) did not change with depth, but showed a considerable variability (CV = 30.1 %) followed by P (CV = 28.3 %), K (CV = 26.7 %) and CEC (CV = 21.8 %). In contrast to this, pH, the C:N ratio and $CaCO_3$ staged the lowest variability across the field (CV < 10 %).

Table 2.6. Descriptive statistics of soil physical-chemical properties averaged in the two soil layers (0-60 cm).

Soil traits	Mean	Min	Max	SD	CV (%)	Kurtosis	Skewness	K-S
Depth 0-60 cm								
% sand	51.7	31.7	76.1	15.6	30.2	-1.6	0.2	*
% silt	36.9	17.0	53.3	12.3	33.4	-1.5	-0.2	*
% clay	11.4	5.70	17.0	3.54	31.1	-1.3	-0.3	*
pH	8.34	8.16	8.65	0.15	1.76	-0.3	0.8	*
CaCO3 (g/kg)	182	160	203	11.7	6.42	-0.7	-0.2	*
C (g/kg)	6.05	3.59	7.93	1.45	23.9	-1.2	-0.4	*
N (g/kg)	0.78	0.48	0.98	0.16	20.9	-1.2	-0.6	*
C:N	7.76	7.17	8.99	0.48	6.19	0.6	0.9	*
P (mg/kg)	6.38	3.60	9.70	1.81	28.3	-0.6	0.4	*
K (cmol+/kg)	0.15	0.11	0.25	0.04	26.7	0.2	0.8	*
Ca (cmol+/kg)	8.38	5.44	10.4	1.74	20.7	-1.3	-0.5	*
Mg (cmol+/kg)	0.71	0.30	1.03	0.27	37.2	-1.4	-0.4	*
Na (cmol+/kg)	0.07	0.04	0.11	0.02	30.1	-0.3	0.4	*
CEC (cmol+/kg)	10.5	6.09	13.7	2.30	21.8	-0.9	-0.5	*
EC (µS/cm)	169	128	187	14.7	8.70	1.7	-1.2	*

Min, minimum; Max, maximum; CV, coefficient of variation; K-S, significance of Kolmogorov-Smirnov test for normal distribution; *, significant at $P \leq 0.05$.

2.2.6. Quality control of Spatio-temporal YSCs

Simple correlation analysis between spatial soil data and crop yield is a first step to understand the yield variability at field level in PA. In this way, correlation provides the direct evidence to study the causes of yield variability through linear relationship between variables. Hence, simple correlations provide the initial information to determine what factors influence the crop yield.

There were significant correlation coefficients were exhibited between selected soil properties (Table 2.7). However, sand contents showed inverse correlation with other soil properties. The soil parameters (% silt and % clay) exhibited positive relations with each other showing the correlation coefficient ranging between 0.87-0.91. Furthermore, ECa is positvely correlated with sand content (r = 0.50), and negatively correlated with silt (-0.52), clay (-0.40) and CEC (-0.20) contents. Hence, ECa relationship with soil parameters

showed that they could be measured by ECa, because ECa is highly co-related with soil texture and CEC. The highest correlation between single soil property and relative yield (YSCs) was found in case of % silt (0.49) followed by CEC (0.42) (Table 2.7). However, sand contents showed an inverse correlation (-0.47) with yield. Correlation between ECa and yield was also negative (r = -0.71), meaning that ECa is highly correlated with studied crop yields which explained 71 % yield variability. However, ECa is a measure of several other soil properties which may or may not affect the crop yield, depending on the level of ECa at field scale. Moreover, there were also other soil or external factors influencing the yield beyond those measured by ECa (Corwin et al., 2003). At this particular site, ECa was found to be a useful parameter for studied crops variability i.e. wheat, sunflower and coriander. A scatter plot showed linear correlation with relative yield (%) through increasing or decreasing levels with respect to specific soil property (Figure 2.4). The relative yield within YSCs showed negative linear correlation with % sand and ECa, whereas positive correlation with silt, clay and CEC contents. Positive linear correlation showed that there were no yield limiting effects contributing to decrease crop yield, whereas factors which showed negative correlation with yield exhibited yield limiting effects on particular crop. In this study site, soil texture (% sand, % silt and % clay) and CEC showed linear correlation with yield data to various degrees (Figure 2.4: 2.4a, 2.4b, 2.4c, 2.4d and 2.4e). In this research the considerable variation in crop yields (within YSCs) across the field was fairly correlated to the parallel variation of selected soil properties. The present results are in line with the findings of Di Virgilio et al. (2007). Therefore, it is important to understand the causes of yield variability through soil related factors for delineating the appropriate management zones that may be expected to substantially improve the final crop productivity.

Table 2.7. Pearson correlations between selected soil properties, ECa and spatio-temporal yield within YSCs

Variables	% sand	% silt	% clay	CEC (cmol+/kg)	ECa (dS/m)	Relative yield (%)
% sand	1					
% silt	-1.00	1				
% clay	-0.94	0.91	1			
CEC (cmol+/kg)	-0.89	0.87	0.90	1		
ECa (dS/m)	0.50	-0.52	-0.40	-0.20	1	
Relative yield (%)	-0.47	0.49	0.40	0.42	-0.71	1

Significant correlations are shown based on 20 soil data point at $P \leq 0.05$

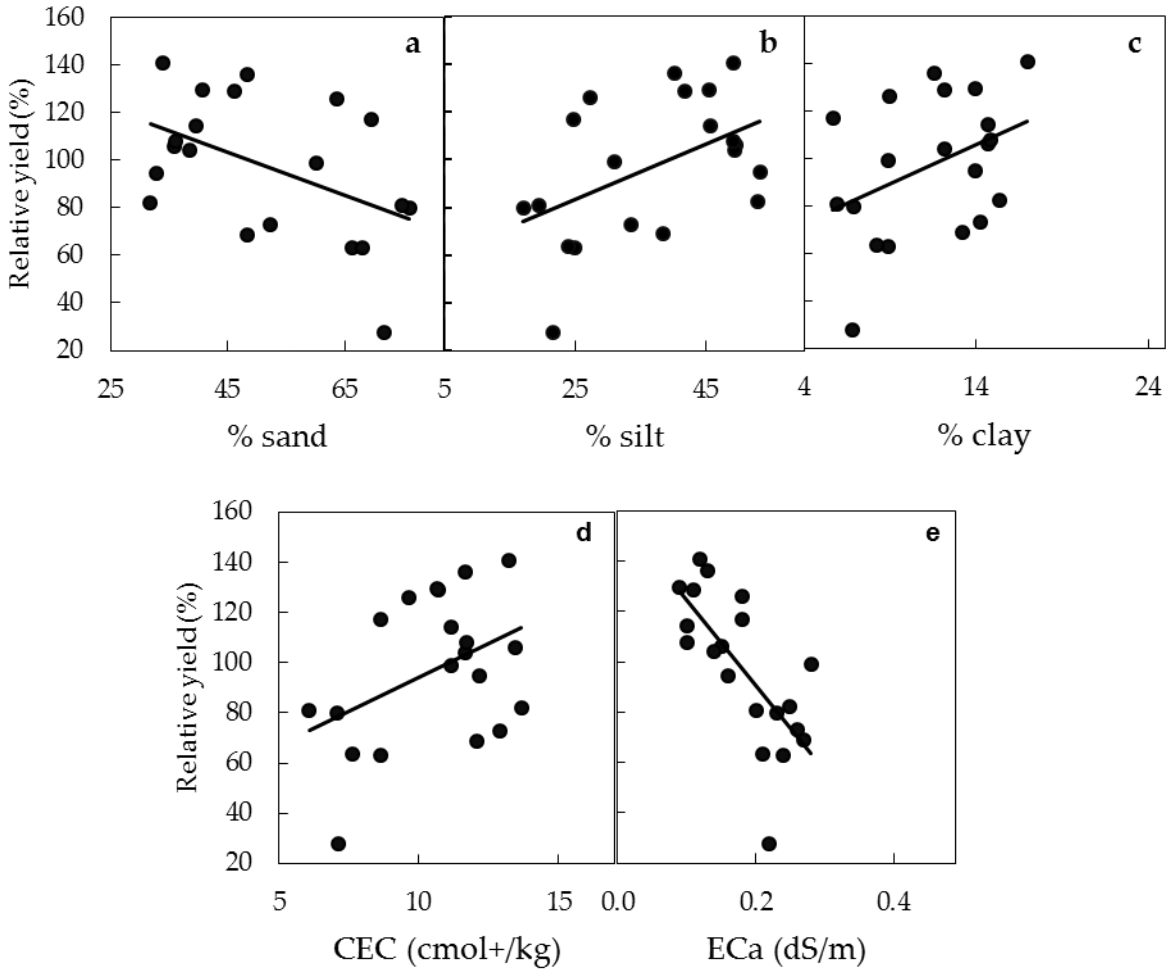

Figure 2.4. Scatter plots of stable soil properties, ECa and spatio-temporal yield (%) within YSCs based on 20 soil data points

Classification of stable soil physiochemical properties (soil depth 0-60 cm) related to spatio-temporal yield variation depicted statistical differences of soil data within each YSCs (Table 2.7). The lowest mean value of sand content (42.9 %) was found consistent with HYS class, performing maximum GY (122 % of average yield), whereas intermediate sand content (54.4 %) was recorded under LYS giving only 80 % yield. However, maximum mean sand (58.1 %) was observed under unstable class at high field uncertainty (CV>30 %), where the relative GY was slightly more (83 %) than LYS class. This fact demonstrates that higher mean value of sand contents did not significantly affect the overall yield within unstable field part under current field conditions (Table 2.7). Compared to this, mean contents of silt, clay and CEC were found to be consistent with the three YSCs. In addition, the values of these soil properties (silt, clay and CEC) were found high in HYS, intermediate in LYS and lowest in unstable class. It is therefore evinced that these soil traits increased the crop yield at higher contents, whereas lower contents had not showed significant adverse effects on crop yields within unstable, as compared to LYS class. The minimum soil ECa was found consistent with HYS class, giving maximum crop yield (122 %) as compared to LYS and unstable. However, slightly higher values of ECa were found in unstable class in which more grain yield was attained 83 % than LYS, meaning that higher ECa under higher variability area (CV>30 %) had not shown the significant negative affects on crop yields. Corwin and Lesch (2003) explained that soil ECa values are not always consistent with crop yield variability, due to complex interactions of soil properties, environmental factors or interaction among them with ECa, influencing final yield. Furthermore, stable soil properties evidenced higher variations (CV) within LYS class, demonstrating that these soil indices had shown slightly negative effects on spatiotemporal crop yields, giving lower yield (80 %) than HYS and unstable class. Consequently, mean values of spatial soil properties had shown considerable statistical differences and were aligned with the spatio-temporal variability within yield stability classes.

Table 2.7. Differences in soil variables among YSCs.

Variables	Yield classes	Data points	Mean	Min	Max	CV (%)	K-S
% sand	HYS	7	42.9	33.8	69.7	29	***
	LYS	6	54.5	31.7	76.1	36	***
	Unstable	7	58.1	39.6	74.7	21	***
% silt	HYS	7	44.2	24.7	49.5	21	***
	LYS	6	34.7	17	53.3	46	***
	Unstable	7	31.5	19.3	45.7	29	***
% clay	HYS	7	12.9	5.67	17	28	***
	LYS	6	10.8	6.77	15.4	35	***
	Unstable	7	10.4	5.93	14.7	31	***
CEC (cmol+/kg)	HYS	7	11.4	8.62	13.4	14	***
	LYS	6	10.1	7.09	13.7	28	***
	Unstable	7	10.1	6.09	12.9	24	***
Standardised ECa (ds/m)	HYS	1202	-0.01	-3.56	3.56	-1	***
	LYS	815	0.01	-3.11	3.01	1	***
	Unstable	634	0.02	-2.93	2.66	0.5	***
Crop yields (relative %) within YSCs	HYS	527	122	100	148	9	***
	LYS	352	80	27	100	19	***
	Unstable	277	83	29	136	32	***

HYS, high yielding and stable; LYS, low yielding and stable; Min, minimum; Max, maximum; CV, coefficient of variation; K-S, signficance of Kolmogorov-Smirnov test for normal distribution; *, significant at $P \leq 0.05$; **, significant at $P \leq 0.01$; ***, significant at $P \leq 0.001$.

At the end, the interesting question is why some areas of the field produced high yield over others, and why other areas changed over time, some years producing high yield and other years producing low yield (unstable zones). To address these questions, we investigated the balance of ambient moisture during the five growing seasons (Table 2.8). During DW 2010, the crop growing period from tillering to heading (initial to mid-season) received total precipitation (206 mm) and was considered a wet period, whereas late-season (ripening stage) suffered from a dry period (-68 mm). Bread wheat

2012 and 2014 also received enough precipitation from tillering to stem elongation stages (initial to developmental stages) (28 and 212 mm, respectively), thereafter a dry period was registered approaching from heading to ripening (maturity stages). The combined results of temperature and precipitation were also investigated for winter cereals and spring dicots (Figure 2.4 and 2.5). The range of total precipitation for winter cereals (DW & BW) was 212-702 mm from October to June, whereas the range for spring dicots (SF & CO) was 222-300 mm from March to August. In some months during mid growing season, very low precipitation occurred as in case of BW 2012. DW 2010 and BW 2014 received enough precipitation during the peak developmental stages (Jan-April). During winter cereals, temperature pattern also changed over seasonal growth among years, exhibiting very low values in winter months (Nov-March) and then increasing values during later months. In spring dicots, the average temperature ranges were from 10 to 25 °C during the growing period. We observed that precipitation in the given region varied greatly from one crop season to another, affecting crop growth and development, and utimately yield. Many past studies indicated that crop yields significantly varied between years over erratic behaviour of water availability during the growing season (Kang et al., 2009; Kukal and Irmak, 2018). However, timing, frequency and intensity of climatic variables, especially precipitation, had also considerable effects on crop growth and yield components (Poudel and Shaw, 2016; Kukal, and Irmak, 2018).

In our study, spring dicots (SF 2011 and CO 2013) suffered more with water deficit periods during whole growing period, and exhibited higher variation (CV = 38 %) during growing season as compared to winter cereals (CV = 29-33 %) (Table 2.2). Moreover, higher rains at early growth stages of winter wheat might be responsible for water logging, denitrification, etc., and in turn limit the final productivity. In the case of the two short cycle spring dicots, precipitation was recorded below potential needs (ETc) during the whole growing period that was, therefore, considered a continuously dry period, because of higher evapotranspiration due to higher temperature during the spring/summer period. Hence, dry periods of spring dicots are more responsible for influences on the grain yield pattern over years, which highly contributed in temporal variability during cropping seasons. Based on the ambient moisture conditions during growing seasons, it appears that wet and dry periods depending on total rainfall, crop evapotranspiration and temperature had a considerable effect on crop behaviour. Generally, crops need more water at heading or ripening stages for successfully completing the growth cycle towards maturity, whereas early stages are less sensitive to

scarce water because crops are only initiated to reproductive stage (Butts-Wilmsmeyer et al., 2019). Karim et al. (2000) stated that dry period at ripening of winter wheat decreased the grain yield upto 65% as compared to irrigated wheat (Karim et al., 2000). Mirzaei et al. (2011) stated that moisture stress at any growth stage of wheat significantly reduced the yield and yield related components, however maturity stages are considered to be more sensitive. Wang et al. (1995) found that moisture stress at maturity decreased nitrogen use efficiency in wheat plants, which considerably limits crop productivity. Nel et al. (2001) concluded that water stress decreased the sunflower seed yield up to 23 %. Moisture stress during growing period of coriander significantly decreased the biomass, plant height, seed yield and even oil contents (Unlukara et al., 2016).

Table 2.8. Meteorological data during the length of growing seasons of the five surveyed crops.

Crop and year	Growth period	Growth stages (Feekes)	Time (days)	P (mm)	ETc (mm)	P-ETc (mm)	Moisture conditions
DW 2010	Ini	Tillering	24	17	9	8	Wet
	Dev	Stem elongation	65	180	26	154	Wet
	Mid	Heading	100	265	221	44	Wet
	Late	Ripening	64	127	195	-68	Dry
SF 2011	Ini	Tillering	35	31	41	-10	Dry
	Dev	Stem elongation	40	29	142	-113	Dry
	Mid	Heading	50	67	278	-211	Dry
	Late	Ripening	30	2	101	-99	Dry
BW 2012	Ini	Tillering	19	35	10	25	Wet
	Dev	Stem elongation	68	43	40	3	Wet
	Mid	Heading	116	77	245	-168	Dry
	Late	Ripening	58	50	180	-130	Dry
CO 2013	Ini	Tillering	20	22	23	-1	Dry
	Dev	Stem elongation	30	36	83	-47	Dry
	Mid	Heading	25	5	141	-136	Dry
	Late	Ripening	15	17	52	-35	Dry
BW 2014	Ini	Tillering	44	96	13	83	Wet
	Dev	Stem elongation	74	188	59	129	Wet
	Mid	Heading	79	86	273	-187	Dry
	Late	Ripening	43	77	139	-62	Dry

DW, durum wheat; SF, sunflower; BW, bread wheat; CO, coriander; CV., coefficient of variation; P, precipitation; ETc, crop evapotranspiration; Ini, Initial; Dev, crop development; Mid, mid-season; Late, late-season.

It is also acknowledged that rainfall or temperature fluctuations during critical growth stages of crops can have substantial influences on final crop productivity (Asfaw et al., 2018). In addition, previous results also showed that minute temperature differences during gowing period cannot significantly affect crop yield, as compared to irrigation or rainfall (Kang et al., 2009; Carter et al., 2016). Iizumi and Ramankutty (2015) demonstrated that higher temperature during spring season suggests to plant first crop 'winter barley' earlier than before, so that farmers can grow second crop as rapeseed and mustard during the remaining part of the growing period to enhance the soil nutrient

status and profit. Our study suggests that, if the weather condition are favorable in a specific year, then unstable zones could be managed as high yielding; otherwise, as low yielding. Additionally, if the dry period occurs during winter wheat heading and then flowering, the following nitrogen doses should be increase to enhance grain protein content of cereals, anyhow this practice is most common in rainfed area's and vary from country to country. We recommended that farmers should use uniform fertilizer rates with respect to space and time by considering the in-season weather conditions. We believe that stable yield zones must be managed by strategic planning, whereas unstable zones by tactical approach, i.e. considering the meteorological conditions during the specific growing season. Therefore, it is very important to receive timely in-season weather information for alternative strategies, keeping the unique set of moisture conditions in mind during the growing season of crops (Basso et al., 2011).

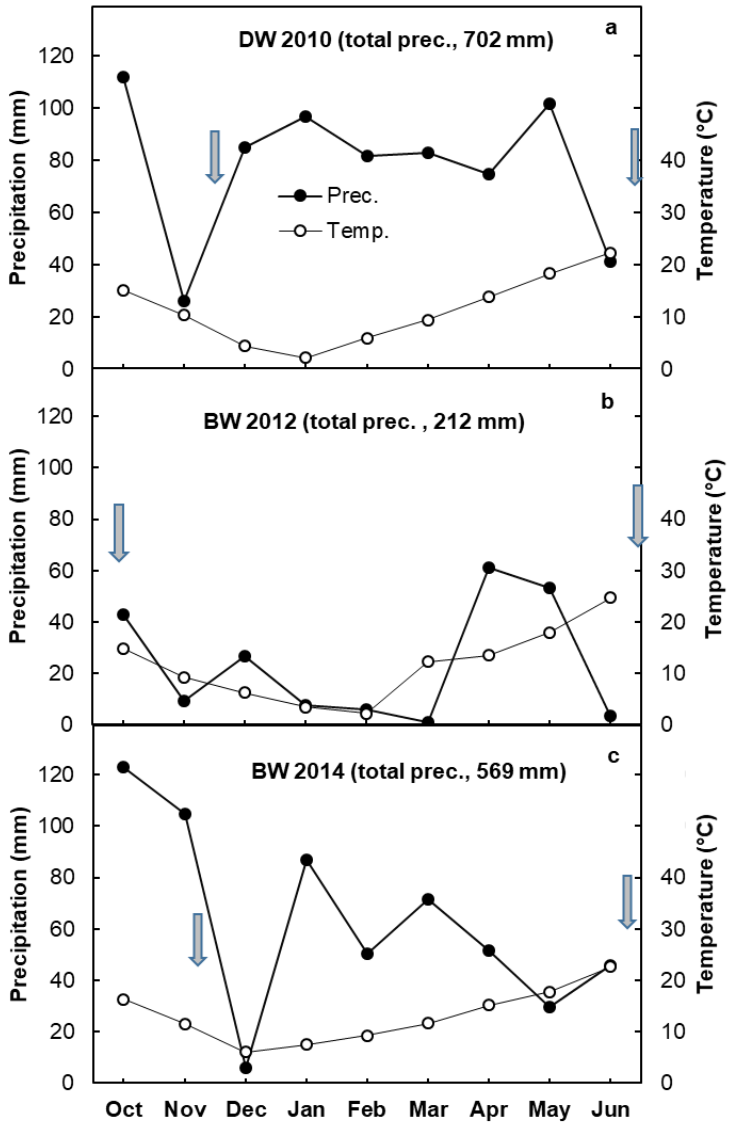

Figure 2.4. Precipitation and temperature patterns extending from October to June according to Bagnouls and Gaussen (1953) in the 3 years with winter cereals (DW 2010, and BW 2012 and 2014). Months where average temperature exceeds the double of total precipitation are considered a dry period. Grey arrows indicate seeding and maturation time.

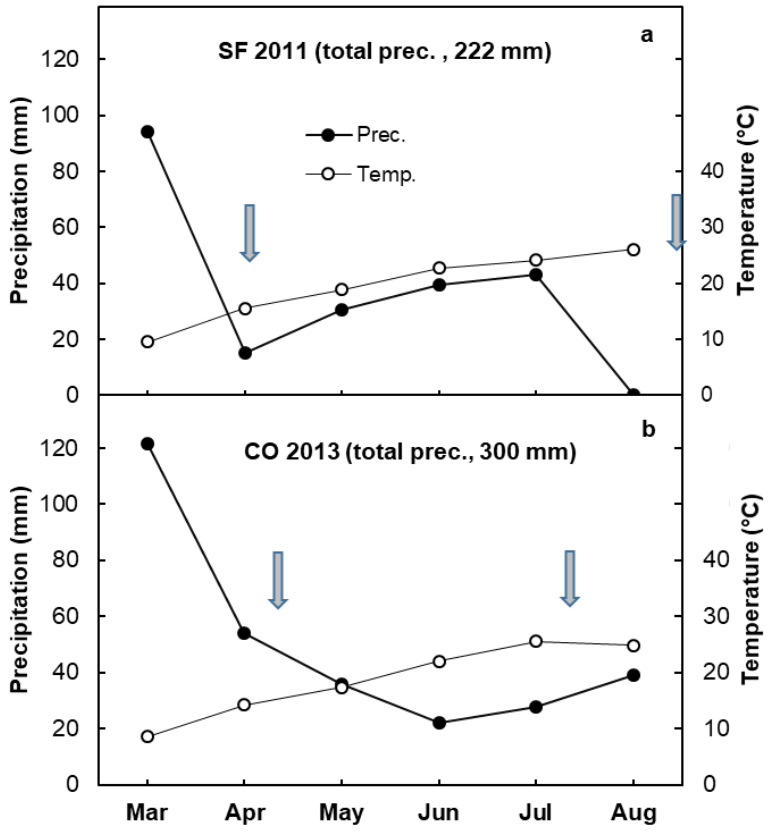

Figure 2.5. Precipitation and temperature patterns extending from March to August according to Bagnouls and Gaussen (1953) in the 2 years with spring dicot (SF 2011 and CO 2013). Months where average temperature exceeds the double of total precipitation are considered a dry period. Grey arrows indicate seeding and maturation time.

2.3. Summary and Conclusions

Site-specific YSCs are the basis in precision agriculture by understanding where variable cropping inputs are needed, based on spatial and temporal characteristics of the field. This paper defined the YSCs based on spatial and temporal maps depicted across the field over a series of five-year crop yields. Spatial variability maps were shown relatively stable, exhibiting high yield in southern part and low yield in the norther part of the field.

Crop spatio-temporal variability over a series of years is considerably alinged with the spatial soil properties and apparent electrical conductivity (ECa) classification within YSCs. However, each single factor may or may not affect the ECa and ultimate yield, which increases the difficulty to understand causes and effects on crop growth and

development. These factors could be related to soil, pests and diseases, meteorology, human activities, and interactions among them influencing crop yields. Thus, varying crop yield within field is a challenge for farming community, unless which factors influence the yield over each year are known.

The consistent low yield in the north part of the field could be cultivated separately from the south part, with tree plantation or vineyear as cultivated in the past (Figure 2.6). Moreover, this area is economically important, covering 2.8 ha, to maximize the yield productivity over existing cultivation. Hence, unstable class does not require the separate cultivation because this area gives enough yield, but changed with time. Preliminary correlation analysis, and classification of selected soil properties with spatiotemporal yield confirmed that YSCs were relatively consistent with spatial soil data. However, in-season information is helpful to understand whether an unstable field area (class) will behave as high or low yielding area in a particular year, hence providing farmers with useful insights about the application of fertilizers in a site-specific way. If the weather pattern of the year is favorable, then unstable classes could be managed as high yielding zones; otherwise, as low yielding zones. The present study demonstrates that YSCs are more practical, cost-effective for variable rate inputs, and target soil-sampling plans for optimizing the crop yields with minimum economic resources and environmental impacts.

Figure 2.6. Field history (1976-2006).

General Discussion and Conclusions

Application of precision agriculture for variable rate decisions within the same field is already being successfully used in farming practices, with the aim of using minimum economic resources involving low environmental impacts. The appraisal of soil and crop characteristics is an important premise to this goal, as precision agriculture relies on timely information to produce crop inputs/practices to be implemented out site specifically.

In this framework, in the first part of this thesis various Landsat imagery were downloaded from different Landsat missions such as Landsat 5, 7 and 8 during the five growing season of DW 2010, SF 2011, BW 2012, CO 2013 and BW 2014. The following vegetation indices (Vis) were calculated: Normalized Difference Vegetation Index (NDVI), Enhanced Vegetation Index (EVI), Soil Adjusted Vegetation Index (SAVI), Green Normalized Difference Vegetation Index (GNDVI), Green Chlorophyll Index (GCI), and Simple Ratio (SR). The first simple correlation was assessed to determine the consistency between vegetation indices and final georeferenced yield data, using the 30 m spatial resolution (SpR) of the above referred satellite missions, for the determination of critical growth stages for each crop. Furthermore, a geostatistical analysis was applied to georeferenced crop yield and remote vegetation data, to determine the SpD in their data distribution and GY maps. For DW 2010, NDVI was shown the best index during elongation stages from node 6 to mid-booting (BBCH growth stage 36-43), indicating a very high consistency with wheat yield. For SF 2011, we found that GNDVI and SR showed the highest correlations from inflorescence to flower declining (BBCH 51-67). For BW 2012, stem elongation from 3rd to 6th node emergence (BBCH 33-36) showed consistent high correlations under all studied VIs, although EVI and SR exhibited slightly higher correlations during the wheat prediction period. For CO 2013, flowering to the beginning of seed ripening (BBCH 63-81) was found a critical time because of enough biomass structure during maturity stages, and EVI, NDVI, and SR were found topmost indices during these stages. For BW 2014, all studied VIs showed the highest correlation from flag leaf to grain filling, where NDVI, GCI, and SR were found best ones (BBCH 37-77). Higher correlations during initial growth stages of surveyed winter cereals are associated with showing the fact that the long-time elapsed from seeding to the time when the first imagery was acquired may have served the plant to better sense the environmental differences, and translate them into a spectral response in good agreement with final GY. Winter wheat showed minimum correlations during maturity stages

because wheat plants go into senescence during maturity, thus decreasing their reactivity to different ambient conditions. The two spring dicots featuring a shorter cycle also necessitated a certain amount of time to attain maximum biomass structure, and good correlations between VIs and GY were achieved at later stages than cereals. Pixel level study showed strong agreements between five classes (i.e., quintiles) of VIs and the corresponding five classes of GY, resulting in a final agreement between 64 and 86 %. It is generally sensed that water availability, nutrient uptake, crop management practices, weather conditions, and diseases may influence crop canopy reflectance to a varying extent, also interacting among them. Therefore, remote VIs cannot 100 % correspond to GY data due to abundant variations in reflectance properties of crop canopy during the growing period.

In this respect, the combined use of Sentinel-2A and Landsat data, providing a larger number of data and a higher SpR, would foster a more detailed assessment that could be especially useful in identifying growth stages in different crops (Griffiths et al., 2019). Data fusion from different platforms would overcome drawbacks related to the use of a single, medium resolution satellite by improving the field temporal sampling.

Future monitoring possibilities fostered by the Copernicus Sentinel 2 mission from the European Space Agency will allow imagery to be acquired from the year 2015 onwards, with spectral channels aligned with Landsat and Spot satellites. Improvements are expected from a higher SpR (10-20 m) and radiometric resolution (reflectance registered with 16 bit). This is coupled with a revisit frequency of 2-3 days, ensuring the creation of dense time series for crop growth monitoring.

Lastly, the use of Landsat collection level-1 data raises the issue of atmospheric data correction. In our study, we decided to apply a simple correction as the DOS1 method despite the good quality data (Tier 1 Level-1 Precision Terrain data), to ensure comparability of surface reflectance among multi-temporal images (Song et al., 2001; Lu et al., 2002). More sophisticated models for atmospheric correction, as those distributed by USGS under Climate Data Records, were not adopted as we could not collect specific in-field measurements. However, usefulness of atmospheric correction is questioned due to the risk of adding more errors (Young et al, 2017), which is especially true in the case of large areas surveyed.

Based on this, good prospects may be envisaged for improved yield forecasts over large agricultural areas, as well as better support to farmers for specific decision management strategies.

In the 2nd part of this thesis, yield stability classes (YSCs) were delineated based on spatio-temporal variability of crop yield over multiple years, as a different approach to site-specific field management. The following three YSCs were produced: high yielding and stable (HYS), low yielding and stable (LYS) and unstable. Crop spatio-temporal variation was investigated in terms of simple correlation and statistical differences of stable soil properties within YSCs. In addition, we examined the moisture balance, i.e. the relationship between precipitation and evapo-transpiration, and temperature trends during the growing season of surveyed crops, as potential factors determining temporal yield variation among years (unstable zones). Yield stability map showed that the southern part of the field always produced high yield, whereas the northern part consistently produced lower yield. Yield stability classes have been showing well-defined size and position of the spatial variability within field, as premise for future field management practices to be deployed in a site-specific way.

Soil analysis determined that a higher level of sand affected crop yield in the northern field portion, whereas a lower sand content did not show a sizeable effect on the spatial pattern of crop yield. YSCs were positively correlated with stable soil properties. However, we observed that higher contents of silt, clay and CEC were consistent with HYS class, giving maximum yield (122 %). However, lowest contents were found in unstable class, given slightly higher yield (83 %) than LYS. The lowest soil apparent electrical conductivity (ECa) was also found consistent with HYS class, and produced highest yield (122 %) than LYS and unstable classes. However, higher ECa values were found inconsistent with LYS and unstable class., which might be due to the complex interaction of soil and environmental factors influencing ECa and ultimate yield.

Observation of meteorological data indicate that the five rainfed crops suffered from an erratic pattern of weather elements, which varied the crop productivity among years. Therefore, in-season weather information is a very important clue for farmers to decide whether unstable zones should be treated as high yielding or low yielding zones during a specific time period. If the weather pattern of the year is favorable, then unstable zones could be managed as high yielding; otherwise, as low yielding. For fertilization, crop simulation models are used for calculating the amount of nitrogen fertilizer based on the crop condition till the time of side-dressing, and on the environmental scenario envisaged for the remaining part of the crop season. In this way, farmers can reduce their risk while making decisions, while at the same time following the principle of applying optimal dosage of nitrogen by considering the profit and environmental impact. Generally, if the drought stress occurs during heading or

flowering, the following nitrogen doses should be increase to enhance protein contents of grain crops, but this practice is most common in dry part of the world and depends on the geographical location of specified country. Hence, farmers should use recommended uniform fertilizer rates with respect to space and time by considering the in-season weather conditions. We have found that stable yield zones must be managed by strategic planning, whereas unstable zones by tactical approach, i.e. following the remote sensing approach or weather scenario within season to determine the management clue with tactical strategic approach.

References

Ahirwar, S., Swarnkar, R., Bhukya, S., & Namwade, G. (2019). Application of drone in agriculture. *International Journal Curr. Microbiological Applied Science*, *8*, 2500-2505.

Allen, R. G., Pereira, L. S., Raes, D., & Smith, M. (1998). Crop evapotranspiration-Guidelines for computing crop water requirements-FAO Irrigation and drainage paper 56. *Fao, Rome*, *300*(9), D05109.

Amado, T. J. C., Pontelli, C. B., Santi, A. L., Viana, J. H. M., & Sulzbach, L. A. D. S. (2007). Variabilidade espacial e temporal da produtividade de culturas sob sistema plantio direto. *Pesquisa Agropecuária Brasileira*, *42*(8), 1101-1110.

Amorosi, A., Centineo, M. C., Dinelli, E., Lucchini, F., & Tateo, F. (2002). Geochemical and mineralogical variations as indicators of provenance changes in Late Quaternary deposits of SE Po Plain. *Sedimentary Geology*, *151*(3-4), 273-292.

Andreo, V. (2013). Remote sensing and geographic information systems in precision farming. *Instituto de Altos Estudios Espaciales "Mario Gulich"-CONAE/UNC Facultad de Matematica. Astronomia y Física–UNC*.

Asfaw, A., Simane, B., Hassen, A., & Bantider, A. (2018). Variability and time series trend analysis of rainfall and temperature in northcentral Ethiopia: A case study in Woleka sub-basin. *Weather and Climate Extremes*, *19*, 29-41.

Ayankojo, I. T., Morgan, K. T., & Mahmoud, K. (2019). Evaluation of Soil Water and Nitrogen Distribution by Site-Specific Irrigation Scheduling Method in Tomato Crop Grown on Sandy Soil. *Soil Science Society of America Journal*.

Baghdadi, N., & Zribi, M. (2016). *Land Surface Remote Sensing in Agriculture and Forest*. Elsevier.

Bagnouls, F. (1953). Saison sèche et indice xérothermique. *Bull Soc His nat Toulouse*, *88*, 193-239.

Barbanti, L., Adroher, J., Damian, J. M., Di Virgilio, N., Falsone, G., Zucchelli, M., & Martelli, R. (2018). Assessing wheat spatial variation based on proximal and remote spectral vegetation indices and soil properties. *Italian Journal of Agronomy*, *13*(1).

Barbanti, L., Vecchi, A., Sher, A., & Di Girolamo, G. (2012, June). Sweet, fibre and forage sorghum (Sorghum bicolor (L.) Moench) resilience to varying seeding time, in view of supplying biomass for energy uses. In *Proceedings of the 20th Biomass Conference and Exhibition, Milan, Italy* (pp. 18-22).

Basnet, B., Kelly, R., Jensen, T., Strong, W., Apan, A., & Butler, D. (2003). Delineation of management zones using multiple crop yield data. In *Proceedings of the 16th*

Triennial Congress of the International Soil Tillage Research Organisation (ISTRO 2003)(pp. 69-75). University of Queensland.

Basso, B., Cammarano, D., & De Vita, P. (2004). Remotely sensed vegetation indices: Theory and applications for crop management. *Rivista Italiana di Agrometeorologia*, *1*(5), 36-53.

Basso, B., Dobrowolski, J., & McKay, C. (2017). From the Dust Bowl to Drones to Big Data: The Next Revolution in Agriculture. *Geo. J. Int'l Aff.*, *18*, 158.

Basso, B., Fiorentino, C., Cammarano, D., & Schulthess, U. (2016). Variable rate nitrogen fertilizer response in wheat using remote sensing. *Precision agriculture*, *17*(2), 168-182.

Basso, B., Ritchie, J. T., Cammarano, D., & Sartori, L. (2011). A strategic and tactical management approach to select optimal N fertilizer rates for wheat in a spatially variable field. *European Journal of Agronomy*, *35*(4), 215-222.

Bellingham, B. K. (2009). Method for irrigation scheduling based on soil moisture data acquisition. *Irrigation District SustainabilityStrategies to Meet the Challenges*, 383.

Benedetti, R., & Rossini, P. (1993). On the use of NDVI profiles as a tool for agricultural statistics: The case study of wheat yield estimate and forecast in Emilia Romagna. *Remote Sensing of Environment*, *45*(3), 311-326.

Bhunia, G. S., Shit, P. K., & Maiti, R. (2018). Comparison of GIS-based interpolation methods for spatial distribution of soil organic carbon (SOC). *Journal of the Saudi Society of Agricultural Sciences*, *17*(2), 114-126.

Blackmore, S. (1999). Remedial correction of yield map data. *Precision agriculture*, *1*(1), 53-66.

Blackmore, S. (2000). The interpretation of trends from multiple yield maps. *Computers and electronics in agriculture*, *26*(1), 37-51.

Blackmore, S. (2003). *The role of yield maps in precision farming* (Doctoral dissertation, Cranfield University).

Blackmore, S., Godwin, R. J., & Fountas, S. (2003). The analysis of spatial and temporal trends in yield map data over six years. *Biosystems engineering*, *84*(4), 455-466.

Boegh, E., Søgaard, H., Broge, N., Hasager, C. B., Jensen, N. O., Schelde, K., & Thomsen, A. (2002). Airborne multispectral data for quantifying leaf area index, nitrogen concentration, and photosynthetic efficiency in agriculture. *Remote sensing of Environment*, *81*(2-3), 179-193.

Botarelli, L., Brunetti, A., Pasquini, A., & Zinoni, F. (1999). Aspetti generali delle osservazioni agrofenologiche. *Collana di A-grofenologia, MiPAF, PF Phenagri, Fenologia per l'Agricoltura. Vol*, *1*, 110.

Brian McConkey, P. B., Lafond, G. P., Moulin, A., & Pelcat, Y. (2004). Optimal time for remote sensing to relate to crop grain yield on the Canadian prairies. *Canadian Journal of Plant Science*, *84*(1), 97-103.

Brisson, N., Gate, P., Gouache, D., Charmet, G., Oury, F. X., & Huard, F. (2010). Why are wheat yields stagnating in Europe? A comprehensive data analysis for France. *Field Crops Research*, *119*(1), 201-212.

Bullock, D. S., & Bullock, D. G. (2000). Economic optimality of input application rates in precision farming. *Precision Agriculture*, *2*(1), 71-101.

Butts-Wilmsmeyer, C., Seebauer, J., Singleton, L., & Below, F. (2019). Weather during key growth stages explains grain quality and yield of maize. *Agronomy*, *9*(1), 16.

Cambardella, C. A., Moorman, T. B., Parkin, T. B., Karlen, D. L., Novak, J. M., Turco, R. F., & Konopka, A. E. (1994). Field-scale variability of soil properties in central Iowa soils. *Soil science society of America journal*, *58*(5), 1501-1511.

Carter, E. K., Melkonian, J., Riha, S. J., & Shaw, S. B. (2016). Separating heat stress from moisture stress: analyzing yield response to high temperature in irrigated maize. *Environmental Research Letters*, *11*(9), 094012.

Chang, J., Clay, D. E., Carlson, C. G., Reese, C. L., Clay, S. A., & Ellsbury, M. M. (2004). Defining yield goals and management zones to minimize yield and nitrogen and phosphorus fertilizer recommendation errors. *Agronomy Journal*, *96*(3), 825-831.

Chavez Jr, P. S. (1988). An improved dark-object subtraction technique for atmospheric scattering correction of multispectral data. *Remote sensing of environment*, *24*(3), 459-479.

Clark, I. (1979). *Practical geostatistics* (Vol. 3, p. 129). London: Applied Science Publishers.

Cohen, W. B., Spies, T. A., & Bradshaw, G. A. (1990). Semivariograms of digital imagery for analysis of conifer canopy structure. *Remote Sensing of Environment*, *34*(3), 167-178.

Congedo, L. (2016). Semi-automatic classification plugin documentation. *Release*, *4*(0.1), 29.

Cornell, J. A., & Berger, R. D. (1987). Factors that influence the value of the coefficient of determination in simple linear and nonlinear regression models. *Phytopathology*, *77*(1), 63-70.

Corwin, D. L. (2005, July). Delineating site-specific crop management units: Precision agriculture application in GIS. In *Proceedings of the 2005 ESRI International Users Conference, San Diego, CA, USA* (pp. 25-29).

Corwin, D. L. (2013). 8 Site-specific management and delineating management zones. *Precision Agriculture for Sustainability and Environmental Protection*, 135-157.

Corwin, D. L., & Lesch, S. M. (2003). Application of soil electrical conductivity to precision agriculture. *Agronomy journal*, *95*(3), 455-471.

Corwin, D. L., & Lesch, S. M. (2005). Characterizing soil spatial variability with apparent soil electrical conductivity: I. Survey protocols. *Computers and electronics in agriculture*, *46*(1-3), 103-133.

Corwin, D. L., Lesch, S. M., Shouse, P. J., Soppe, R., & Ayars, J. E. (2003). Identifying soil properties that influence cotton yield using soil sampling directed by apparent soil electrical conductivity. *Agronomy Journal*, *95*(2), 352-364.

Cuculeanu, V., Tuinea, P., & Bălteanu, D. (2002). Climate change impacts in Romania: Vulnerability and adaptation options. *GeoJournal*, *57*(3), 203-209.

da Silva, J. M. (2006). Analysis of the spatial and temporal variability of irrigated maize yield. *Biosystems engineering*, *94*(3), 337-349.

Dadhwal, V. K., & Ray, S. S. (2000). Crop assessment using remote sensing-part-II: Crop condition and yield assessment. *Indian Journal of Agricultural Economics*, *55*(2), 55-67.

Dashtpagerdi, M. M., Vagharfard, H., & Honarbakhsh, A. (2013). Application of cross-validation technique for zoning of groundwater levels in Shahrekord plain. *Agricultural Sciences*, *4*(07), 329-333.

Daughtry, C. S. T., Walthall, C. L., Kim, M. S., De Colstoun, E. B., & McMurtrey Iii, J. E. (2000). Estimating corn leaf chlorophyll concentration from leaf and canopy reflectance. *Remote sensing of Environment*, *74*(2), 229-239.

De Caires, S. A., Wuddivira, M. N., & Bekele, I. (2015). Spatial analysis for management zone delineation in a humid tropic cocoa plantation. *Precision Agriculture*, *16*(2), 129-147.

Demirbaş, N. (2018). Precision Agriculture in Terms of Food Security: Needs for The Future. *Precis. Agric*, *27*.

Di Virgilio, N., Monti, A., & Venturi, G. (2007). Spatial variability of switchgrass (Panicum virgatum L.) yield as related to soil parameters in a small field. *Field crops research*, *101*(2), 232-239.

Domínguez, J. A., Kumhálová, J., & Novák, P. (2017). Assessment of the relationship between spectral indices from satellite remote sensing and winter oilseed rape yield. *Agron. Res*, *15*(1), 55-68.

Dresselhaus, T., & Hückelhoven, R. (2018). Biotic and Abiotic Stress Responses in Crop Plants.

Duncan, H. A. (2012). Locating the variability of soil water holding capacity and understanding its effects on deficit irrigation and cotton lint yield.

Elachi, C., & Van Zyl, J. J. (2006). *Introduction to the physics and techniques of remote sensing* (Vol. 28). John Wiley & Sons.

Elwadie, M. E., Pierce, F. J., & Qi, J. (2005). Remote sensing of canopy dynamics and biophysical variables estimation of corn in Michigan. *Agronomy Journal*, *97*(1), 99-105.

Feller, C., Bleiholder, H., Buhr, L., Hack, H., Hess, M., Klose, R., ... & Weber, E. (1995). Phanologische Entwicklungsstadien von Gemusepflanzen I. Zwiebel-, Wurzel-, Knollen-und Blattgemuse. *Nachrichtenblatt des Deutschen Pflanzenschutzdienstes*, *47*(8), 193-205.

Field, C. B., Barros, V. R., Mastrandrea, M. D., Mach, K. J., Abdrabo, M. K., Adger, N., ... & Burkett, V. R. (2014). Summary for policymakers. In *Climate change 2014: impacts, adaptation, and vulnerability. Part A: global and sectoral aspects. Contribution of Working Group II to the Fifth Assessment Report of the Intergovernmental Panel on Climate Change* (pp. 1-32). Cambridge University Press.

Flynn, P. (2003). Biotic vs. abiotic—distinguishing disease problems from environmental stresses. *ISU Entomology*. Retrieved 16 May 2013.

Fraisse, C. W., Sudduth, K. A., & Kitchen, N. R. (2001). Delineation of site-specific management zones by unsupervised classification of topographic attributes and soil electrical conductivity. *Transactions of the ASAE*, *44*(1), 155.

Fraisse, C. W., Sudduth, K. A., Kitchen, N. R., & Fridgen, J. J. (1999). Use of unsupervised clustering algorithms for delineating within-field management zones. *St. Joseph: American Society of Agricultural Engineers*.

Frieler, K., Schauberger, B., Arneth, A., Balkovič, J., Chryssanthacopoulos, J., Deryng, D., ... & Olin, S. (2017). Understanding the weather signal in national crop-yield variability. *Earth's future*, *5*(6), 605-616.

Geipel, J., Link, J., & Claupein, W. (2014). Combined spectral and spatial modeling of corn yield based on aerial images and crop surface models acquired with an unmanned aircraft system. *Remote Sensing*, *6*(11), 10335-10355.

Georgi, C., Spengler, D., Itzerott, S., & Kleinschmit, B. (2018). Automatic delineation algorithm for site-specific management zones based on satellite remote sensing data. *Precision agriculture*, *19*(4), 684-707.

Gibbons, G. (2000). Turning a farm art into science-an overview of precision farming. *URL: http://www. precisionfarming. com*.

Gitelson, A. A. (2016). 15 Remote Sensing Estimation of Crop Biophysical Characteristics at Various Scales. In *Hyperspectral Remote Sensing of Vegetation*; Thenkabail, P.S., Lyon, J. G., Huete, A., Eds.; CRC Press: Boca Raton, FL, USA, pp. 329–354.

Gitelson, A. A., Gritz, Y., & Merzlyak, M. N. (2003). Relationships between leaf chlorophyll content and spectral reflectance and algorithms for non-destructive chlorophyll assessment in higher plant leaves. *Journal of plant physiology*, *160*(3), 271-282.

Gitelson, A. A., Kaufman, Y. J., & Merzlyak, M. N. (1996). Use of a green channel in remote sensing of global vegetation from EOS-MODIS. *Remote sensing of Environment*, *58*(3), 289-298.

Gitelson, A. A., Vina, A., Ciganda, V., Rundquist, D. C., & Arkebauer, T. J. (2005). Remote estimation of canopy chlorophyll content in crops. *Geophysical Research Letters*, *32*(8).

Gomes, F.P. (1985). Curso de estatística experimental. Sixth edition; Nobel: Piracicaba, Brasil, p. 430.

Goovaerts, P. (1997). *Geostatistics for natural resources evaluation*. Oxford University Press: New York, USA.

Griffin, T. W., Lowenberg-DeBoer, J., Lambert, D. M., Peone, J., Payne, T., & Daberkow, S. G. (2004). Adoption, profitability and making better use of precision farming data. Staff paper# 04-06. *Purdue University, Dept. of Agricultural Economics, West Lafayette, IN, USA*.

Griffiths, P., Nendel, C., & Hostert, P. (2019). Intra-annual reflectance composites from Sentinel-2 and Landsat for national-scale crop and land cover mapping. *Remote sensing of environment*, *220*, 135-151.

Guedes Filho, O., Vieira, S. R., Chiba, M. K., Nagumo, C. H., & Dechen, S. C. F. (2010). Spatial and temporal variability of crop yield and some Rhodic Hapludox properties under no-tillage. *Revista Brasileira de Ciência do Solo*, *34*(1), 1-14.

Gunzenhauser, B., & Shanahan, J. (2011). Using multi-year yield analysis to create management zones for variable rate seeding. *Johnston: DuPont Pioneer*.

Gupta, R. D., Arora, S., Gupta, G. D., & Sumberia, N. M. (2010). Soil physical variability in relation to soil erodibility under different land uses in foothills of Siwaliks in NW India. *Tropical Ecology*, *51*(2), 183.

Hanks, J., & Ritchie, J. T. (1991). Modeling Plant and Soil Systems: Agronomy Monograph No. 31. *ASA-CSSASSSA, Madison, WI*.

Hanna, A. Y., Harlan, P. W., & Lewis, D. (1982). Soil available water as influenced by landscape position and aspect 1. *Agronomy Journal*, *74*(6), 999-1004.

Hatfield, J. L., & Prueger, J. H. (2010). Value of using different vegetative indices to quantify agricultural crop characteristics at different growth stages under varying management practices. *Remote Sensing*, *2*(2), 562-578.

Hatfield, J. L., Asrar, G., & Kanemasu, E. T. (1984). Intercepted photosynthetically active radiation estimated by spectral reflectance. *Remote Sensing of Environment*, *14*(1-3), 65-75.

Hatfield, J. L., Gitelson, A. A., Schepers, J. S., & Walthall, C. L. (2008). Application of spectral remote sensing for agronomic decisions. *Agronomy Journal*, *100*(Supplement_3), S-117.

Hedley, C. B., Bradbury, S., Ekanayake, J., Yule, I. J., & Carrick, S. (2010, November). Spatial irrigation scheduling for variable rate irrigation. In *Proceedings of the New Zealand Grassland Association* (Vol. 72, pp. 97-102). New Zealand Grassland Association.

Herbei, M. V., & Sala, F. (2015). Use landsat image to evaluate vegetation stage in sunflower crops. *AgroLife Scientific Journal*, *4*(1), 79-86.

Higley, L. G., & Peterson, R. K. (Eds.). (2001). *Biotic Stress and Yield Loss*. CRC Press.

Holmes, A. (2017). Transforming variability to profitability–variable seed rates in New Zealand maize. In *7th Asian-Australasian Conference on Precision Agriculture*.

Homdee, T., Pongput, K., & Kanae, S. (2016). A comparative performance analysis of three standardized climatic drought indices in the Chi River basin, Thailand. *Agriculture and Natural Resources*, *50*(3), 211-219.

Huete, A. R. (1988). A soil-adjusted vegetation index (SAVI). *Remote sensing of environment*, *25*(3), 295-309.

Huete, A., Didan, K., Miura, T., Rodriguez, E. P., Gao, X., & Ferreira, L. G. (2002). Overview of the radiometric and biophysical performance of the MODIS vegetation indices. *Remote sensing of environment*, *83*(1-2), 195-213.

Huggins, D. R., & Alderfer, R. D. (1995, January). Yield variability within a long-term corn management study: Implications for precision farming. In *Site-specific*

management for agricultural systems (No. sitespecificman, pp. 417-426). American Society of Agronomy, Crop Science Society of America, Soil Science Society of America.

Iizumi, T., & Ramankutty, N. (2015). How do weather and climate influence cropping area and intensity?. *Global Food Security*, *4*, 46-50.

Inman, D., Khosla, R., Reich, R., & Westfall, D. G. (2008). Normalized difference vegetation index and soil color-based management zones in irrigated maize. *Agronomy journal*, *100*(1), 60-66.

Isaaks, E. H., & Srivastava, R. M. (1989). Applied geostatistics. Oxford Univ. Press, New York. *Applied geostatistics. Oxford Univ. Press, New York.*

Jaynes, D. B., Colvin, T. S., & Kaspar, T. C. (2005). Identifying potential soybean management zones from multi-year yield data. *Computers and electronics in agriculture*, *46*(1-3), 309-327.

Jensen, J. R. (2007). Remote Sensing of the Environment: An Earth Resource Prerspective, 608 Pearson Prentice Hall. *United States*.

Johnson, C. K., Mortensen, D. A., Wienhold, B. J., Shanahan, J. F., & Doran, J. W. (2003). Site-specific management zones based on soil electrical conductivity in a semiarid cropping system. *Agronomy journal*, *95*(2), 303-315.

Jordan, C. F. (1969). Derivation of leaf-area index from quality of light on the forest floor. *Ecology*, *50*(4), 663-666.

Journel, A. G., & Journel, A. G. (1989). *Fundamentals of geostatistics in five lessons* (Vol. 8). Washington, DC: American Geophysical Union.

Kang, Y., Khan, S., & Ma, X. (2009). Climate change impacts on crop yield, crop water productivity and food security–A review. *Progress in natural Science*, *19*(12), 1665-1674.

Karim, M. A., Hamid, A., & Rahman, S. (2000). Grain growth and yield performance of wheat under subtropical conditions: II. Effect of water stress at reproductive stage. *Cereal Research Communications*, 101-107.

Kayad, A. G., Al-Gaadi, K. A., Tola, E., Madugundu, R., Zeyada, A. M., & Kalaitzidis, C. (2016). Assessing the spatial variability of alfalfa yield using satellite imagery and ground-based data. *PloS one*, *11*(6), e0157166.

Kersten, G. E., Mikolajuk, Z., & Yeh, A. G. O. (2000). *Decision support systems for sustainable development: a resource book of methods and applications*. Springer Science & Business Media.

Khosla, R., Fleming, K., Delgado, J. A., Shaver, T. M., & Westfall, D. G. (2002). Use of site-specific management zones to improve nitrogen management for precision agriculture. *Journal of Soil and Water Conservation*, *57*(6), 513-518.

Khosla, R., Westfall, D. G., Reich, R. M., Mahal, J. S., & Gangloff, W. J. (2010). Spatial variation and site-specific management zones. In *Geostatistical applications for precision agriculture* (pp. 195-219). Springer, Dordrecht.

Klosterman, S., & Richardson, A. D. (2017). Observing spring and fall phenology in a deciduous forest with aerial drone imagery. *Sensors*, *17*(12), 2852.

Kravchenko, A. N., & Bullock, D. G. (2000). Correlation of corn and soybean grain yield with topography and soil properties. *Agronomy Journal*, *92*(1), 75-83.

Kuiawski, A. C. M. B., Safanelli, J. L., Bottega, E. L., Oliveira Neto, A. M. D., & Guerra, N. (2017). Vegetation indexes and delineation of management zones for soybean1. *Pesquisa Agropecuária Tropical*, *47*(2), 168-177.

Kukal, M. S., & Irmak, S. (2018). Climate-driven crop yield and yield variability and climate change impacts on the US great plains agricultural production. *Scientific reports*, *8*(1), 3450.

Kumhálová, J., & Matějková, Š. (2017). Yield variability prediction by remote sensing sensors with different spatial resolution. *International Agrophysics*, *31*(2), 195-202.

Kumhálová, J., Zemek, F., Novák, P., Brovkina, O., & Mayerová, M. (2014). Use of Landsat images for yield evaluation within a small plot. *Plant, Soil and Environment*, *60*(11), 501-506.

Labus, M. P., Nielsen, G. A., Lawrence, R. L., Engel, R., & Long, D. S. (2002). Wheat yield estimates using multi-temporal NDVI satellite imagery. *International Journal of Remote Sensing*, *23*(20), 4169-4180.

Lancashire, P. D., Bleiholder, H., Boom, T. V. D., Langelüddeke, P., Stauss, R., Weber, E., & Witzenberger, A. (1991). A uniform decimal code for growth stages of crops and weeds. *Annals of applied Biology*, *119*(3), 561-601.

Large, E. C. (1954). Growth stages in cereals illustration of the Feekes scale. *Plant pathology*, *3*(4), 128-129.

Lark, R. M., & Stafford, J. V. (1996 a). Classification as a first step in the interpretation of temporal and spatial variability of crop yield. *Aspects of Applied Biology,* 46, 139–142.

Lark, R. M., & Stafford, J. V. (1996 b). Consistency and change in spatial variability of crop yield over successive seasons: methods of data analysis. In: 3rd International

Conference on Precision Agriculture. In: Robert, P.C., Rust, R.H., Larson, W.E. (Eds.). Madison, Wisconsin, USA, pp. 141-149.

Leopold, U., Heuvelink, G. B., Tiktak, A., Finke, P. A., & Schoumans, O. (2006). Accounting for change of support in spatial accuracy assessment of modelled soil mineral phosphorous concentration. *Geoderma*, *130*(3-4), 368-386.

Lesch, S. M., Rhoades, J. D., & Corwin, D. L. (2000). ESAP-95 Version 2.01 R: User manual and tutorial guide: Research Rpt. 146, USDA-ARS George E. *Brown, Jr. Salinity Laboratory, Riverside, CA*.

Lesch, S. M., Strauss, D. J., & Rhoades, J. D. (1995). Spatial prediction of soil salinity using electromagnetic induction techniques: 2. An efficient spatial sampling algorithm suitable for multiple linear regression model identification and estimation. *Water resources research*, *31*(2), 387-398.

Li, Y., Shi, Z., Wu, C. F., Li, H. Y., & Li, F. (2008). Determination of potential management zones from soil electrical conductivity, yield and crop data. *Journal of Zhejiang University Science B*, *9*(1), 68-76.

Lindblom, J., Lundström, C., Ljung, M., & Jonsson, A. (2017). Promoting sustainable intensification in precision agriculture: review of decision support systems development and strategies. *Precision Agriculture*, *18*(3), 309-331.

Long, D. S. (1998). Spatial autoregression modeling of site-specific wheat yield. *Geoderma*, *85*(2-3), 181-197.

Lu, D., Mausel, P., Brondizio, E., & Moran, E. (2002). Assessment of atmospheric correction methods for Landsat TM data applicable to Amazon basin LBA research. *International Journal of Remote Sensing*, *23*(13), 2651-2671.

Ma, L., Liu, Y., Zhang, X., Ye, Y., Yin, G., & Johnson, B. A. (2019). Deep learning in remote sensing applications: A meta-analysis and review. *ISPRS journal of photogrammetry and remote sensing*, *152*, 166-177.

Maestrini, B., & Basso, B. (2018a). Drivers of within-field spatial and temporal variability of crop yield across the US Midwest. *Scientific reports*, *8*(1), 14833.

Maestrini, B., & Basso, B. (2018b). Predicting spatial patterns of within-field crop yield variability. *Field crops research*, *219*, 106-112.

Maimaitijiang, M., Ghulam, A., Sidike, P., Hartling, S., Maimaitiyiming, M., Peterson, K., . & Burken, J. (2017). Unmanned Aerial System (UAS)-based phenotyping of soybean using multi-sensor data fusion and extreme learning machine. *ISPRS Journal of Photogrammetry and Remote Sensing*, *134*, 43-58.

Mallarino, A. P., & Wittry, D. J. (2004). Efficacy of grid and zone soil sampling approaches for site-specific assessment of phosphorus, potassium, pH, and organic matter. *Precision Agriculture*, *5*(2), 131-144.

Mariani, L., & Ferrante, A. (2017). Agronomic management for enhancing plant tolerance to abiotic stresses—drought, salinity, hypoxia, and lodging. *Horticulturae*, *3*(4), 52.

Marino, S., & Alvino, A. (2019). Detection of Spatial and Temporal Variability of Wheat Cultivars by High-Resolution Vegetation Indices. *Agronomy*, *9*(5), 226.

Maynou, F. (1998). The application of geostatistics in mapping and assessment of demersal resources, Nephrops norvegicus in the northwestern Mediterranean: a case study. *Scientia Marina*, *62*(S1), 117-133.

McKinion, J. M., Jenkins, J. N., Akins, D., Turner, S. B., Willers, J. L., Jallas, E., & Whisler, F. D. (2001). Analysis of a precision agriculture approach to cotton production. *Computers and Electronics in Agriculture*, *32*(3), 213-228.

McKinion, J. M., Willers, J. L., & Jenkins, J. N. (2010). Spatial analyses to evaluate multi-crop yield stability for a field. *Computers and Electronics in Agriculture*, *70*(1), 187-198.

Meier, U. (2001). Growth stages of mono-and dicotyledonous plants. BBCH monograph, 2nd edn. Federal Biological Research Centre for Agriculture and Forestry.

Metzger, M. J., Bunce, R. G. H., Jongman, R. H., Mücher, C. A., & Watkins, J. W. (2005). A climatic stratification of the environment of Europe. *Global ecology and biogeography*, *14*(6), 549-563.

Militino, A., Ugarte, M., & Pérez-Goya, U. (2017). Stochastic spatio-temporal models for analysing NDVI distribution of GIMMS NDVI3g images. *Remote Sensing*, *9*(1), 76.

Mirik, M., Steddom, K., & Michels Jr, G. J. (2006). Estimating biophysical characteristics of musk thistle (Carduus nutans) with three remote sensing instruments. *Rangeland ecology & management*, *59*(1), 44-54.

Mirzaei, A., Naseri, R., & Soleimani, R. (2011). Response of different growth stages of wheat to moisture tension in a semiarid land. *World Appl Sci J*, *12*(1), 83-89.

Mishra, B., Babel, M. S., & Tripathi, N. K. (2014). Analysis of climatic variability and snow cover in the Kaligandaki River Basin, Himalaya, Nepal. *Theoretical and applied climatology*, *116*(3-4), 681-694.

Mkonda, M., & He, X. (2017). Are rainfall and temperature really changing? Farmer's perceptions, meteorological data, and policy implications in the Tanzanian semi-arid zone. *Sustainability*, *9*(8), 1412.

Mogili, U. R., & Deepak, B. B. V. L. (2018). Review on application of drone systems in precision agriculture. *Procedia computer science*, *133*, 502-509.

Mohsenipour, M., Shahid, S., Chung, E. S., & Wang, X. J. (2018). Changing pattern of droughts during cropping seasons of Bangladesh. *Water resources management*, *32*(5), 1555-1568.

Moral, F. J., Terrón, J. M., & Da Silva, J. M. (2010). Delineation of management zones using mobile measurements of soil apparent electrical conductivity and multivariate geostatistical techniques. *Soil and Tillage Research*, *106*(2), 335-343.

Moshia, M. E., Khosla, R., Davis, J. G., Westfall, D. G., & Doesken, K. (2015). Precision manure management on site-specific management zones: Topsoil quality and environmental impact. *Communications in soil science and plant analysis*, *46*(2), 235-258.

Moshia, M. E., Khosla, R., Longchamps, L., Reich, R., Davis, J. G., & Westfall, D. G. (2014). Precision manure management across site-specific management zones: grain yield and economic analysis. *Agronomy Journal*, *106*(6), 2146-2156.

Mulla, D. J. (2013). Twenty five years of remote sensing in precision agriculture: Key advances and remaining knowledge gaps. *Biosystems engineering*, *114*(4), 358-371.

Nawar, S., Corstanje, R., Halcro, G., Mulla, D., & Mouazen, A. M. (2017). Delineation of soil management zones for variable-rate fertilization: A review. In *Advances in agronomy* (Vol. 143, pp. 175-245). Academic Press.

Nel, A. A., Loubser, H. L., & Hammes, P. S. (2001). The effect of water stress during grain filling on the yield and processing quality of sunflower seed. *South African Journal of Plant and Soil*, *18*(3), 114-117. Unlukara, A., Beyzi, E., Ipek, A., & Gurbuz, B. (2016). Effects of different water applications on yield and oil contents of autumn sown coriander (Coriandrum sativum L.). *Turkish Journal of Field Crops*, *21*(2), 200-209.

Neményi, M., Mesterházi, P. Á., Pecze, Z., & Stépán, Z. (2003). The role of GIS and GPS in precision farming. *Computers and Electronics in Agriculture*, *40*(1-3), 45-55.

Neupane, J., & Guo, W. (2019). Agronomic Basis and Strategies for Precision Water Management: A Review. *Agronomy*, *9*(2), 87.

Odeha, I. O. A., McBratney, A. B., & Chittleborough, D. J. (1994). Spatial prediction of soil properties from landform attributes derived from a digital elevation model. *Geoderma*, *63*(3-4), 197-214.

Orsini, L., & Remy, J. C. (1976). Utilisation du chlorure de cobaltihexamine pour la détermination simultanée de la capacité d'échange et des bases échangeables des sols. *Sci. Sol*, *4*, 269-275.

Oshunsanya, S. O., Oluwasemire, K. O., & Taiwo, O. J. (2017). Use of GIS to delineate site-specific management zone for precision agriculture. *Communications in soil science and plant analysis*, *48*(5), 565-575.

Pajares, G. (2015). Overview and current status of remote sensing applications based on unmanned aerial vehicles (UAVs). *Photogrammetric Engineering & Remote Sensing*, *81*(4), 281-330.

Panda, S. S., Ames, D. P., & Panigrahi, S. (2010). Application of vegetation indices for agricultural crop yield prediction using neural network techniques. *Remote Sensing*, *2*(3), 673-696.

Panneton, B., & Brouillard, M. (2002). Use of fuzzy mapping to extract management zones from yield maps AIC 2002. *CSAE/SCGR*, Mansonville, QC, Canada.

Panneton, B., Brouillard, M., & Piekutowski, T. (2001, June). Integration of yield data from several years into a single map. In *Proc III ECPA-European Conference on Precision Agriculture, Montpellier, France, June* (pp. 18-21).

Pearson, R. L., & Miller, L. D. (1972, October). Remote mapping of standing crop biomass for estimation of the productivity of the shortgrass prairie. In *Remote sensing of environment, VIII* (p. 1355).

Pebesma, E. J. (2004). Multivariable geostatistics in S: the gstat package. *Computers & Geosciences*, *30*(7), 683-691.

Peralta, N. R., Costa, J. L., Balzarini, M., Franco, M. C., Córdoba, M., & Bullock, D. (2015). Delineation of management zones to improve nitrogen management of wheat. *Computers and Electronics in Agriculture*, *110*, 103-113.

Pinheiro Lisboa, I.P., Melo Damian, J., Roberto Cherubin, M., Silva Barros, P., Ricardo Fiorio, P., Cerri, C., & Eduardo Pellegrino Cerri, C. (2018). Prediction of Sugarcane Yield Based on NDVI and Concentration of Leaf-Tissue Nutrients in Fields Managed with Straw Removal. *Agronomy*, *8*(9), 196.

Plant, R. E., Munk, D. S., Roberts, B. R., Vargas, R. L., Rains, D. W., Travis, R. L., & Hutmacher, R. B. (2000). Relationships between remotely sensed reflectance data and cotton growth and yield. *Transactions of the ASAE*, *43*(3), 535.

Poudel, S., & Shaw, R. (2016). The relationships between climate variability and crop yield in a mountainous environment: a case study in Lamjung District, Nepal. *Climate*, *4*(1), 13.

Prasad, A. K., Chai, L., Singh, R. P., & Kafatos, M. (2006). Crop yield estimation model for Iowa using remote sensing and surface parameters. *International Journal of Applied Earth Observation and Geoinformation*, *8*(1), 26-33.

Qi, J., Huete, A. R., Moran, M. S., Chehbouni, A., & Jackson, R. D. (1993). Interpretation of vegetation indices derived from multi-temporal SPOT images. *Remote Sensing of Environment*, *44*(1), 89-101.

Rab, M. A., Fisher, P. D., Armstrong, R. D., Abuzar, M., Robinson, N. J., & Chandra, S. (2009). Advances in precision agriculture in south-eastern Australia. IV. Spatial variability in plant-available water capacity of soil and its relationship with yield in site-specific management zones. *Crop and Pasture Science*, *60*(9), 885-900.

Reynolds, C. A., Yitayew, M., Slack, D. C., Hutchinson, C. F., Huete, A., & Petersen, M. S. (2000). Estimating crop yields and production by integrating the FAO Crop Specific Water Balance model with real-time satellite data and ground-based ancillary data. *International Journal of Remote Sensing*, *21*(18), 3487-3508.

Robertson, G. P. (1998). GS+ geostatistics for the environmental sciences: GS+ user's guide. *Plainwell: Gamma Design Software*, *152*, 1.

Rocha, A. V., & Shaver, G. R. (2009). Advantages of a two band EVI calculated from solar and photosynthetically active radiation fluxes. *Agricultural and Forest Meteorology*, *149*(9), 1560-1563.

Rodríguez, Y. C., El Anjoumi, A., Gómez, J. D., Pérez, D. R., & Rico, E. (2014). Using Landsat image time series to study a small water body in Northern Spain. *Environmental monitoring and assessment*, *186*(6), 3511-3522.

Rouse Jr, J., Haas, R. H., Schell, J. A., & Deering, D. W. (1974). Monitoring vegetation systems in the Great Plains with ERTS. In Proceedings of the Third Earth Resources Technology Satellite Symposium: Washington, DC, USA, 10-14 December 1973; pp. 309–317.

Rütting, T., Aronsson, H., & Delin, S. (2018). Efficient use of nitrogen in agriculture. *Nutrient Cycling in Agroecosystems*, 110, 1-5.

Sadrykia, M., Delavar, M. R., & Zare, M. (2017). A GIS-based decision making model using fuzzy sets and theory of evidence for seismic vulnerability assessment under uncertainty (case study: Tabriz). *Journal of Intelligent & Fuzzy Systems*, *33*(3), 1969-1981.

Schlenker, W., & Roberts, M. J. (2008). *Estimating the impact of climate change on crop yields: The importance of nonlinear temperature effects* (No. w13799). National Bureau of Economic Research: Cambridge, MA, USA.

Schmidhalter, U., Maidl, F. X., Heuwinkel, H., Demmel, M., Auernhammer, H., Noack, P. O., & Rothmund, M. (2008). Precision farming–adaptation of land use management to small scale heterogeneity. In *Perspectives for agroecosystem management* (pp. 121-199). Elsevier.

Schrijver, R., Poppe, K., & Daheim, C. (2016). Precision agriculture and the future of farming in Europe. *Teaduslike ja tehnoloogiliste valikute hindamise üksus.[online] http://www. europarl. europa. eu/RegData/etudes/STUD/2016/581892/EPRS_STU (2016) 581892_EN. pdf (01.05. 2018)*.

Scudiero, E., Teatini, P., Manoli, G., Braga, F., Skaggs, T., & Morari, F. (2018). Workflow to establish time-specific zones in precision agriculture by spatiotemporal integration of plant and soil sensing data. *Agronomy*, *8*(11), 253.

Shah, F., & Wu, W. (2019). Soil and crop management strategies to ensure higher crop productivity within sustainable environments. *Sustainability*, *11*(5), 1485.

Shanahan, J. F., Schepers, J. S., Francis, D. D., Varvel, G. E., Wilhelm, W. W., Tringe, J. M., ... & Major, D. J. (2001). Use of remote-sensing imagery to estimate corn grain yield. *Agronomy Journal*, *93*(3), 583-589.

Shiru, M., Shahid, S., Alias, N., & Chung, E. S. (2018). Trend analysis of droughts during crop growing seasons of Nigeria. *Sustainability*, *10*(3), 871.

Shrestha, S. L., Maharjan, K. L., & Joshi, N. P. (2012). Relationship between climate variables and yields of food crops in Nepal: Cases of Makwanpur and Ilam Districts. *Journal of International Development and Cooperation*, *18*(4), 37-54.

Simelli, I., & Tsagaris, A. (2015) "The Use of Unmanned Aerial Systems (UAS) in Agriculture." In HAICTA, pp. 730-736.

Simões, M. D. S., Rocha, J. V., & Lamparelli, R. A. C. (2005). Spectral variables, growth analysis and yield of sugarcane. *Scientia Agricola*, *62*(3), 199-207.

Sims, D. A., & Gamon, J. A. (2003). Estimation of vegetation water content and photosynthetic tissue area from spectral reflectance: a comparison of indices based on liquid water and chlorophyll absorption features. *Remote sensing of environment*, *84*(4), 526-537.

Singla, S. K., Garg, R. D., & Dubey, O. P. (2018). Spatiotemporal analysis of LANDSAT Data for Crop Yield Prediction. *Journal of Engineering Science & Technology Review*, *11*(3).

Slayback, D. A., Pinzon, J. E., Los, S. O., & Tucker, C. J. (2003). Northern hemisphere photosynthetic trends 1982–99. *Global Change Biology*, *9*(1), 1-15.

Smith, R. J., Raine, S. R., McCarthy, A. C., & Hancock, N. H. (2009). Managing spatial and temporal variability in irrigated agriculture through adaptive control. *Australian Journal of Multi-disciplinary Engineering*, *7*(1), 79-90.

Song, C., Woodcock, C. E., Seto, K. C., Lenney, M. P., & Macomber, S. A. (2001). Classification and change detection using Landsat TM data: when and how to correct atmospheric effects?. *Remote sensing of Environment*, *75*(2), 230-244.

Stafford, J. V., Lark, R. M., & Bolam, H. C. (1999). Using yield maps to regionalize fields into potential management units. In: Robert, P.C., Rust, R.H., Larson, W.E. (Eds.), Proceedings of the 4th International Conference on Precision Agriculture. ASA, CSSA, SSSA, Madison, WI, USA, p. 225-237.

Steiner, J. L., Briske, D. D., Brown, D. P., & Rottler, C. M. (2018). Vulnerability of Southern Plains agriculture to climate change. *Climatic change*, *146*(1-2), 201-218.

Stępień, M., Gozdowski, D., Samborski, S., Dobers, E. S., Szatyłowicz, J., & Chormański, J. (2016). Validation of topsoil texture derived from agricultural soil maps by current dense soil sampling. *Journal of Plant Nutrition and Soil Science*, *179*(5), 618-629.

Sudduth, K. A., & Drummond, S. T. (2007). Yield editor. *Agronomy Journal*, *99*(6), 1471-1482.

Swindell, J. E. G. (1997). Mapping the spatial variability in the yield potential of arable land through GIS analysis of sequential yield maps. In *Precision agriculture'97: papers presented at the first European Conference on Precision Agriculture, Warwick University Conference Centre, UK, 7-10 September 1997*. Oxford; Herndon, VA: BIOS Scientific Pub., c1997..

Sys, C., Van Ranst, E., & Debaveye, J. Land Evaluation. Part I: principles in land evaluation and crop production calculations. General Administration for Development Cooperation, Agricultural Publications nr. 7, GADC, Brussels, Belgium, 1991.

Tanjii, K. K. (1990). *Agricultural salinity assessment and management* (No. 04; S620, T3.).

Taylor, J. C., Wood, G.A., & Thomas, G. (1997). Mapping yield potential with remote sensing. In *Procs. of the First European Conference on Precision Agriculture, London, UK.*, pp. 713-720.

Tian, L., Yuan, S., & Quiring, S. M. (2018). Evaluation of six indices for monitoring agricultural drought in the south-central United States. *Agricultural and forest meteorology*, *249*, 107-119.

Tilman, D. (1999). Global environmental impacts of agricultural expansion: the need for sustainable and efficient practices. *Proceedings of the National Academy of Sciences*, *96*(11), 5995-6000.

Toscano, P., Castrignanò, A., Di Gennaro, S. F., Vonella, A. V., Ventrella, D., & Matese, A. (2019). A Precision Agriculture Approach for Durum Wheat Yield Assessment Using Remote Sensing Data and Yield Mapping. *Agronomy*, *9*(8), 437.

Tucker, C. J., Pinzon, J. E., Brown, M. E., Slayback, D. A., Pak, E. W., Mahoney, R., ... & El Saleous, N. (2005). An extended AVHRR 8-km NDVI dataset compatible with MODIS and SPOT vegetation NDVI data. *International Journal of Remote Sensing*, *26*(20), 4485-4498.

Van Leeuwen, W. J. D., & Huete, A. R. (1996). Effects of standing litter on the biophysical interpretation of plant canopies with spectral indices. *Remote sensing of Environment*, *55*(2), 123-138.

Van Uffelen, C. G. R., Verhagen, J., & Bouma, J. (1997). Comparison of simulated crop yield patterns for site-specific management. *Agricultural Systems*, *54*(2), 207-222.

Verhagen, A., Booltink, H. W. G., & Bouma, J. (1995). Site-specific management: balancing production and environmental requirements at farm level. *Agricultural systems*, *49*(4), 369-384.

Viña, A., Gitelson, A. A., Nguy-Robertson, A. L., & Peng, Y. (2011). Comparison of different vegetation indices for the remote assessment of green leaf area index of crops. *Remote Sensing of Environment*, *115*(12), 3468-3478.

Wang, F., Qi, M., Wang, H., & Changjiu, Z. (1995). *The response of winter wheat to water stress and nitrogen fertilizer use efficiency* (No. INIS-MA--002). Joint FAO/IAEA Div. of Nuclear Techniques in Food and Agriculture.

Wiegand, C. L., Maas, S. J., Aase, J. K., Hatfield, J. L., Pinter Jr, P. J., Jackson, R. D., ... & Lapitan, R. L. (1992). Multisite analyses of spectral-biophysical data for wheat. *Remote Sensing of Environment*, *42*(1), 1-21.

Woodcock, C. E., Strahler, A. H., & Jupp, D. L. (1988). The use of variograms in remote sensing: I. Scene models and simulated images. *Remote Sensing of Environment*, *25*(3), 323-348.

Woolley, J. T. (1971). Reflectance and transmittance of light by leaves. *Plant physiology*, *47*(5), 656-662.

Xiao, Y., Gu, X., Yin, S., Shao, J., Cui, Y., Zhang, Q., & Niu, Y. (2016). Geostatistical interpolation model selection based on ArcGIS and spatio-temporal variability

analysis of groundwater level in piedmont plains, northwest China. *SpringerPlus*, *5*(1), 425.

Yang, C., Peterson, C. L., Shropshire, G. J., & Otawa, T. (1998). Spatial variability of field topography andwheat yield in the palouse region of the Pacific Northwest. *Transactions of the ASAE*, *41*(1), 17-27.Zandalinas, S. I., Mittler, R., Balfagón, D., Arbona, V., & Gómez-Cadenas, A. (2018). Plant adaptations to the combination of drought and high temperatures. *Physiologia plantarum*, *162*(1), 2-12.

Young, N. E., Anderson, R. S., Chignell, S. M., Vorster, A. G., Lawrence, R., & Evangelista, P. H. (2017). A survival guide to Landsat preprocessing. *Ecology*, *98*(4), 920-932.

Yousefi, M. R., & Razdari, A. M. (2015). Application of GIS and GPS in precision agriculture (a review). *International Journal of Advanced Biological and Biomedical Research*, *3*(1), 7-9.

Yue, J., Feng, H., Yang, G., & Li, Z. (2018). A comparison of regression techniques for estimation of above-ground winter wheat biomass using near-surface spectroscopy. *Remote Sensing*, *10*(1), 66.

Zarco-Tejada, P. J., Ustin, S. L., & Whiting, M. L. (2005). Temporal and spatial relationships between within-field yield variability in cotton and high-spatial hyperspectral remote sensing imagery. *Agronomy Journal*, *97*(3), 641-653.

Zhang, Q., Yang, Z., Li, Y., Chen, D., Zhang, J., & Chen, M. (2010). Spatial variability of soil nutrients and GIS-based nutrient management in Yongji County, China. *International Journal of Geographical Information Science*, *24*(7), 965-981.

Supplementary Materials

Table S1.1. Descriptive statistics of remote VIs derived from Landsat imagery during growing period of durum wheat in 2010.

BBCH	Mean	Median	Min	Max	SD	CV%	K-S
			NDVI				
31	0.29	0.29	0.23	0.35	0.03	8.8	ns
32	0.29	0.29	0.24	0.36	0.03	11.5	ns
36	0.59	0.58	0.44	0.71	0.08	13.6	*
43	0.71	0.72	0.5	0.83	0.10	14.2	*
55	0.66	0.68	0.51	0.73	0.06	8.7	ns
			EVI				
31	0.31	0.31	0.24	0.36	0.03	9.8	ns
32	0.33	0.33	0.27	0.4	0.04	10.9	ns
36	0.49	0.49	0.34	0.63	0.09	17.4	**
43	0.66	0.65	0.44	0.83	0.12	17.7	ns
55	0.73	0.74	0.48	0.83	0.07	10.1	**
			SAVI				
31	0.17	0.17	0.14	0.2	0.02	9.1	ns
32	0.19	0.19	0.16	0.23	0.02	9.3	ns
36	0.30	0.30	0.22	0.37	0.05	15.3	**
43	0.40	0.40	0.29	0.49	0.06	14.8	ns
55	0.44	0.45	0.3	0.5	0.04	9.3	ns
			GNDVI				
31	0.21	0.21	0.18	0.24	0.02	7.4	ns
32	0.23	0.23	0.2	0.27	0.02	8.1	ns
36	0.39	0.39	0.3	0.48	0.05	13.1	ns
43	0.49	0.49	0.37	0.58	0.06	12.9	ns
55	0.51	0.51	0.37	0.55	0.04	7.9	**
			GCI				
31	0.53	0.54	0.44	0.62	0.05	9.3	ns
32	0.60	0.60	0.5	0.72	0.06	10.5	ns
36	1.33	1.30	0.88	1.83	0.28	21.1	ns
43	2.06	2.00	1.24	2.83	0.49	23.9	ns
55	2.10	2.10	1.21	2.47	0.29	13.7	ns
			SR				
31	1.72	1.73	1.57	1.87	0.08	4.6	ns
32	1.72	1.71	1.55	1.91	0.1	5.8	ns
36	2.93	2.84	2.17	3.73	0.48	16.4	**
43	4.14	3.95	2.63	5.64	0.94	22.7	ns
55	4.01	4.03	2.65	4.55	0.43	10.7	ns

SD, standard deviation: CV, coefficient of variation: K-S, Kolmogorov-Smirnov test for normal distribution; ns, non-significant; *, significant at $P \leq 0.05$; **, significant at $P \leq 0.01$.

Table S1.2. Descriptive statistics of remote VIs derived from Landsat imagery during growing period of sunflower in 2011.

BBCH	Mean	Median	Min	Max	SD	CV%	K-S
			NDVI				
30	0.47	0.48	0.39	0.54	0.02	4.8	ns
32	0.66	0.66	0.57	0.73	0.04	6.5	ns
51	0.70	0.7	0.56	0.79	0.06	9.2	**
67	0.52	0.55	0.35	0.64	0.09	16.2	**
75	0.28	0.28	0.21	0.38	0.03	12.2	ns
			EVI				
30	0.51	0.52	0.44	0.56	0.03	5.8	*
32	0.90	0.91	0.7	1.09	0.12	12.8	**
51	0.76	0.76	0.55	0.92	0.11	14.4	**
67	0.54	0.55	0.35	0.71	0.1	19	ns
75	0.24	0.24	0.19	0.31	0.02	10.2	ns
			SAVI				
30	0.32	0.33	0.28	0.35	0.02	5.4	**
32	0.52	0.52	0.4	0.61	0.06	10.7	ns
51	0.49	0.49	0.37	0.58	0.06	12.4	**
67	0.34	0.35	0.24	0.44	0.06	16.5	ns
75	0.16	0.16	0.13	0.19	0.01	9.3	ns
			GNDVI				
30	0.37	0.38	0.33	0.39	0.02	4.2	**
32	0.53	0.54	0.45	0.6	0.04	7.5	ns
51	0.55	0.55	0.45	0.62	0.05	8.5	**
67	0.40	0.41	0.31	0.48	0.05	12.8	**
75	0.22	0.22	0.19	0.26	0.02	7.7	ns
			GCI				
30	1.19	1.21	1.01	1.31	0.08	6.4	ns
32	2.33	2.33	1.64	3	0.37	15.8	ns
51	2.49	2.51	1.72	3.23	0.45	18.2	*
67	1.39	1.42	0.91	1.9	0.28	20.5	ns
75	0.57	0.56	0.46	0.72	0.06	9.8	ns
			SR				
30	2.42	2.43	2.23	2.6	0.09	3.9	ns
32	4.17	4.16	3.15	5.3	0.61	14.7	**
51	4.53	4.53	3.15	5.95	0.86	19	*
67	2.81	2.85	2	3.72	0.49	17.5	ns
75	1.62	1.62	1.46	1.81	0.08	5.2	ns

SD, standard deviation: CV, coefficient of variation: K-S, Kolmogorov-Smirnov test for normal distribution; ns, non-significant; *, significant at $P \leq 0.05$; **, significant at $P \leq 0.01$.

Table S1.3. Descriptive statistics of remote VIs derived from Landsat imagery during growing period of bread wheat in 2012.

BBCH	Mean	Median	Min	Max	SD	CV%	K-S
			NDVI				
33	0.47	0.46	0.37	0.61	0.07	14.6	**
36	0.54	0.50	0.44	0.67	0.08	14.1	*
41	0.52	0.51	0.4	0.61	0.06	12.3	*
63	0.80	0.81	0.64	0.88	0.06	7.3	**
83	0.51	0.51	0.46	0.56	0.03	5.3	ns
			EVI				
33	0.45	0.43	0.35	0.58	0.07	16.7	**
36	0.34	0.38	0.01	0.71	0.27	79.2	*
41	0.30	0.43	-0.12	0.5	0.2	67.8	*
63	0.11	0.11	0.02	0.13	0.03	23.8	*
83	0.54	0.58	0.14	0.65	0.11	19.8	*
			SAVI				
33	0.25	0.24	0.21	0.32	0.04	14.4	**
36	0.18	0.20	0	0.36	0.14	80.0	*
41	0.10	0.15	-0.01	0.18	0.07	69.4	*
63	0.45	0.47	0.1	0.54	0.1	23.3	*
83	0.28	0.30	0.07	0.34	0.06	20.3	*
			GNDVI				
33	0.33	0.32	0.28	0.39	0.04	11.1	*
36	0.14	0.22	-0.27	0.42	0.24	168.3	*
41	-0.73	-0.16	-11.14	0.14	1.31	179.3	*
63	0.53	0.57	0.06	0.63	0.13	25.1	*
83	0.32	0.35	-0.08	0.41	0.1	31.4	*
			GCI				
33	1.00	0.95	0.78	1.31	0.17	17.0	*
36	0.60	0.73	-0.25	1.5	0.69	114.4	*
41	0.21	0.38	-0.27	0.44	0.26	122.7	*
63	2.61	2.69	0.45	3.49	0.75	29.0	**
83	1.05	1.10	0.12	1.39	0.27	25.5	*
			SR				
33	2.28	2.20	1.91	2.84	0.3	13.1	**
36	1.89	1.97	0.77	3.25	0.94	49.6	*
41	1.21	1.37	0.73	1.46	0.26	21.9	*
63	4.87	5.00	1.68	6.37	1.2	24.7	ns
83	2.33	2.38	1.2	2.79	0.32	13.6	*

SD, standard deviation: CV, coefficient of variation: K-S, Kolmogorov-Smirnov test for normal distribution; ns, non-significant; *, significant at $P \leq 0.05$; **, significant at $P \leq 0.01$.

Table S1.4. Descriptive statistics of remote VIs derived from Landsat imagery during growing period of coriander in 2013.

BBCH	Mean	Median	Min	Max	SD	CV%	K-S
			NDVI				
34	0.08	0.08	0.07	0.08	0	2.7	**
55	0.33	0.34	0.25	0.38	0.04	10.6	**
63	0.62	0.63	0.46	0.7	0.07	11.2	*
71	0.68	0.70	0.5	0.78	0.08	12.0	*
81	0.65	0.66	0.51	0.74	0.07	10.3	*
			EVI				
34	0.27	0.27	0.25	0.29	0.01	3.3	ns
55	0.43	0.43	0.4	0.45	0.01	2.6	ns
63	0.59	0.60	0.43	0.71	0.09	15.8	*
71	0.64	0.66	0.5	0.73	0.07	11.1	*
81	0.63	0.65	0.5	0.69	0.05	8.4	*
			SAVI				
34	0.08	0.08	0.08	0.09	0	2.0	ns
55	0.28	0.29	0.23	0.32	0.02	8.3	**
63	0.43	0.44	0.34	0.51	0.06	13.0	*
71	0.53	0.54	0.43	0.59	0.05	9.5	*
81	0.45	0.46	0.38	0.49	0.03	6.7	*
			GNDVI				
34	0.11	0.11	0.1	0.11	0	1.9	ns
55	0.37	0.37	0.29	0.41	0.03	8.1	*
63	0.60	0.61	0.52	0.65	0.04	7.3	*
71	0.67	0.68	0.57	0.72	0.05	7.0	*
81	0.62	0.63	0.55	0.66	0.03	5.3	*
			GCI				
34	0.24	0.24	0.23	0.25	0.01	2.2	ns
55	1.16	1.20	0.83	1.38	0.14	12.3	*
63	3.06	3.12	2.19	3.74	0.52	17.1	*
71	4.19	4.33	2.82	5.31	0.8	19.0	*
81	3.36	3.49	2.49	3.92	0.43	12.9	*
			SR				
34	1.17	1.16	1.15	1.18	0	0.4	**
55	2.01	2.05	1.67	2.24	0.15	7.7	**
63	3.34	3.40	2.52	3.99	0.5	14.9	*
71	5.86	6.02	3.73	7.9	1.32	22.5	*
81	4.52	4.68	3.24	5.36	0.66	14.6	*

SD, standard deviation: CV, coefficient of variation: K-S, Kolmogorov-Smirnov test for normal distribution; ns, non-significant; *, significant at $P \leq 0.05$; **, significant at $P \leq 0.01$.

Table S1.5. Descriptive statistics of remote VIs derived from Landsat imagery during growing period of bread wheat in 2014.

BBCH	Mean	Median	Min	Max	SD	CV%	K-S
			NDVI				
32	0.69	0.68	0.57	0.8	0.07	10.8	**
37	0.79	0.78	0.69	0.85	0.05	6.0	**
55	0.84	0.84	0.78	0.87	0.03	3.0	**
77	0.81	0.83	0.7	0.87	0.05	5.7	*
85	0.40	0.45	0.19	0.55	0.1	25.6	*
			EVI				
32	0.45	0.43	0.35	0.55	0.07	15.6	**
37	0.59	0.57	0.48	0.69	0.07	12.2	*
55	0.78	0.78	0.69	0.85	0.05	5.9	ns
77	0.59	0.60	0.47	0.67	0.05	9.2	**
85	0.38	0.41	0.24	0.5	0.08	20.9	*
			SAVI				
32	0.41	0.39	0.32	0.49	0.05	13.3	**
37	0.61	0.60	0.52	0.7	0.06	9.9	*
55	0.57	0.57	0.52	0.61	0.03	4.9	**
77	0.49	0.50	0.41	0.54	0.04	7.7	**
85	0.28	0.28	0.2	0.38	0.05	19.2	ns
			GNDVI				
32	0.60	0.59	0.52	0.67	0.05	8.3	**
37	0.59	0.58	0.52	0.65	0.05	7.6	**
55	0.72	0.72	0.67	0.75	0.02	3.4	**
77	0.65	0.66	0.57	0.7	0.03	5.2	**
85	0.40	0.38	0.29	0.53	0.07	17.2	*
			GCI				
32	3.11	2.86	2.24	4.18	0.65	21.1	*
37	2.97	2.81	2.2	3.82	0.55	18.7	*
55	5.13	5.15	4.09	6	0.6	11.6	**
77	3.85	3.90	2.79	4.62	0.53	13.8	**
85	1.43	1.27	0.86	2.37	0.43	30.2	*
			SR				
32	5.05	4.53	3.43	7.23	1.29	25.6	*
37	7.49	7.12	5.21	10.09	1.68	22.4	*
55	6.26	6.31	5.25	7.09	0.57	9.1	**
77	4.78	4.87	3.58	5.6	0.57	12.0	**
85	2.43	2.45	1.72	3.5	0.48	19.7	ns

SD, standard deviation: CV, coefficient of variation: K-S, Kolmogorov-Smirnov test for normal distribution; ns, non-significant; *, significant at $P \leq 0.05$; **, significant at $P \leq 0.01$.

Acknowledgements

My deepest reverence of gratitude to "**Almighty Allah"**, the Most Beneficent and Most Merciful, who blessed me with good health, the will and capability to undertake and complete this research for this thesis. I offer my humblest thanks to the **Holly Prophet 'Muhammad' (Peace be upon him)** who is forever a torch of guidance for mankind to a right direction of life.

I feel highly privileged to express the deep sense of gratitude to my respected supervisor **Dr. Lorenzo Barbanti**, Assistant Professor, Department of Agricultural and Food Sciences, DISTAL, University of Bologna, Italy; having support, encouragement, inspiring guidance and motivation to start high scientific research and compilation of this PhD dissertation.

I would like to extend my profound sense of gratitude to my co-supervisor **Dr. Roberta Martelli** for her scholastic guidance and valuable suggestions. Countless thanks to **Dr. Flavio Lupia,** Scientific Researcher, CREA Research Centre for Agricultural Policies and Bioeconomy, Rome Italy, **and Dr. Elia Scudiero,** Research Agronomist, United State Department of Agriculture (USDA), Riverside, California USA, for their advice, support and training in the compilation of scientific papers during my PhD programme. The help extended by **Dr. Gloria Falsone** for her supervision and assistance in soil analysis during study period. I am thankful to **PhD unit, the PhD Coordinator, Chairperson and whole staff members** who's inspired me to do my work in time and moral encouragement by taking keen interest in my research work.

Lastly, I would also like to record the sincerest thanks to **Dr. Dennis Corwin,** Senior Scientific Officer, Salinity Laboratory, ARS-USDA, California USA, for his generous transfer of knowledge and invaluable words of advice that will always serve as beacon throughout the course of my research horizon.

I express my humble gratitude to my loving parents and all my family members for their prayers, love, affection and help. Their aspirations are the torch of my destination.

May Allah Almighty bless them.

(ABID ALI)